POLITECNICO DI MILANO

Facoltà di Ingegneria

Dipartimento di Elettronica, Informazione e Bioingegneria

Master of Science in

Environmental and Land Planning Engineering

A framework to test multiple optimality principles in landscape evolution under river dynamics

Supervisor:

PROF. ANDREA CASTELLETTI

Assistant Supervisor:

POSTDOC. SIMONE BIZZI

Alta Scuola Politecnica Assistant Supervisors:

PROF.SSA MARINA DE MAIO

Master Graduation Thesis by:

ANDREA COMINOLA
Student Id n. 765644

EMANUELE MASON
Student Id n. 765334

Academic Year 2011-2012

POLITECNICO DI MILANO

Facoltà di Ingegneria

Dipartimento di Elettronica, Informazione e Bioingegneria

Corso di Laurea Magistrale in

Ingegneria per l'Ambiente e il Territorio

Una framework per testare differenti principi di ottimalità nell'evoluzione geomorfologica del territorio guidata dalla dinamica fluviale

Relatore:

PROF. ANDREA CASTELLETTI

Correlatore:

POSTDOC. SIMONE BIZZI

Correlatore Alta Scuola Politecnica Assistant:

PROF.SSA MARINA DE MAIO

Tesi di Laurea Magistrale di:

ANDREA COMINOLA
Student Id n. 765644

EMANUELE MASON
Student Id n. 765334

Anno Accademico 2011-2012

COLOPHON

This document was typeset using the typographical look-and-feel `classicthesis` developed by André Miede. The style was inspired by Robert Bringhurst's seminal book on typography "*The Elements of Typographic Style*". `classicthesis` is available for both LaTeX and LyX:

http://code.google.com/p/classicthesis/

Happy users of `classicthesis` usually send a real postcard to the author, a collection of postcards received so far is featured here:

http://postcards.miede.de/

Andrea Cominola and Emanuele Mason: *A framework to test multiple optimality principles in landscape evolution under river dynamics*, March 2013

Final Version as of April 5, 2013 (`classicthesis` version 1.0).

A Cecilia e Francesca, che ci sopportano

— A & E

ACKNOWLEDGMENTS

We would like to express our sincere gratitude to the persons who encouraged and supported this Master thesis, providing us with knowledge and help for carrying it on until the end.

Thanks to Professor Andrea Castelletti, who engaged us in this challenging work and many other experiences. We are grateful for his unconditional trust and help. His advices and the time spent together were useful for developing this thesis, but especially precious for having fostered our growth and the participation to many wonderful experiences like our American months, American Geophysical Union (AGU)2012 and European Geophysical Union (EGU)2013 conferences. He also provided us many interesting suggestions for our future careers, we will keep in mind.

Thanks to Simone Bizzi. His constant support, commitment and optimism were fundamental for stimulating us and showing us that there are different ways of approaching the different issues and their tricky aspects. His sincere excitement when approaching unresolved scientific problems has been one of the major support to face the unknown aspects of this work. We hope to be able to carry it with us in future.

Thanks to Professor Kyungrock Paik. He showed a continuous interest in our thesis and his suggestions were precious in all the work phases, since the beginning, when he gave us the opportunity to start working on his model, until the end, for the results interpretation.

Thanks to Professor Patrick Reed and his research group. They kindly hosted us during our research months at PennState University in State College (PA, USA) and provided all the help and assistance we needed for every kind of purpose in those months. Working with Patrick's research group was a very enriching experience, we will not forget in the future. Patrick's question "who cares about your work?" was a new starting point for going beyond the thesis topic as an academic matter, allowing us to explore the bigger picture into which find a place for this research.

Thanks to Marina De Maio. She showed great interest in deepening the topic of our thesis and accepted with great enthusiasm to co-supervise it.

The months spent at PennState University working on this thesis were possible thanks to the finances offered by the scholarship "Politecnico di Milano - a.a. 2011/12 per tesi all'estero", we both could take advantage of.

CONTENTS

LIST OF FIGURES

LIST OF TABLES

LISTINGS

ACRONYMS

AGU	American Geophysical Union
AM	Adaptive Metropolis
AMALGAM	A Multi ALgorithm Genetically Adaptive Multiobjective
C++	C plus plus
DEM	Digital Elevation Model
D8	Eight Direction
DE	Differential Evolution
DF	Depression Filling
EGU	European Geophysical Union
εNSGA-II	epsilon Nondominated Sorting Genetic Algorithm II
EA	Evolutionary Algorithm

EE	Energy Expenditure
EEE	Equal Energy Expenditure
EEL	Energy Expenditure in any Link
GA	Genetic Algorithm
GD8	Global Eight Direction
GDE_3	Generalized Differential Evolution 3
GIS	Geographic Information System
GLE	Genetic Landscape Evolution
IDW	Inverse Distance Weighting
HPC	High Performance Computing
LAP	Least Action Principle
LSD	Local Steepest Direction
MIT	Massachusetts Institute of Technology
MO	Multi Objective
MOEA	Multi Objective Evolutionary Algorithm
MOP	Multi Objective Problem
NFE	Number of Function Evaluations
NASA	National Aeronautics and Space Administration
NSGA	Nondominated Sorting Genetic Algorithm
NSGA-II	Nondominated Sorting Genetic Algorithm II
OCN	Optimal Channel Network
OMOPSO	Optimal Multi Objective Particle Swarm Optimization
PM	Polynomial Mutation
PSO	Particle Swarm Optimization
SBX	Simulated Binary Crossover
$SPEA_2$	Strength Pareto Evolutionary Algorithm 2
SRTM	Shuttle Radar Topography Mission
TEE	Total Energy Expenditure
TIN	Triangular Irregular Network

USGS	United States Geological Survey
VEGA	Vector Evaluated Genetic Algorithm
XML	eXtensible Markup Language
YAML	YAML Ain't Markup Language

ABSTRACT

Proper techniques and knowledge for modeling landscape evolution under river dynamics are fundamental to assess their resilience to extreme events, climate change, and to improve planning and management strategies.

Since landscape and river evolution occur at various spatial and temporal scale, with many factors and drivers, understanding and modeling them is highly complex. Among the approaches proposed in the literature, the idea of a least action principle has been suggested many times as a simpler approach than a physically based one when applied at the basin scale. This theory assumes that natural river networks self-organize in order to satisfy the "optimality" criterion of least energy expenditure. Yet, since its mathematical formulation implies too many degrees of freedom if compared to the available equations, the problem cannot be solved easily. For this reason, various simplifications have been proposed by different authors. Thanks to DEMs and increased computational power, it is possible to study the 3D structure of river networks, but the suggested simplifications fail to characterize both the whole complexity of rivers branching and their longitudinal bed profiles.

In an attempt to test the hypotheses behind these simplifications, we assessed the suitability of using a multi-objective optimization framework. The core of the framework is a newly developed model which makes a synthetic landscape evolve over a 3D spatial domain. Multiple alternative river network evolutions, corresponding to as many trade-offs among the different and conflicting proposed formulations of the optimality principles, are computed exploiting evolutionary multi-objective algorithms. 3D features of generated landscapes and river networks are compared with natural ones through Horton's and Hack's laws.

Results show that multi-objective framework highlights the existent conflicts among the objectives proposed so far in literature and reproduce the 3D structure of river networks, according to them. Furthermore, the framework pointed out which limitations are due to modeling flaws: some improvements are proposed.

This work might help the identification of the real formulation of the optimality principle and foster the debate around the theory of optimality in landscape evolution processes.

SOMMARIO

La presenza di tecniche appropriate e conoscenze di processo per modellizzare l'evoluzione morfologica dei territori soggetti a dinamiche fluviali è fondamentale per valutare la loro resilienza di fronte a eventi estremi, al cambiamento climatico, e migliorare le politiche di pianificazione e gestione delle risorse. Dal momento che l'evoluzione morfologica del territorio e delle reti fluviali avviene su ampie scale spazio-temporali, ed è guidata da molti fattori, la sua modellazione risulta molto complessa. Tra gli approcci presenti in letteratura, l'idea di un principio di minima energia è stato proposto più volte, risultando più semplice di un approccio fisicamente basato, quando applicato a scala di bacino. Questa teoria presuppone che le reti fluviali in natura si organizzino autonomamente in maniera da rispettare il criterio di ottimalità di minima energia. Tuttavia, la sua formulazione matematica è complicata; per questo molte semplificazioni sono state proposte in letteratura. Sebbene l'uso di DEM e la disponibilità di potenza di calcolo permettano di studiare la struttura 3D delle reti fluviali, le semplificazioni proposte falliscono nel descrivere contemporaneamente la ramificazione delle reti e il profilo longitudinale dei fiumi. Al fine di testare le ipotesi a supporto delle semplificazioni, questo lavoro si pone l'obiettivo di testare l'utilizzo di una framework di ottimizzazione multi obiettivo. Il cuore della framework è un modello che fa evolvere un territorio sintetico nelle tre dimensioni. Vengono simulate differenti evoluzioni fluviali, corrispondenti ai diversi tradeoff tra formulazioni differenti e conflittuali del principio di ottimalità proposto in letteratura, sfruttando l'utilizzo di algoritmi genetici. Le caratteristiche 3D dei terreni simulati e delle reti fluviali sono confrontate con quelle naturalli, grazie alle leggi di Horton di Hack. I risultati mostrano che la framework multi obiettivo è in grado di evidenziare i conflitti esistenti tra gli obiettivi finora proposti in letteratura e riprodurre, in accordo con essi, la struttura 3D delle reti fluviali. Inoltre, la framework permette di individuare quali limiti sono dovuti al processo modellistico: per questi alcuni miglioramenti sono proposti. Questo lavoro può aiutare l'individuazione della corretta formulazione del principio di ottimalità e incentivare il dibattito circa la teoria di ottimalità nel processi di evoluzione morfologica del territorio.

ESTRATTO

La presenza di tecniche appropriate e conoscenze di processo per modellare l'evoluzione morfologica dei territori soggetti a dinamiche fluviali è fondamentale per valutare la loro resilienza di fronte a eventi estremi e migliorare le politiche di pianificazione e gestione delle risorse.

L'evoluzione geomorfologica del terreno è uno dei temi più caldi tra quelli studiati in geomorfologia e può essere definita come un processo continuo il cui risultato sono

> le interazioni tra forma e processo che si riflettono in cambiamenti misurabili sul territorio, lungo scale temporali sia umane che geologiche. [see 41, p. 247]

In particolare, tra tutti i processi che influenzano l'evoluzione geomorfologica del territorio, come le attività tettoniche e l'interazione tra il suolo e gli agenti climatici, lo sviluppo delle reti fluviali ha un ruolo molto rilevante. Infatti i flussi d'acqua cambiano forma ai versanti, regolano i processi di erosione e sedimentazione e, iterativamente, formano le reti fluviali. Questi processi coinvolgono sia trasferimenti di massa di terreno (proprio tramite erosione, trasporto e sedimentazione), sia cambiamenti della distribuzione di energia: il movimento dei flussi d'acqua lungo il terreno fa si che l'energia potenziale delle gocce di pioggia si trasformi in energia cinetica e parte sia dissipata a causa dell'attrito con il suolo.

Sembra chiaro come l'evoluzione morfologica del territorio e delle reti fluviali avvenga su ampie scale spazio-temporali, e sia guidata da molti fattori: per questo la sua modellazione risulta molto complessa. Tra gli approcci presenti in letteratura, l'idea di un principio di minima energia è stato proposto più volte, a partire dagli studi preliminari di Leopold and Langbein nel 1962. Questa teoria presuppone che le reti fluviali, in natura, si organizzino autonomamente in maniera da rispettare il criterio di ottimalità di minima energia, il cosiddetto Least Action Principle (LAP). Un confronto tra questo approccio di studio e quello fisicamente basato mostra come, l'approccio basato sul LAP sia di più semplice applicazione, per studi condotti a scala di bacino. Infatti, sebbene un approccio fisicamente basato sia in grado di descrivere in dettaglio i sottoprocessi e le loro interazioni, all'interno della dinamica di evoluzione di reti fluviali e territorio, è allo stesso tempo limitato dal numero di parametri da calibrare e aggiornare nel tempo. Per questo, l'approccio fisicamente basato viene solitamente utilizzato a scala di sezione e tratti di canali. Diversamente, l'approccio basato sul principio di minima energia, detto di

ottimalità, sebbene non permetta lo studio delle dinamiche dei sottoprocessi, può essere usato per simulare il comportamento di suolo e reti fluviali a scala di bacino, nel seguente modo:

- una formulazione del principio di ottimalità viene stabilita come ipotesi iniziale;
- sulla base della formulazione del criterio di ottimalità scelta, si risolve un problema di minimizzazione (anche detto di ottimizzazione) per simulare il comportamento delle reti fluviali e del territorio sul quale si sviluppano.

Tuttavia, la formulazione del principio di minima energia è complicata, nel senso che ci sono troppi gradi di libertà, se confrontati con il numero di equazioni disponibili per la sua formulazione. Per questo, molte versioni semplificate sono state proposte in letteratura; tra queste ricordiamo i principi di *minimo consumo di energia totale* TEE, *minimo consumo di energia in ogni link della rete* EEL, *minimo consumo di energia per unità di area* EE e *ugual consumo di energia per unità di area* EEE, proposti da Rodríguez-Iturbe et al.[55]. Sebbene l'uso di DEM e la disponibilità di potenza di calcolo permettano di studiare la struttura 3D delle reti fluviali, le semplificazioni proposte per il principio di ottimalità falliscono nel descrivere contemporaneamente la ramificazione delle reti (quindi la loro struttura bidimensionale) e il profilo longitudinale dei fiumi. Un tentativo in questa direzione è stato fatto da Paik, il quale ha simulato l'evoluzione geomorfologica con un modello genetico di evoluzione del territorio (Genetic Landscape Evolution (GLE)) in 3D, che però, nonostante i buoni risultati nel descrivere la conformazione planare delle reti, non ne descriveva realisticamente lo sviluppo nella terza dimensione, la quota.

Al fine di testare le ipotesi dalle quali sono state proposte le formulazioni semplificate del principio di minima energia, questo lavoro si pone l'obiettivo di testare l'efficacia di una framework di ottimizzazione multi-obiettivo. In una framework del genere, le diverse formulazioni del principio di minima energia diventano i criteri da ottimizzare (da qui l'aggettico multi-obiettivo), quindi le ipotesi iniziali, mentre gli output saranno dei modelli di terreno sintetico, con le relative reti fluviali, ottimizzate secondo i criteriche stabiliti. La loro attendibilità dovrà essere valutata, confrontando le loro caratteristiche idrologiche con quelle delle reti fluviali presenti in natura. In questa maniera, le formulazioni scelte per i criteri potranno essere valutate, analizzando i trade-off ed i possibili conflitti esistenti tra di esse, così come la loro influenza sulla forma degli output sintetici. Il fine ultimo di questo approccio di studio, che non è comunque scopo della tesi, ma per il quale la tesi offre materiale di analisi e lavoro, è trovare la corretta, unica, formulazione del principio di minima energia, adatta ad essere applicata a DEM, che permetta di descrivere i processi di evoluzione geomorfologica del territorio e delle sue reti fluviali.

La framework che è stata implementata per raggiungere gli obiettivi di questo lavoro, si compone di tre elementi, come riportato nel diagramma in figura 4.1:

- il cuore della framework è un modello che fa evolvere un territorio sintetico nelle tre dimensioni, ne estrae le reti fluviali e calcola i corrispondenti valori dei criteri selezionati. I criteri selezionati per i nostri esperimenti sono le formulazioni di quelli già citati proposti da Rodríguez-Iturbe et al., cioè TEE, EEL, EE e EEE;

- un ottimizzatore che sfrutta una serie di algoritmi genetici è interfacciato al modello, al fine di minimizzare i valori dei criteri scelti e fare evolvere il sistema in accordo con essi;

- un set di strumenti di analisi dei risultati completa la framework. Questa ultima parte permette di confrontare gli output sintetici con delle reti fluviali naturali: indici idrologici derivanti dalle leggi di Horton e di Hack vengono valutati per le reti sintetiche e confrontati con i range di valori tipici tra le reti naturali. Tecniche di clusterizzazione e statistica sono inglobate in questa parte, per un' analisi completa dei risultati.

I risultati ottenuti sulla base di alcuni esperimenti (descritti nel capitolo 5) mostrano che la framework multi-obiettivo è in grado di evidenziare i conflitti esistenti tra gli obiettivi finora proposti in letteratura e riprodurre, in accordo con essi, la struttura 3D delle reti fluviali. A tal proposito, i ritrovati principali sono stati:

- l'ipotesi di conflitto tra alcune formulazioni del principio di ottimalità sono comprovate dalle soluzioni ottime trovate (che compongono la cosiddetta frontiera di Pareto);

- la framework ha permesso di formulare i diversi criteri con in maniera consona a modelli di terreno digitali DEM;

- risultati promettenti sono stati raggiunti, sia nel riprodurre le caratteristiche 2D delle reti, sia nello studiare le loro caratteristiche tridimensionali, tramite l'analisi delle pendenze e dei profili longitudinali dei fiumi.

Inoltre, la framework ha permesso di individuare quali limiti sono dovuti al processo modellistico: per questi alcuni miglioramenti sono proposti, quali l'integrazione di un interpolatore spaziale nel modello.

Il contributo di questo lavoro è quindi rivolto sia a fini modellistici, che di *system understanding*:

- dal punto di vista di *system understanding*, uno sforzo importante è stato dedicato nel formalizzare meglio il problema dell'evoluzione geomorfologica soggetta al principio di ottimalità. Lo stesso sforzo è stato poi impiegato nel cercare di capire le caratteristiche delle differenti formulazioni di questo principio e il loro legame con la morfologia di territorio e reti fluviali;
- dal punto di vista modelistico, è la prima volta che una framework completa viene implementata per lo studio a multi-obiettivo e in 3D del problema affrontato. Questo strumento quindi rappresenta l'output materiale della tesi, che può essere utilizzato per rispondere alle numerose domande aperte, rimandate a ricerche future.

Da questo lavoro può partire l'individuazione della corretta formulazione del principio di ottimalità e il dibattito circa la teoria di ottimalità nel processi di evoluzione morfologica del territorio viene incentivato.

PREFACE

This document represents the Master Graduation Thesis written by Andrea Cominola and Emanuele Mason as the final project of their Master of Science in Environmental Engineering.

The idea of working on a multi-objectives framework for studying landscape evolution under river dynamics firstly came up in March 2012, while speaking with Professor Andrea Castelletti and Simone Bizzi, who respectively supervised and co-supervised this thesis. The idea of putting together issues related to geomorphology and modeling approaches typical of control theories constituted the starting point for concretely working on the thesis. From that moment on, the two students worked intensively on the choosen topic until March 2013.

The bigger part of the work was performed at Politecnico di Milano, apart from the period between October and December 2012, when the two students had the opportunity to perform part of their research at PennState University in State College (PA, USA). The students closely worked with Patrick Reed and his research group, and for the whole period cooperated with Professor Kyungrock Paik from Korea University. They both co-supervised the thesis. In particular, they started working by analyzing a recent GLE model developed by Professor Paik, who provided them with all the needed material. Finally, Marina De Maio from Politecnico di Torino co-supervised the thesis as Alta Scuola Politecnica co-supervisor.

MOTIVATION

As the students firstly could intuitively think and then could verify while working, modeling landscape and river evolution is a big challenge. As they had the opportunity to verify also while attending the AGU2012 and EGU2013 conferences, many theories exist, but not many significant works exist related to landscape evolution analysis based on optimality criteria.

The motivation for working on that topic derives from several aspects. First of all, personal interest captured the students' willingness to start this thesis.

Secondly, the idea of developing scientific improvements with respect to a very challenging topic as the one of landscape evolution under river dynamics, providing new tools, approaches and results, fostered their work.

Finally, their strongest motivation and hope is that, even if a single work might bring little improvements to scientific and technical dis-

ciplines, the framework developed in this thesis could be concretely used. In particular, since many issues rise, it is hoped that many future researches will focus on the topic. At the same time, the students are certain that the framework might rise the interest of hydrologists and geomorphologysts and be used for real case study analysis, integrated with other existing tools.

Part I

THEORY

This first part of the thesis introduces the theoretical concepts characterizing the study of landscape and river evolution and the framework which was developed within this work.

1 INTRODUCTION

Every river appears to consist of a main trunk, fed from a variety of branches, each running in a valley proportional to its size, and all of them together forming a system of vallies, communicating with one another, and having such a nice adjustment of their declivities that none of them join the principal valley on too high or too low a level

— Playfair. *Illustrations of the Huttonian theory of the earth*, 1802

Landscape evolution is one of the main topics geomorphological science deals with. It can be defined as a continuous process resulting from

> the interactions between form and process that are played out as measurable changes in landscapes over geologic as well as human time scales [see 41, p. 247].

Among the processes which affect landscape evolution, river networks development assumes a relevant role. In fact, water and sediment interactions shape hillslopes, regulate soil erosion and sedimentation, and organize river networks, iteratively. Since landscape evolution and river organization occur at various spatial and temporal scale, involving a great amount of factors and drivers, the understanding and modeling of them is highly complex.

Many modeling approaches can be found in the pertinent literature. Among them, the idea of a least action principle governing river networks evolution has been proposed many times as a simpler approach than a physically based one when applied at the basin scale. This theory assumes that river networks, as observed in nature, self-organize and act on soil transportation in order to satisfy the "optimality" criterion of least energy expenditure.

Yet, since its mathematical formulation implies too many degrees of freedom if compared to the available equations, the problem cannot be solved easilly. For this reason, various simplifications, like 2D analisys or single section focus, have been proposed by different authors. The simplifications depend on which time and spatial scale we are focusing on, and then on the type of framework we are interested in, i. e. for system understanding or modeling for management. Thanks to DEMs and increased computational power, it is now possible to study the 3D structure of river networks. For this purpose the suggested simplifications fail to characterize both the whole complexity of river networks branching and longitudinal bed profiles.

Considering this statement, the following questions rise:

- May the principle be used to represent the landscape evolution process in time and space process using Digital Elevation Models?
- Would a multi-objective framework be suitable to take advantage of the existing knowledge and to assess the tradeoffs among different simplified version of the "optimality" criterion in order to find the proper expression for 3D modeling?

The main objective of this thesis is to give an answer to these questions. In the attempt to pursue this objective, we detailed a multi-criteria optimization framework to describe river and landscape evolution in a 3D spatial domain. It is composed by:

- a model which, given a discretized landscape i. e. a DEM, builds the relative river network and evaluates the value of the criteria. For building the algorithm of the model, the main features of a GLE model, developed by Professor Kyungrock Paik from Korea University were taken as a basis, re-elaborated and improved;[1]
- an optimizer which generates synthetic landscapes, exploiting evolutionary algorithms, and, coupled to the model, performs the optimization of multiple objectives;
- a set of analysis tools and methods for assessing the features of the synthetic landscapes, generated by the model.

The joint analysis of multiple objectives might help the identification of the real optimality principle and foster the debate around the theory of optimality in landscape evolution processes. Furthermore, the framework is expected to point out which limitations are due to modeling flaws and which instead depends on the criteria considered.

1.1 THE CONTENTS OF THIS THESIS

The mentioned topics will be debated in the next chapters of this thesis, according to the following structure:

- Chapter 2 provides the basic theoretical knowledge about the topic of landscape evolution under river dynamics. After that, the deliverable contribution of this thesis, i. e. the multi-objective framework, is introduced;
- the framework is formalized with mathematical terms in chapter 3 . Moreover, all its features and the way it works are characterized, together with its outputs and the methodology for analyzing them;

1 For a description of Professor Paik's GLE model, see [38].

- in chapter 4 the elements of the framework described in the previous chapter are detailed from the technical point of view of implementation. Input parameters, model settings, algorithm technicalities both for the model and the results analysis tools are deepened.
- Finally, the main simulation results are presented and analyzed in chapter 5 , describing the model setting used for generating them, the main findings and the criticalities. After that, the fore is left to a short conclusion, with final remarks and suggestions for future research.

2

LANDSCAPE EVOLUTION UNDER RIVER DYNAMICS

Whenever a theory appears to you as the only possible one, take this as a sign that you have neither understood the theory nor the problem which it was intended to solve

— Popper, *Objective Knowledge: An Evolutionary Approach*, 1979

This chapter is intended to make the reader familiar with the topic of landscape evolution under river dynamics and the processes it involves, in terms of matter transportation and energy transformation. There is the description and the comparison of the main approaches adopted in scientific and technical disciplines for understanding and reproducing this phenomenon. Before concluding the chapter, the methodology adopted for the work described within this thesis is briefly introduced.

2.1 LANDSCAPE AND RIVERS EVOLUTION

Basic theoretical contents are given to depict the frame around this work.

As it was already explained in the introduction, the objective of this thesis is to approach the complex phenomena of landscape and river evolution through a simulation model based on optimality criteria. However, before focusing the attention on the model it is necessary to provide some basic knowledge about the phenomena themselves, in order to better understand the basic hypothesis and the features of the model.

A clear definition of landscape evolution is given by traditional geomorphology discipline, which states:

> landscape evolution describes exclusively time-dependent changes from rugged youthful topography, through the rounded hillslopes of maturity, to death as a flat plain. [see 41, p. 247]

It appears, from this definition, that the process of landscape evolution covers multiple scales, both in terms of space and time, during which the landscape modifies its shape, and therefore mass distribution, going through different chronological phases. It is a dynamic process that develops over geologic and human time scales too and it is driven by multiple agents. In fact, as Pazzaglia highlights in his 2003 paper, quoting a previous paper by Davis, many processes including "surface wash, ground water, temperature change, freeze-thaw, chemical weathering, root and animal bioturbation" [see 41, p.

251] contribute to shape the Earth landscape. However, it is possible to say that the following three factors are the most important categories of drivers:

- tectonic activities;
- interaction between soil and climatic and atmospheric agents;
- interaction between terrain and water fluxes.

Since the aim of this thesis is studying the just mentioned process of landscape evolution under the effects of river dynamics, the analysis is not going to deepen in detail the other factors shaping the landscape and our attention will be focused on the interaction between river networks and the terrain. It becomes then important to characterize river networks and their basins in relationship with the terrain they develop on and, for this purpose, Rodríguez-Iturbe et al.'s words look appropriate:

> well-developed river basins are made up of two interrelated systems: the channel networks and the hillslopes [...] Hillslopes are the runoff-producing elements which the network connects [see 55, p. 1095].

Considering that, it emerges that river networks formation and landscape evolution processes are strongly interdependent, therefore they cannot be independently explained. In simple words, landscape configuration is responsible for the formation of river networks and river networks are, in turn, responsible for shaping the landscape, interactively. This intense and continuous interaction rules the physics of the overall system (i. e. the combination of soil and river networks), causing:

- changes in mass distribution;
- energy transfer and transformation.

> As raindrops fall on a landscape, travelling toward the ocean, they mobilize surface-forming materials, such as sand and gravel, and dissipate their energy. Through this process, fluxes of the sediment-water mixture form and then move through their respective paths, i. e. streams or rivers. These fluxes exhibit spatially varying mass and energy distributions. [see 38, p. 684]

These two phenomena will be detailed in the following sections.

2.1.1 *Changes in mass distribution: the process of matter movement*

The first point of view our study of the phenomena starts from regards mass transfer and transportation: firstly their phenomenology is described, then the mathematical formalization of their main features is given.

2.1.1.1 *Phenomenology*

The water flowing onto the landscape moves a large amount of soils downstream.

Phenomena of matter movement which cause changes in soil mass distribution are usually grouped together under the term "solid matter transport". In particular, under this category, the following three sub-processes are grouped:

- erosion;
- matter transfer;
- sedimentation.

These three processes take often place sequentially and their driver is the action of a flowing fluid: a portion of soil is eroded (i. e. removed) by the flow, it is carried by the flow itself and then settles in a different place from the original one, through sedimentation.

The prolonged action of this erosion-sedimentation cycle, along thousands of years, shapes the landscape. In fact, when the water flows, nourished by raining events, and snow melting start assuming preferential paths on the hillslopes, the process of river channels formation and landscape evolution develops according to the following phases, well described by Liu and Lu [29]:

RAPID INCISION: the flow starts carving the terrain, forming V-shaped valleys;

WIDENED INCISION: flow incision goes on, together with landslides and avalanches, widening the valley;

DYNAMIC EQUILIBRIUM: channels assume a milder slope, the rate of sediment from upstream increases and the V-shaped valley becomes U-shaped.

The transition from V-shaped to U-shaped valley is well represented in figure 2.1.

Moreover, the result of erosion, transport and deposition is the typical concave shape of a natural river longitudinal profile: as represented in figure 2.2, its slope tends to decrease going from upstream to downstream.

Considering solid matter transfer in open water channels, it is possible to say that the dragging action of the flowing current acts on river bed and banks. As a consequence, the portion of matter removed can be transported by the flow alternatively:

Figure 2.1: On the left: V-shaped valley, Riobamba (Ecuador). On the right: U-shaped valley, Glen Geusachan (UK).

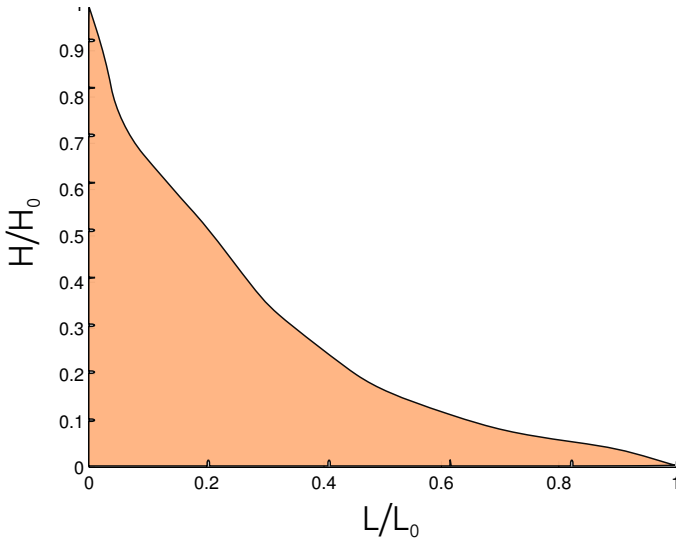

Figure 2.2: An example of concave river profile: the longitudinal profile of Suceava river (Romania). H is the stream altitude at the point of measurement, H_0 is the stream altitude from the river mouth at the headwater, L is the stream distance from the river mouth at the point of measurement, L_0 is the stream distance from the river mouth at the headwater.
Data source: [48].

- as suspended in the flow;
- as dragged on the bottom of the channel.

Moreover, going more in detail, a channel has a specific sediment transport capacity: if the rate of sediment is below this threshold, no sedimentation happens, but

> if the rate of sediment supply is larger than the capacity of the channel to move it, the surplus sediment drops out and begins to cover the channel bottom. [see 9, p. 5]

2.1.1.2 *Mathematical modeling*

Existing mathematical models focus on different aspects and processes of the whole system.

Even if the previous description of erosion, solid matter transport and sedimentation appears simplified, it should be already clear that those processes hide a great complexity, given the number of elements that take part in them and their interactions. In fact, they depend again on both:

- factors related to WATER FLOWS. They include precipitation abundance and its transformation into runoff;
- factors related to the SOIL. They include shape factors, like slope and side length, structural elements (i. e. kind of soil, texture, grain size and permeability) and other factors (like vegetation, soil usage and agricultural cultures).

For this reason, great effort was dedicated by hydrogeologists in providing a mathematical description of erosive processes. In general the goal is quantifying the rate of erosion and the rate of solid matter transported. A complete listing and analysis of the existent formulas and methods of evaluating them is not the objective of this thesis. In this section it is just important to understand which factors are involved and how the process of solid matter transport can be formalized. Therefore, not all the proposed mathematical formulations are described here, but only their relevant goals and some examples, without making the dissertation too heavy.[1]

Specifically, it is possible to distinguish among different models, for solid matter movement description, depending on their target:

MODELS FOR HILLSLOPE EROSION: they consider the mountainside scale and try to link the loss of soil on the mountainside to the amount of matter which reach the outlet of the basin. They allow the evaluation of the *Sediment Delivery Ratio* along a time horizon, as formalized with equation (2.1)

$$SDR = \frac{P}{A} \tag{2.1}$$

1 For the reader willing to deepen her/his knowledge about sediment transport, the following books are suggested: J.R.L. Allen. *Principles of Physical Sedimentology*. Allen & Unwin London, 1985 [1] and W.H. Graf and S. Altinakar. *Fluvial Hydraulics: flow and transport processes in channels of simple geometry*. Wiley, 1998 [11].

where:

- SDR is the sediment delivery ratio;
- P is the sediment production;
- A is the soil loss.

Such kind of models can be either physically based, requiring the use of differential equations, or empirical ones, like the *Universal Soil Loss Equation* and its newer versions, which are the most used.[2]

MODELS FOR BANK EROSION: they are very important in order to quantify bank erosion and be able to build effective embankments. Specifically, they usually follow these three steps:

1. a threshold parameter ϕ_c, called critical Shields' parameter is evaluated thanks to Shields' abacus, as
$$\phi_c = f(Re) \tag{2.2}$$
where Re is Reynold's number;
2. ϕ, which is Shields' parameter for the given river and flow, is evaluated as
$$\phi = \frac{\tau}{(\gamma_s - \gamma)d} \tag{2.3}$$
where:
   - τ is the shear stress;
   - γ_s is the specific weight of the sediment;
   - γ is the specific weight of the fluid;
   - d is the particles diameter.
3. ϕ_c and ϕ are compared: if the value of ϕ is over ϕ_c, bank erosion happens.

MODELS FOR MATTER TRANSFER IN RIVERBED: their aim is to quantify the amount of solid matter transported by the water flowing in the channel. As already said, it depends both on the characteristics of the water flow and the solid matter features. It can be quantified adopting three types of approaches, i. e. a physical based one, a probabilistic one or an empiric one; here, only the formulation given by the first approach is quoted, in order to understand the contributing elements.[3]

2 For a reference, see W. H. Wischmeier, D. D. Smith, et al. "Predicting Rainfall Erosion Losses-A guide to conservation planning." In: *Predicting rainfall erosion losses-A guide to conservation planning* (1978) [70].

3 For references on the probabilistic and empiric approach, see, respectively, H.A. Einstein. *The Bed-load Function for Sediment Transportation in Open Channel Flows*. Technical bulletin (United States. Dept. of Agriculture). U.S. Department of Agriculture, 1950 [9] and E. Meyer-Peter and R. Müller. "Formulas for bed-load transport." In: *Proceedings of the 2nd Meeting of the International Association for Hydraulic Structures Research*. International Association of Hydraulic Research Delft. 1948, pp. 39–64 [32]

The just mentioned formulation is given by DuBoys [8], as follows:

$$q_s = n\varepsilon\frac{(n-1)v_s}{2} \tag{2.4}$$

where:

- q_s is the bed material load per unit width;
- ε is the thickness of material of the riverbed;
- n is the number of layers considered for dividing the bottom of the riverbed;
- v_s is the velocity of each layer.

Moreover, since, as previously said in this section, sediments are transported both as suspended in the flow and over the river bed, a more detailed analysis would also evaluate the amount of suspended sediments as a fraction of the total rate of sediment load.

As it was said at the beginning of section 2.1, landscape evolution under river dynamics entails two processes (i. e. matter transport and energy transformation). The principal concepts related to matter transfer were just treated, therefore it is time to devote the same effort for understanding the ones related to energy.

2.1.2 *Energy and entropy-related issues in landscape evolutionary process*

> The only useful energy nature provides to a unit mass of raindrops falling on the slope of a watershed is its potential energy above a datum, say, the sea level. [see 71, p. 311]

Potential energy of raindrops is converted to kinetic energy and friction loss. This is the driving force of erosion.

This sentence written by Yang in his 1971 article, expresses well and simply the starting point for energy-related analysis when speaking about landscape evolution connected to river development. In fact, it is possible to affirm that the potential energy and its dissipation by friction is the source of landscape evolution. When raindrops start flowing on the hillslopes following their way toward the basin outlet, their potential energy is converted into kinetic energy and friction loss, and the work produced shapes the terrain with the dynamics described in the previous sections, forming channels and river networks. As a consequence, since the current landscape is the result of the action of raindrops (and consequently rivers) flowing on it for millions of years, it is also the result of their energy expenditure. Starting from this statements, the following concepts become relevant:

- Energy expenditure;
- Entropy;

They are going to be treated in the following two paragraphs.

2.1.3 *Energy expenditure*

The amount of energy spent by water flows is assessed by evaluating friction loss and geomorphological work.

The process of potential energy transformation explained in the previous paragraph is the result of the movement of water flowing onto the soil, therefore it is driven by the forces allowing the flow itself. As Rodríguez-Iturbe et al. [55] explain in their 1992 paper, the forces driving water flows are the gravity force, in one direction, and the the resistant force due to the soil friction, in the opposite direction:

WEIGHT: its component along the slope is the force which causes the flow of water. It can be expressed as F_w in equation (2.5),

$$F_w = \gamma d L w S \tag{2.5}$$

where:

- γ is the specific weight of the fluid;[4]
- d is the channel depth;
- L is the channel length;
- w is the channel width;
- S is the slope.

RESISTANT FORCE: assuming as a simplification a rectangular section of the channel, it can be expressed as

$$F_r = \tau(2d + w)L \tag{2.6}$$

where τ is the stress per unit area and $(2d + w)L$ represents the wetted area of channel.

Considering the two just mentioned forces, it is possible to quantify the rate of energy expenditure for a channel having length L and discharge Q. In fact, when the water flows in the downstream direction, its initial potential energy moves into kinetic energy while part of it gets lost because of the interaction with soil and resistant friction force. Assuming that water flows with constant velocity, an equilibrium between the two forces will exist, therefore $F_w = F_r$. Equalling equation (2.5) and equation (2.6), one obtains:

$$\tau = \gamma S R \tag{2.7}$$

being $R = \frac{A}{P_w}$ the ratio between wetted area A and wetted perimeter P_w i. e. the hydraulic radius. Since, as Rodríguez-Iturbe et al. state, in the case of turbulent incompressible flow the boundary shear stress τ can be defined as

$$\tau = C_f \rho v^2 \tag{2.8}$$

4 $\gamma = 9810 N/m^3$ for water with temperature of 4°C

where C_f is a dimensionless coefficient of resistance, equalling equation (2.7) and equation (2.8) , it is possible to obtain the rate of energy expenditure per unit weight of fluid per unit length of channel as expressed in equation equation (2.9) :

$$S = \frac{C_f v^2}{Rg} \tag{2.9}$$

It is now easy to understand that the rate of energy expenditure for a channel having length L and discharge Q will be:

$$P = C_f \rho \frac{v^2}{R} QL \tag{2.10}$$

In addition to this expenditure there is a second term representing the energy expenditure for the "maintenance of the channel" i. e. the work carried for transporting sediments and caring the channel [55]. This second term depends on a coefficient K related to the soil, on the shear stress τ^m with m constant and on the wetted perimeter P_w. Adding this, completely define the ENERGY EXPENDITURE of a channel as:

$$P = C_f \rho \frac{v^2}{R} QL + K\tau^m P_w L \tag{2.11}$$

If some energy concepts related to river dynamics have just been explained, also the following one, i. e. entropy, must be addressed in order to introduce the concept of minimum energy expenditure which will be fundamental with respect to overall objective of the thesis.

2.1.4 *Entropy*

Entropy is a concept that can be applied to river systems in order to improve their understanding.

The concept of entropy in landscape evolution was first introduced by Leopold and Langbein in 1962, and then again developed by Yang in 1971. Basically, the concept of entropy in river evolution is related to the same concept in thermodynamics. There, entropy is defined as follows:

$$\Phi = \int \frac{dE}{T}, \tag{2.12}$$

being T the absolute temperature and E the thermal energy per unit mass of substance.

According to Leopold and Langbein and Yang, it is possible to imagine an analogy between thermodynamics and river elements:

- elevation Z in river evolution assumes the same role of the temperature in thermodynamics;
- potential energy loss H in river evolution assumes the same role of the thermal energy in thermodynamics.

It becomes licit to redefine equation (2.12) as follows:

$$\Phi = \int \frac{dH}{Z_m} \tag{2.13}$$

being Z_m the average total fall from the beginning of first order stream to the end of the m-th order stream.[5]

Basing their analysis on this analogy, the mentioned authors assert that a system moves toward stationarity with a minimum rate of production of entropy. As a consequence, it is possible to write equation (2.14) , which represents the concept behind the one of minimum energy expenditure in river evolution deepened in section 2.3 .[6]

$$\frac{d\Phi}{dt} = \text{minimum} \tag{2.14}$$

2.2 STATE OF THE ART ANALYSIS APPROACHES

Studies about landscape evolution try both to understand the system processes and to provide reliable management tools.

Now that the main drivers and features of the complex phenomenon of landscape evolution under river dynamics should be clear, some questions rise:

1. Who is interested in studying this evolutionary process? and why?
2. How is it possible to describe it in a complete way?

2.2.1 *Goals intended to be reached*

The answer to the first question should be accurately balanced, since it constitutes part of the motivation for having carried out this work and, also, the perspective for future research or work this thesis would be addressed to. Fortunately, the cross analysis of the existent literature helped the authors of this thesis to provide an answer to this question. It is possible to say that two kinds of interests drive the research on the considered topic: scientific and technical.

In fact, the pioneers of this field of study were hydrologists and geomorphologists who were attracted by the regularity of some patterns in natural landscapes and started to study landscape and river evolution "for the sake of knowledge". The first interest was then focused on understanding the processes going on in the nature, in order to find some general laws formalizing them and produce descriptive models. Any further improvement in these kind of models would enrich the knowledge available to the scientific community.

5 The ordering procedure to classify river branches will be introduced in subsection 3.4.1. Here is enough to know that the streams originating from springs have order 1 while streams closer to the outlet of a river have higher order.

6 The term "minimum" has to be intended as the minimum compatible with the external conditions.

On the other side, the development of technical disciplines related to goals such as management of natural resources (especially water) or soil protection needs models reproducing landscape and river evolution. With this kind of tools, the following issues can be exploited:

- to forecast the dynamics of a landscape and support decision making processes in planning strategies and localization of infrastructures (such as dams, artificial river banks, and so on);
- to help the forecast of the landscape response and resilience following extreme events;
- to better know and manage the availability of resources of a territory.

If the interests in studying landscape and river evolution appear to be many, the second question still remain unsolved. So, how is it possible to describe that processes in a complete way?

2.2.2 *Methodologies to reach the goals*

The answer is neither unique nor simple. In scientific and technical literature on the topic, different approaches to study landscape and river evolution processes can be found. They differ by dimension of the study domain, by scale of the processes faced, by goals achieved ans so on.

In particular, the following different categories of approach were identified to better explain the main differences:

- physically-based approach;
- optimality-based approach and probability-based approach.

2.2.3 *Physically-based approach*

At the scale of river sections, this approach allows to reproduce in a model the state of the art knowledge of the processes.

Physically based models approach the topic of landscape evolution under river dynamics with a descriptive perspective. They try to describe the current physical processes i. e. water flow and matter transfer, and then to reproduce them using the parameters through which they are characterized. They consider in the most complete way as possible the processes and the elements involved in water and matter movement.

Usually, as also Pazzaglia asserts, "Physical models typically isolate one part of the geomorphic system" [see 41, p. 257], therefore they are usually built on a smaller scale than the one of a river network. They focus on parts of a river channel, between sections as the one represented in figure 2.3, to study what happens in terms of water and matter movement when the flows goes from the upstream one to the downstream one.

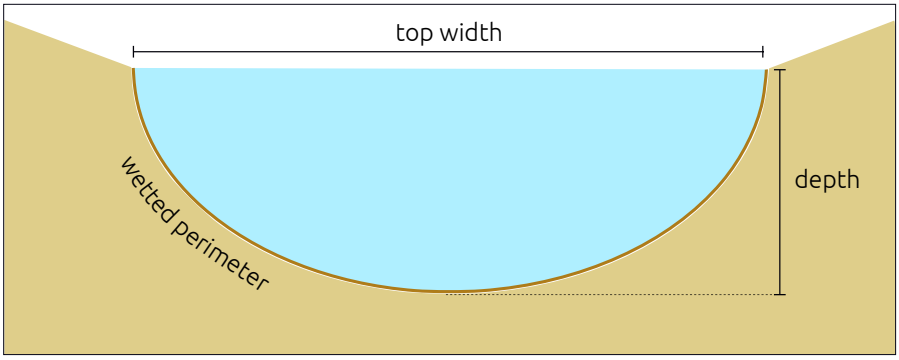

Figure 2.3: Sketch of river section.

To do this, they make use of physical laws, when they are known, and fill the unknown with empirical relations that contains parameters as the ones quoted in the equations mentioned in subsection 2.1.1. The best example for that is given by Nanson and Huang in the following three equations [35]:

FLOW CONTINUITY:

$$Q = WDV \tag{2.15}$$

FLOW RESISTANCE:

$$V = \sqrt{\frac{8}{f} g R S_f} \tag{2.16}$$

SEDIMENT FLUX:

$$\frac{Q_s}{W} = c_d(\tau_0 - \tau_c)^{1.5-1.8} \tag{2.17}$$

Looking at the equations it is possible to identify parameters related both to the water flow, channel section and soil characteristics, but especially to their interaction. In fact, there is:

- channel width W, average depth D, hydraulic radius R and slope S_f describing the section;[7]
- average flow velocity V and discharge Q characterizing the water flow;
- friction factor f and a coefficient c_d linked to the grain size of the soil;
- flow carrying capacity for sediment discharge $Q_s c$, shear stress τ_0 and critical shear stress τ_c characterizing the interaction between the fluid component and the solid one.

2.2.3.1 *Strengths and limits of physically-based approach*

Physically-based approach allows deep understanding of sub-processes in landscape evolution but fails to deal with basin and network scale modeling.

The physical base of this approach allows to build descriptive and management models that are justifiable and reliable. The process of landscape evolution is rationally divided into sub processes, which are analyzed and explained and eventually recomposed into the whole system by explicitly studying their interrelations. The physical base also means that the quantities involved have a real counterpart, which can be measured directly to calibrate the models. The goal achieved is a scientific and rational understanding of the phenomena involved in landscape evolutions.

On the other side, the use of this approach at the basins scale is not common, even if possible. As Pazzaglia says, "Physical models [...] rarely show the behavior of an alluvial channel, for example, in the context of broader landscape change" [see 41, p. 257]. Models based on physical approach are usually applied on a segment of a river channel between two sections, whose geometry and characterizing parameters must be measured. Recalling equation (2.11) makes clear the difficulties related to the number of parameters.

$$P = C_f \rho \frac{v^2}{R} Q L + K \tau^m P_w L \tag{2.18}$$

A model applying this equation needs a value for C_f and K, the geometry of the river for each section the simulation is performed into and a coupled hydraulic model to evaluate v, P, R and Q. In the absence of measures for these quantities, a mathematical calibration can be challenging because of the range they can assume. Also, if any of these values is changing over time, the model needs to know it. Moreover its hydraulic part and the geometry of the channel are interconnected and, therefore, the additional degrees of freedom must be tackled with extra relations.

This characteristics heavily limited the use of physical based approach in landscape evolution models at basin scale.[8]

Before introducing the second category of study approach, i. e. optimality-based approach and probability-based approach, some other concepts are introduced in the next paragraphs.

2.3 THE IDEA OF A LEAST ACTION PRINCIPLE

The optimality based approach is the idea guiding researchers that deal with landscape evolution at a basin scale.

It has been shown the strength of the physical approach to understand landscape evolution, but also its limitation, comes when modeling at basin scale. It should be underlined that the scale and choice

7 with $D = \frac{A}{W}$ being A the wetted area (blue in figure 2.3), w the width of the channel measured at the top of the section, and $R = \frac{A}{P}$ being P the wetted perimeter.

8 Although one example can be found in [42] and its bibliography references.

of modeling approaches closely reflect the targets of the research performed, e. g. to study river system resilience to climatic changes. For such a goal, equation (2.11) needs to be deeply simplified.

This process of reduction lead Leopold and Langbein [28], Yang [71], Rodríguez-Iturbe et al. [55] and many others to deepen the study of energy expenditure and minimum entropy at river basin scale. They came up with different mathematical formalizations of an optimality principle, in accordance with the specific topic of their research. But they share one clear idea: river systems follow a kind of optimality.

This idea will be clarified in the following sections.

2.3.1 *Least action principle*

Reductions of physical laws to scale up the study of river systems at a basin level lead to the idea of an optimal principle.

Given the fact that, according to Leopold and Langbein and Yang, equation (2.14) represents the law governing the evolution of a system toward its most probable state, it is also possible to state the following sentence:

> The river channel has the possibility of internal adjustment among hydraulic variables to meet the requirement for maximum probability, and these adjustments tend also to achieve minimization of work. [see 28, p. A7]

This minimum work condition is also called Least Action Principle LAP.

Theories which support the LAP affirm the idea that a river, and consequently the landscape, evolves in a way that its energy expenditure is minimum. Nevertheless, there is disagreement on how to traduce in mathematical terms the concept of minimum energy expenditure when speaking of river evolution, since equation (2.11) may be reduced in alternative ways according to the research target, e. g. if intended to be applied to the network as a whole or to study the three dimensional structure of a landscape. As a consequence, scientists have been focusing on the research for a proper formalization of the criterion to be minimized. The result of their activity is a great number of proposed criteria expressing the LAP with different perspectives. So far, none of them is satisfactory to fully reproduce the complexity of a river network while capturing its 3D structure.

Many of them were listed and explained by Paik and Kumar in "Optimality approaches to describe characteristic fluvial patterns on landscapes" and by Paik in "Search for the optimality signature of river network development." The ones closely related to this work will be shown below.

2.3.1.1 *Stream Power*

A first example of an optimal principle as a reduction of the physical laws is the so called *Unit Stream Power*, formulated by Yang [72] directly from equation (2.14) as:

$$\frac{dY}{dt} = VS = \text{minimum} \tag{2.19}$$

where:

- V is the average flow velocity;
- S is the slope.

and entropy Φ is substituted with Y, the average fall of a stream, since they are proportional.

2.3.1.2 *Principles of energy expenditure*

We are now ready to present the optimal principle used in this thesis. It has been proposed by Rodríguez-Iturbe et al. in "Energy Dissipation, Runoff Production, and the Three-Dimensional Structure of River Basins," a paper that has become a milestone of the discipline and is the reference for other studies.[9]

In the paper, Rodríguez-Iturbe et al. enunciate three specifications of the LAP that, according to their theories, are respected by river networks.

MINIMUM ENERGY EXPENDITURE IN ANY LINK According to this principle, energy expenditure is at its minimum in any link of the river network.

EQUAL ENERGY EXPENDITURE According to this principle, the energy expenditure relative to a unit area is constant anywhere in the network.

MINIMUM TOTAL ENERGY EXPENDITURE This principle expresses the idea that the sum of the energy expenditure of all the links in a network should also be a minimum.

The paper authors used this three principles to identify a mathematical formalization of the LAP they used to describe the planar structure of river networks. The second principle ensures that

$$P_1 = \frac{P}{P_w L} = \text{const} \tag{2.20}$$

and being $v = \frac{Q P_w}{A}$ and $\tau = C_f \rho v^2$, equation (2.11) becomes

$$P_1 = C_f \rho v^3 + K C_f^m \rho^m v^{2m} = \text{const} \tag{2.21}$$

9 It has almost 180 citations according to Google Scholar and 142 according to Web Of Knowledge

which means the velocity is constant throughout the network, being constant all the other quantities in the equation.

Substituting the width $w = \frac{Q}{vd}$ and grouping all the constants in equation (2.21), the following expression is obtained:

$$P = \frac{QL}{d} \times \text{const} + dL \times \text{const} \tag{2.22}$$

According to the first principle, in a link of the network P must be at its minimum. Therefore, it should be that $\frac{dP}{d(d)} = 0$, which implies $Q \propto d^2$. Substituting this result in equation (2.22) , the optimal energy expenditure can be rewritten as:

$$P = kQ^{0.5}L \tag{2.23}$$

Finally according to the third principle, the energy expenditure in the river network as a whole should be a minimum, i. e. the sum over the N links of the network of their energy expenditure should be

$$P = k\sum_{i=1}^{N} Q_i^{0.5}L_i = \text{minimum} \tag{2.24}$$

The different formulations of the LAP are in contrast one another.

It is possible to comment that, even if all the three principles express the LAP, they are not equal, i. e. the optimization of one of them not necessarily implies the optimization of the others. This is stated in the paper by Rodríguez-Iturbe et al. [55] and suggests the idea that these principles captures opposite "parts" of the LAP. As we will see in the next chapters, this opposition is called conflict in the system management field which usually deals with opposite criteria. The meaning is that the fulfillment of one of them is in contrast with the fulfillment of one or more of the others. This point confirms the presence of different proposed criteria and the debate around the different listed principles of minimum energy expenditure is so open.

In the next paragraph the applications of these principles are shown and contextualized. The reader will be guided through the application of optimal principle in landscape evolution. We will assess different methodological approaches retrieved from the literature, in order to introduce and clarify the purpose of this thesis.

2.3.2 *Probability-based approach*

According to this category of approach, landscape and rivers evolve in order to move toward their most probable state. The definition of most probable state is close to the concept of optimality, therefore we have listed this approach here.

The first, and probably most important work in this direction is represented by the one carried out by Leopold and Langbein in 1962. In their paper, the authors assert that river networks self-organize in

order to reach the configuration with the most probable distribution of energy, which, as shown in subsection 2.1.4 "represents maximum entropy" [28].

In particular, they simulated a random-walk model for reproducing the longitudinal profile of a river. It showed that, on average, the profiles obtained as the output of the model have a concavity comparable to the one visible in natural rivers. They also simulated another constrained random-walk model for reproducing the 2D pattern of an entire river network. They assert that "random pattern represents a most probable network in a structurally and lithologically homogeneous region" [see 28, p. A15].

Despite the results, as Perron et al. states,

> Such studies have provided new insights into the structure of natural river networks, but cannot directly relate river network form to the erosional mechanisms that shape the topography [see 43, p. 100].

2.3.3 *Optimality-based approach*

Approaches based on the idea of the LAP more than the probability based one, assume that river networks evolve according to a particular criterion corresponding to the minimization of a certain mathematical formulation. Accordingly, river and landscape weathering can be simulated by solving a minimization problem, also called optimization problem. The choice of the criterion to be optimized becomes the initial assumption. Then, the comparison between natural river networks and optimized ones verifies the correctness of this initial assumption. The smaller scale phenomena e. g. rate of erosion, channel dimensions, grain size dimension and others, are not detailed as in the physical-based approach. The only thing that matters is the configuration of the landscape and the network above it to quantify the selected criteria.

2.3.3.1 *Total energy expenditure and OCN*

One important work within this approach is represented by the already mentioned "Energy Dissipation, Runoff Production, and the Three-Dimensional Structure of River Basins" by Rodríguez-Iturbe et al. and the subsequent [51]. They tried to test the principle of minimum total energy expenditure showed in equation (2.24) on a 2D network, in the following way:

A. an initial network is perturbated with random noise;

B. step 1 is repeated many times, in order to have many sample networks;

c. for each sample network the value TEE of total energy expenditure is computed as in equation (2.24)

$$P = k \sum_{i=1}^{N} Q_i^{0.5} L_i \tag{2.25}$$

d. the network with minimum value of E is selected and evaluated according to Horton's bifurcation ratio and length ratio indexes.[10]

The results of the combination of the three principles of energy expenditure into equation (2.25) results in a unified picture of the most empirical findings related the structure of river networks. In fact,

> it is concluded that a comprehensive framework for the investigation of geophysical structures, different from their mere geometrical description or from modeling of the growth process responsible for their construction is achieved through OCN approaches. [see 51, p. 1645–1646]

> Also, the geomorphological description of OCNs has been studied in detail, revealing an almost perfect match with well-known empirical or experimental result. [see 52, p. 2194]

Nonetheless, as recognized by Paik [38], the approximation of a landscape with a 2D network lacks the direction gravity acts on. The good results from OCNs were possible only because the elevation, even if is not explicitely included into TEE (equation (2.25)) it is considered by the river network setup, which organizes values of Q according to it. In order to develop a framework to fully study river networks and landscape features, it is required to completely include the third dimension: elevation.

2.3.3.2 *Genetic Landscape Evolution*

After the previously described work, another important step in exploring this modeling approach is constituted by the work performed by Paik in 2011 [38], who tries to include the third dimension i. e. elevation, in order to extend the application of the approach. As in the previous case, a single objective is considered: the one of minimum TEE, defined as the above equation (2.24).

Paik comments his results saying that "simulation results [...] exhibit a self-similar tree structure of natural river networks" [see 38,

10 These indexes are common measure of river networks. For a wide description of Horton ratios and other hydrological indexes, see chapter 3 .

p. 690], but "Optimized river networks show no pattern in their longitudinal profile" [see 38, p. 690], so the description of the third dimension remains still partial. In fact the longitudinal profile of a river shows a typical concave feature as in figure 2.2 . The profile should be steeper for highest elevations and more flat as the river approaches its delta. Missing this characteristic from Paik's results means that both (or either) the model and the proposed criteria are not able to fully understand the complexity of the evolutionary process.

2.4 A MULTI-OBJECTIVE FRAMEWORK

Given the theoretical framework and the premises explained in the previous sections, it is necessary now to clarify the objective of this thesis, already mentioned in the introduction. The general, OVERALL OBJECTIVES of disciplines studying landscape and river evolution are to try to accurately describe that process and being able to reproduce it with modeling tools. As a sub-objective, we identify a more SPECIFIC OBJECTIVE: testing optimality principles followed by whole landscape evolution through a multi-objective approach based on a 3D representation.

In fact, it appears from the assessment of the existent study approaches, performed in section 2.2 , that optimality principles approach is promising in terms of scalability and can be applied successfully to the whole basin. It seems so that as for the methodology, the approach based on optimality criteria represents a good compromise between accuracy and complexity. Nevertheless, as it is also confirmed by the considered literature, at present, a single, satisfactory, formulation of the optimal principle has not been formulated yet: the already proposed optimality criteria, as they are considered separately, partially describe the process e. g. Paik's proposed TEE criterion was not able to make his model reproduce the typical concave profile of main network channels. Given the previous considerations, the question we would address is: may a multiple-objective approach explain more exhaustively the considered process of landscape evolution?

This does not imply that landscape and river networks evolve according to multiple criteria; instead, it means that, given the proven limits of single-objective models, a multi-objective approach would be a more complete analysis tool and help to find the formulation of the optimal principle followed by nature.

In order to pursue the declared specific objective, a framework for testing multiple optimality criteria was built by the authors of this thesis. It will be described in detail in the following chapters, but before entering the technical issues, the optimality criteria which will be considered are now listed and defined.

2.4.1 *Optimality principles: TEE, EEL, EE, EEE*

Four optimality principles have been chosen to be minimized as objectives in the multi-objective framework analysis that will be described in the next chapters. The four objectives were chosen mainly on the basis of the already cited Rodríguez-Iturbe et al.'s and Paik's articles [55] [39]. Each of them is now described and the reason for the choice is justified:

MINIMUM TOTAL ENERGY EXPENDITURE It represents the third criteria expressed in [55], as already explained in subsection 2.3 . It is the same objective used by Paik in [38]. It express the minimization of energy expenditure by the river network as a whole. Its formulation is obtained from the criterion expressed in equation (2.24) :[11]

$$\text{TEE} = \min\left(\sum_{i=1}^{N} Q_i^{0.5} L_i\right) \tag{2.26}$$

where N is the total number of links of the network. It has the following units:

$$\text{TEE}[=]\sqrt{\frac{m^3}{s}}m \tag{2.27}$$

This criteria has proven to be able to reproduce the 2D structure of river networks in [55], [51] and [38].

MINIMUM ENERGY EXPENDITURE IN ANY LINK Since Rodríguez-Iturbe et al. [55] state that the energy expenditure should be minimum not only in the network as a whole, but also in any link of the network, this second objective is introduced:

$$\text{EEL} = \min\left(\text{Var}(\mathbf{Q^{0.5}L})\right) \tag{2.28}$$

where N is the total number of links of the network and $\mathbf{Q^{0.5}L}$ is the vector containing the product $Q_i^{0.5} L_i$ for every i-th link, with $i \in [1 : N]$. Being the minimization of a variance, it is dimensionless.

This objective has to be considered jointly with TEE: by itself it does not minimize the energy expenditure in any link of the network, but, by imposing that the TEE should be distributed equally in the network, it helps reaching the minimum in any link. On the other hand, it also means that each link of the network should be able to reach the same level of energy expenditure.

11 Constant k does not affect minimization, therefore is not reported in equation (2.26)

MINIMUM ENERGY EXPENDITURE PER UNIT AREA This third objective corresponds to the minimization of the energy expenditure per unit area in the whole network.

Rewriting the energy expenditure per unit area of the channel P_1 in equation (2.21) as

$$P_1 = \frac{\rho g Q S}{w + 2d} + K C_f^m \rho^m \nu^{2m} \tag{2.29}$$

and recalling that the first principle $\frac{dP}{d(d)} = 0$ implies $d \propto Q^{0.5}$ and $w \propto Q^{0.5}$, one can write

$$P = c_1 Q^{0.5} S + c_2. \tag{2.30}$$

For a given flow condition c_1 and c_2 are two constants and therefore

$$Q^{0.5} S = \text{const} \tag{2.31}$$

Principles of this form have been found also by studies on stable sections in rivers where is stated the idea that this quantity should be also a minimum [35].

Finally we are ready to express the EE as follows:

$$EE = \min \left(\sum_{i=1}^{N} Q_i^{0.5} S_i \right) \tag{2.32}$$

where N is the total number of links of the network. It has the following units:

$$EE[=] \sqrt{\frac{m^3}{s}} \tag{2.33}$$

It is hoped that the explicit introduction of slope into the objective formulation helps the generation of concave profiles for the main channels of the network.

EQUAL ENERGY EXPENDITURE PER UNIT AREA This objective interprets the principle of equal energy expenditure proposed by Rodríguez-Iturbe et al. [55]. Since, as written in equation (2.31) it should be verified that $Q_i S_i = \text{const}$ over the network links, the same condition can be imposed by writing:

$$EEE = \min \left(\text{Var}(\mathbf{Q^{0.5}S}) \right) \tag{2.34}$$

where $\mathbf{Q^{0.5}S}$ is the vector containing the product $Q_i^{0.5} S_i$ for every i-th link, with $i \in [1 : N]$. Again, since the objective is the minimization of a variance, it is dimensionless. As for TEE and EEL, this objective should be considered together with EE. It is closer to the translation of a constraint into an objective than an objective by itself.

Wrapping up the content of this chapter, the basic knowledge about landscape evolution under river dynamics was provided. Then the principal methods for analyzing this phenomenon are assessed and it has been presented the framework proposed in this thesis, together with its aim and the objectives considered. The formalization of the mentioned framework is going to be explained in the next two chapters.

3

TESTING OPTIMALITY PRINCIPLES: A FRAMEWORK

Order and simplification are the first steps toward the mastery of a subject — the actual enemy is the unknown

— Mann and Woods, *The magic mountain*, 1924

The idea guiding this work was exposed in the previous chapter, but now it requires a formalization effort in order to be implemented and used. The formalization splits the methodology, adopted to verify the hypothesis, from the hypotheses to test itself and, hopefully, constitutes the second contribution of this thesis to the field.

As a first stage, the problem is formalized in a verbal way, then it is translated into mathematical terms. That constitutes the basis to identify the steps required to test the hypotheses, which are explained sequentially. Secondly, the steps are abstracted from the problem, becoming the framework which this thesis is addressed to. The framework is then critically discussed, in order to underline new aspects and opportunities of improvement.

3.1 PROBLEM FORMALIZATION

The main hypotheses we want to test with this work are:

LAP principle and its formulations are tested through the framework built during this thesis work.

- landscape evolution under river dynamics may be explained as if it follows an optimality principle;
- this unique principle might be discovered by testing many formulations of LAP.

These hypotheses imply that it is accepted as true that river evolution follows an optimality principle, but that none of the optimality principles tested so far is capable of properly reproducing the rivers behaviour. Therefore, the proposed solution is to test many principles and analyze the conflicts that arise among them, in order to underline some of the characteristics of the real principle.

3.1.1 *Mathematical formalization*

It is now necessary to redefine what landscape evolution and river dynamics are, in order to translate the above sentences in a mathematically treatable way.

3.1.1.1 *Landscape entities*

A landscape may be represented as a function of two space variables, i. e. two coordinates:

$$z = f(x, y) \tag{3.1}$$

where z is the elevation at the point defined by (x, y). The water flow over this landscape may be represented by a two-dimensional vector field, being $\mathbf{q}(x, y)$ the discharge per unit of contour length and being its direction parallel to the gradient vector associated to equation (3.1):

$$\mathbf{q} \propto -\nabla f = -\left(\frac{\partial f}{\partial x}\hat{\imath} + \frac{\partial f}{\partial y}\hat{\jmath}\right). \tag{3.2}$$

Mass conservation principle applied to the flow of water leads to

$$\nabla \mathbf{q} = p(x, y) - \frac{\partial d}{\partial t} \tag{3.3}$$

where $p(x, y)$ is the rainfall excess rate and $\frac{\partial d}{\partial t}$ represents the partial derivative of flow depth over the landscape with respect to time. In this thesis, a steady state solution is searched for, and therefore $\frac{\partial d}{\partial t} = 0$ and $\nabla \mathbf{q} = p(x, y)$.

Similarly to the water flow, also the flow of sediments may be modeled with a vector field $\mathbf{q_s}(x, y)$ parallel to $\mathbf{q}$. Mass conservation on sediments transportation leads to

$$\nabla \mathbf{q_s} = U(x, y) - b_t \tag{3.4}$$

where $U(x, y)$ models the rate of tectonic uplift and b_t is the rate at which bedrock height or soil depth change in (x, y). b_t may be either negative or positive and represents deposition or erosion caused by river dynamics. This entities will be deepened later and their inclusion into the model will be explained.

3.1.1.2 *Precipitation*

Precipitation $p(x, y)$ is called effective precipitation[1] and actually is

$$p = f(x, y, t, \ldots) \tag{3.5}$$

depending on other characteristics such as temperature, permeability, etc. . . . Given the focus of this work, we simplify the above expression by writing the average value as

$$p = \bar{p} = \mathbb{E}[p(\cdot)] \tag{3.6}$$

1 In hydrology, according to the United States Geological Survey (USGS) definition, « Effective precipitation (rainfall) [is] that part of the precipitation that produces runoff.» [26], i. e. the precipitation in excess of infiltration capacity, evaporation, transpiration, and other losses.

and we will use an unique value of precipitation for the whole modeled landscape.

Function $f(\cdot)$ in equation (3.1) is unknown, probably not linear, therefore its values will not be searched in a mathematical way. Instead, we will identify this function with a look-up table[2]. This will be further explained in the paragraph about discretization, in subsection 3.2.1 .

3.1.1.3 *Optimal landscape*

According to the hypothesis that rivers follow optimality principles, it is possible to write

$$f(\cdot) = \arg \min_{f(\cdot)\in F(\cdot)} g(x, y, z) = \arg \min_{f(\cdot)\in F(\cdot)} g(x, y, \bar{p}, f(\cdot)) \tag{3.7}$$

where $g(\cdot)$ is the mathematical formulation of the optimality principle[3]. The same hypothesis ensures that

$$\exists!\ f(\cdot) \in F(\cdot) \mid f(\cdot) = \arg\min g(x, y, \bar{p}, f(\cdot)) \tag{3.8}$$

The identification of the above equation (3.8) , given a guessed $g(\cdot)$ function, will be the scope of this thesis.

Given the problem as it has been formalized in the first paragraphs of this chapter, it is now possible to describe the macro-elements which compose the framework for testing optimality principles in landscape evolution under river dynamics. They are the following three:

THE MODEL: it is the part of the framework responsible for the evaluation of $g(x, y, f(\cdot))$. It is described in section 3.2;

THE OPTIMIZATION: it is the phase of the framework responsible for the identification of $f(\cdot)$. The methodology is characterized in section 3.3;

THE EVALUATION THROUGH NATURALITY INDEXES: it is the part of the framework responsible for the assessment of the outputs provided by the previous two. Its features are described in section 3.4.

3.2 THE MODEL

The model extracts drainage networks from a landscape model and evaluates the values of the optimality principles to test.

From this point further, we will refer to the model meaning the implementation of the evaluation of $g(x, y, f(\cdot))$ as defined in equation (3.7). All the $g(\cdot)$ functions we evaluated require some common hydrological variables, like discharge or drained area. As a consequence, the evaluation is split into four steps:

2 i. e. a finite form of function in which a certain number of tuple z, x, y is known and represented in a four dimensions numerical matrix.

3 or the cost function, using the jargon of control theory.

A. extraction of the drainage networks from the elevation surface, i. e. the identification of the drainage direction from each point (x, y);[4]

B. evaluation of channels length and slope in the drainage network;

C. evaluation of the discharge flowing through the channels;

D. assessment of the value of the optimality principle.

The first two steps are faced by O'Callaghan and Mark [36] in their classic "The extraction of drainage networks from digital elevation data." They identify several steps, among which interior pit removal, drainage direction assignment and drainage accumulation are interesting with respect to this work.

DEPRESSION FILLING the interior pit removal phase is commonly called depression filling. It is a common operation when dealing with field data, which present a lot of so called false depressions, caused by the measuring process. These would be translated into lakes or ponds, without having any relation with reality. In this context, this operation ensures that every point has an outlet and prevents from modeling lakes. In comparison with [36], the phase is anticipated because a different algorithm from [45] will be used. This topic will be deepened in the next chapter.

DRAINAGE DIRECTION ASSIGNMENT , sometimes called flow routing, requires the identification of the directions field. This step is the skeleton for the extraction of the drainage network from a terrain model. The idea is that water chooses to flow toward the steepest descent direction. Many methods to perform this operation exist: the most used and famous is called Eight Direction (D8), used also by [36]. It performs a local search among the neighborhoods of a point to find the direction of steepest descent. The number eight in its name comes from the discretization of the possible directions (see subsection 3.2.1.2). Here, an improved method derived from D8 method, called GD8 algorithm from [37] will be used.

DRAINAGE ACCUMULATION is the phase which assigns to each point of the drainage network the area draining into that point. Given the simplifications introduced in equation (3.6), the precipitation is equally distributed over the whole landscape. Therefore, this phase also outputs the discharge at any point of the drainage network.

4 In geomorphology, a drainage system or network is the pattern formed by streams, rivers, and lakes in a particular drainage basin. Geomorphologists and hydrologists often view streams as part of drainage basins [44].

The operations just described are commonly used in Geographic Information System (GIS) with hydrological capabilities. A GIS is a system designed to capture, store, manipulate, analyze, manage, and present all types of geographical data. Computer-based GIS became widely diffused in recent years. Nevertheless, none of them has the capability to connect with a surface optimizer, while they have many other features which would be useless for this work, such as geolocalization. Therefore, a totally new software was developed to perform these operations, starting from its basis and giving us the possibility to control each part of the evaluation process. Its practical implementation is shown in chapter 4 and appendix A.1, but some important concepts for understanding it are introduced in the next paragraphs.

3.2.1 *Discretization*

In mathematics, discretization concerns the process of transferring continuous models and equations into discrete counterparts. This process is usually carried out as a first step toward making them suitable for numerical evaluation and implementation on digital computers.

3.2.1.1 *Landscape discretization*

Since our experiment runs on computers, we need to discretize the elevation field. Again, this problem has already been faced by a number of scientists, engineers and private companies. A DEM is a digital model or three-dimensional representation of a terrain surface. A DEM can be represented as a raster or as a vector-based Triangular Irregular Network (TIN).[5]

In this work, raster are used thanks to their easier implementation and wider diffusion[36]. The landscape, i. e. the function $f(\cdot)$ as defined in subsection 3.1.1.1, is therefore represented by a bi-dimensional matrix. Each cell of the matrix contains an elevation value, which is assigned to an elementary surface $dx \times dy$. The DEM cells are assumed square, i. e. $dx = dy$, and the length dx defines the scale of the DEM itself, i. e. its resolution. The cell is sometimes named pixel [39].

This definition means that the entities involved in equation (3.8) are now defined as

$$x \in X \subset \mathbb{N}_0 \qquad y \in Y \subset \mathbb{N}_0 \qquad z \in Z \subset \mathbb{N}_0 \tag{3.9}$$

$\mathbb{N}_0$ is used instead of the full $\mathbb{Z}$ to simplify the implementation. x, y and z can be translated if needed. The surface $z(\cdot)$ becomes a matrix containing the z-value at each x row and y column.

5 i. e. A raster is a grid of squares, each of which contains a data that is representative of the whole square. They are also known as a heightmap when representing elevation.

3.2.1.2 *Drainage Networks discretization*

The drainage network is also discretized, accordingly to the discretization of the landscape. Since the landscape is composed by cells with a certain area, each of them will generate a surface runoff when it is raining on it.

In literature and in common GIS applications, the flow routing is deterministic: all the runoff from a cell flows toward another single cell. Given the landscape representation, it is clear that the possible flow directions are only eight[6]. This also means that there are only two possible lengths for the drainage line connecting the centers of two cells: the cell length, dx, and the diagonal length of the cell $\sqrt{2}dx$.

Another quantity which characterizes a drainage network is the slope in the main channel. Given a discretized length and a discretized elevation, the possible values of slope are a subset of rational numbers.

Finally the drained area at a location (x, y) of the DEM is the upward area whose rainfall is drained into (x, y) itself. In this work, the drained area of a cell becomes equal to the number of cells which drain into the cell itself and, therefore, it is discretized as well.

3.2.2 *Model inputs*

As seen, function $g(\cdot)$, i.e. the optimal principle, may be evaluated by the model. To do that, the model requires to know the landscape, the function $f(\cdot)$. Given the discretized representation of the DEM, the model actually needs one value of $f(\cdot)$ for each DEM cell.

Since a DEM can cover many square kilometers and, therefore, is composed by thousands of cells, the number of inputs is very large. The experiments presented in chapter 5 are performed on DEMs having 2500 cells (or pixels). The elevation values for each cell come from the optimizer: using the terms of multi-objective optimization discipline, they are the control variables.

However, the great number of elevation values required constitutes an additional obstacle for the optimization algorithm to understand the relation between controls and objectives, i.e. between the landscape elevations and the optimality criterion. Additionally, the algorithm used here relies on a certain randomness that is shifted to the landscape. In order to strengthen the relation between the landscape and the criterion, and to reduce the random noise of the surface, a spatial interpolator is introduced and integrated in the model for some experiments shown in chapter 5 . Consequently, a smaller number of control variables is requested to the optimization algorithm, which can focus more on the search for the optimum. These values are then interpolated to find the function $f(\cdot)$ over the whole landscape.

6 Each DEM cell is surrounded by only eight neighbouring cells.

Many spatial interpolators were evaluated: among them, Inverse Distance Weighting (IDW) was chosen. It is very simple and it does not require many parameters nor setup. Therefore, it was used as a first try. Its details are explained in subsection 4.1.3 .

3.3 THE SEARCH FOR THE LANDSCAPE: OPTIMIZATION

Optimization looks for the landscapes which minimize the optimality criteria.

The method to evaluate $g(\cdot)$ has been shown: it requires the elevation surface, i. e. function $f(\cdot)$, defined by equation (3.8):

$$\exists!\ f(\cdot) \in F(\cdot) \mid f(\cdot) = \arg\min g(x, y, \bar{p}, f(\cdot)). \tag{3.10}$$

The identification of $f(\cdot)$ is, therefore, the search for the minimum of function $g(\cdot)$.

3.3.1 *Multi-objective optimization*

As already said in section 2.4, the optimality principles proposed in literature, i. e. the functions $g(\cdot)$, fail to reproduce the whole complexity of landscape evolution. Therefore, a many-principle approach is applied. Practically, this means that there are multiple $g(\cdot)$ functions, so it is not possible to identify a single minimum point.

The mathematical names for this problem are multiobjective optimization or programming, multicriteria optimization, or Pareto optimization. The field they belong to is studied under the topic of multiple criteria decision making and is concerned with mathematical optimization problems, involving more than one objective function to be optimized simultaneously. Multiobjective optimization has been applied in many fields of science, including engineering, economics and logistics, where optimal decisions need to be taken in the presence of trade-offs between two or more conflicting objectives[7].

For a nontrivial multiobjective optimization problem, a single solution that simultaneously optimizes each objective function, i. e. each $g(\cdot)$ function in this problem, does not exist. In that case, the objective functions are said to be conflicting, and a possibly infinite number of Pareto optimal solutions might exist. A solution is called nondominated, Pareto optimal or efficient if none of the objective functions can be improved in value without impairment in some of the other objective values. Without additional preference information, all Pareto optimal solutions can be considered mathematically equally good.

Mathematically speaking, Cohon and Marks ([5] cited in [17]) framed the multiobjective design problem as a "vector optimization" subject

7 Minimizing weight while maximizing the strength of a particular component, and maximizing performance whilst minimizing fuel consumption and emission of pollutants of a vehicle are examples of multiobjective optimization problems involving two and three objectives, respectively.

to a set of constraints defining the feasible region of the decision space. We will call it Multi Objective Problem (MOP) as in [4]. Equation (3.11) formally defines the multiobjective design problem as the minimization of a vector, $G(\mathbf{x})$, composed of K objective functions, $g(\mathbf{x})$:

$$\underset{\mathbf{x}\in\Omega}{\text{minimize}} \quad G(\mathbf{x}) = [g_1(\mathbf{x}), g_2(\mathbf{x}), \ldots, g_k(\mathbf{x})] \tag{3.11}$$

$$\text{subject to} \quad c_m(\mathbf{x}) \leqslant 0, \quad \forall m \in \xi \tag{3.12}$$

where $\mathbf{x} = [x_1, x_2, \ldots, x_n]$ is a vector of L decision variables in the decision space Ω. Equation (3.12) optionally subjects $F(\mathbf{x})$ to one or more inequality constraints defined by ξ. Therefore it is possible to define Λ as the set of decisions in Ω that satisfy these constraints.

Given the framework presented above, equation (3.10) , which defines the solutions of the problem here presented, has to be rewritten as:

$$\exists f_i(\cdot) \in F(\cdot) \mid f_i(\cdot) = \arg\min (J_1, J_2, \ldots, j_k)\,. \tag{3.13}$$

$$J_k = g_k(\mathbf{x}) \tag{3.14}$$

$$\begin{aligned} \text{s.t.} \quad & \mathbf{x} \in \Lambda \subset \Omega \\ & \mathbf{x} = [x, y, \bar{p}, z] \\ & z = f(x, y, \bar{p}) \\ & i = 1, 2, \ldots, \infty \end{aligned} \tag{3.15}$$

where

- $f_i(\cdot)$ is i-th function that belongs to the set of Pareto optimal solutions;
- k is the number of principle;
- x, y, z are subject to equation (3.9) .

3.3.2 *Dealing with multiple solutions*

It is now clear that adopting many principles of optimality leads to a set of multiple solutions. This set is called Pareto front. One might wonder what the physical meaning of such a result is, remembering that we are trying to simulate natural landscapes. The simpler explanation is that each solution is the effect of different weights applied to the objectives. In other words, it is possible to build a single objective optimization problem which leads to that solution, being the single objective a proper weighted sum of the multiple optimality principles. If one assumes that there is only one "proper" solution among the points of the Pareto front, this means that the real principle is

the weighted sum of the principles used to obtain that solution[8]. So the question is now shifted on the method to recognize the "proper" solution: we will present it in section 3.4 .

3.3.3 *Multi-objective algorithms*

In literature, many algorithms exist for solving multi-objective problems. None of them can be said to be generally superior to all the others [33]. They can be classified roughly into two main groups by noticing that many of them are focused

> [...] on converting the problem into a single or a family of single objective optimization problems with a real-valued objective function termed the scalarizing function. [see 33, p. 63 and following]

The simplified problem is then solved with theories and methods of scalar optimization. The approach is called scalarization.

Among the others, a further classification has to be made. Historically, multi-objective optimization has been linked with decision making, where the goal is to identify the solution the decision maker is looking for. Therefore, some of the algorithms rely on the expertise of the decision maker. These algorithm are called preference-based methods by Cohon (cited in [33]) and cannot be used for the problem here faced.

The remaining algorithms identify the set of Pareto optimal solutions (or an approximation of that) without additional information. As Coello Coello perfectly summed up in his review "Evolutionary multi-objective optimization"

> [...]the Operations Research community has developed approaches to solve MOPs since the 1950s. Currently, a wide variety of mathematical programming techniques to solve MOPs are available in the specialized literature. However, mathematical programming techniques have certain limitations when tackling MOPs. For example, many of them are susceptible to the shape of the Pareto front and may not work when the Pareto front is concave or disconnected. Others require differentiability of the objective functions and the constraints. Also, most of them only generate a single solution from each run. Thus, several runs (using different starting points) are required in order to generate several elements of the Pareto optimal set. [see 4, ch. 3, p. 3]

8 Other explanations are possible: e. g. nature is random and therefore a single landscape shape as a response to river dynamics does not exist. These kind of explanations require a much larger theoretical study of the problem and are therefore left to researchers with greater experience on the subject.

To avoid any assumption on the solution, i. e. on the shape of $f(\cdot)$ and $g(\cdot)$ functions, a more general algorithm is needed. In case of discretization and limited feasibility space Ω, it is possible to try each value and then selecting the Pareto optimal solutions among them. The problem tackled in this thesis accepts different controls and, taking for example a DEM composed by 51×51 cells,where the control for each of them can assume 18 values, the total combinations of controls would be 8.11×10^{3013}, therefore this method can not be used. Instead of trying each control combination, it is possible to try some of them and choose the next tentative to try according to some heuristic. Following this idea,

> ...evolutionary algorithms deal simultaneously with a set of possible solutions (the so-called population) which allows us to find several members of the Pareto optimal set in a single run of the algorithm. Additionally, evolutionary algorithms are less susceptible to the shape or continuity of the Pareto front (e. g. they can easily deal with discontinuous and concave Pareto fronts)[9].

This is the idea evolutionary algorithms are based on.

3.3.4 *Evolutionary algorithms*

As previously explained, given the poor *a priori* information available about the problem and the solution, a MOEA seems the best choice. However the main drawback of an EA is that the set of solutions is just the best available approximation of the real Pareto front. It is impossible to know how good the approximation is.

Another important drawback is pointed out by Hadka and Reed in "Diagnostic assessment of search controls and failure modes in many-objective evolutionary optimization": they empirically showed

> that parameterization can greatly impact the performance of an MOEA, and for many top-performing algorithms, this issue becomes severely challenging as the number of objectives increases [18].

Since parameterization is problem-specific, it is impossible to know which one is the best for the MOP here faced before solving it.

A good approach for facing the parameterization issue can be found in [17] and [49]. They used a sampling method (Latin Hypercube) to generate a set of possible parameterizations for the evolutionary algorithm they want to test. Then they solved the problem using each parameter set many times, to overcome the influence of the random seed used. The set of solutions is then taken as the best solutions across

9 [4], pag 3.

all parameterizations, all seeds and all algorithms. The EAs, their parameterization and the number of different random seeds used is our framework are detailed in section 4.4, section 4.5 and section 5.1.

3.3.4.1 *Advantages of MOEAs*

The choice of applying MOEAs to solve the optimization problem arises firstly from Paik's work [38]: he used a Genetic Algorithm (GA) to solve its single objective minimization problem. The same approach can be easily extended to multiple principles. It has the additional advantage of producing an entire Pareto front in a single run, while it needs few mathematical properties for the problem to be minimized, compared to other Multi Objective (MO) algorithms. Thanks to the availability of state of the art MOEAs under open source licenses free of charge, the quality of the solution found by a MOEA is not an issue.

3.3.5 *Defining the control variables range*

In subsection 3.2.2 , the concept of control variable was introduced. Usually, when defining control variables, also a range of values they can assume is established. In the case of Paik's single objective GLE model, each DEM cell was subjected to a control variable which could change the elevation cell by lowering or increasing it. Each control variable could assume the values $[-100, 0, +100]$ centimeters. As it is described in [38], the model was sequentially iterated 15 times, therefore each cell could vary its elevation by a value in the range $[-1500, +1500]$ centimeters, discretized with step 100.

As it is said in subsection 3.3.2 , a Pareto front composed by multiple solutions is produced as output of our framework, at the end of each execution. Consequently, it becomes difficult to make the framework iterate many times. In fact, at the end of each sequential iteration, a new Pareto front for every starting condition (i. e. for every point of the Pareto front obtained at the previous iteration) would be created. As a consequence, the dimensionality of the solutions set would exponentially grow at each iteration (e. g. if the first iteration produced a Pareto front composed by 1000 points, 1000 other Pareto fronts would be present at the end of the second iteration, and so on) and the solutions analysis would be extremely difficult.

In order to overcome this problem, our framework is designed to perform just one single iteration, but:

- for the first experiments, which will be commented in chapter 5, the range of values each control variable can assume is extended, in order to give each DEM cell the same freedom as in Paik's GLE model;

- when the IDW interpolator is integrated in the model, the elevation itself of some DEM cells becomes a control variable (while the others are obtained through interpolation), and it can assume almost every value higher than 0.

Specific information about control variables range setting for each experiment will be provided in chapter 5.

3.4 NATURALITY INDEXES

Naturality indexes are used to evaluate the different solutions of the Pareto front, by comparing the synthetic DEMs and river networks to natural ones.

It has been explained in subsection 3.3.2 that adopting a MO approach leads to multiple solutions and, therefore, the problem of how to evaluate the Pareto front arises. Evaluating the solutions belonging to the Pareto front means evaluating the hypotheses the problem is built on, i. e. the initial guessing about $g(\cdot)$ functions, the modules of the model and the discretization values chosen.

From section 3.1, the process studied here is landscape evolution under river dynamics: examples of this exist almost everywhere on the Earth surface. In literature, some methods to assess common geomorphological features of such a system are cited. The most important features we will try to assess are drainage network organization and channels slope characteristics, in order to consider both 2D ad 3D features of river networks. In particular, the indexes adopted for assessing these features are based on Horton's law and Hack's law, as explained in the next paragraphs.

3.4.1 *Horton's laws*

Historically, the first and most important numerical indexes to asses river geomorphology are Horton's laws [19]. The following part is a summary of chapter 1.2 from [53].

The first law expresses the deep regularity of river networks, in terms of relations between the parts. It is called Horton's law of stream numbers and is expressed as

$$\frac{N(\omega)}{N(\omega+1)} = R_B \tag{3.16}$$

where $N(\omega)$ is the number of streams of order ω and R_B is called *bifurcation ratio*. $N(\omega)$ is estimated with the ordering procedure showed in figure 3.1 developed by Strahler ([64] and [65]) based on Horton's original work.

The second law characterizes the regularity of river networks by analyzing stream lengths. It is called Horton's law of stream length:

$$\frac{\bar{L}(\omega+1)}{\bar{L}(\omega)} = R_L \tag{3.17}$$

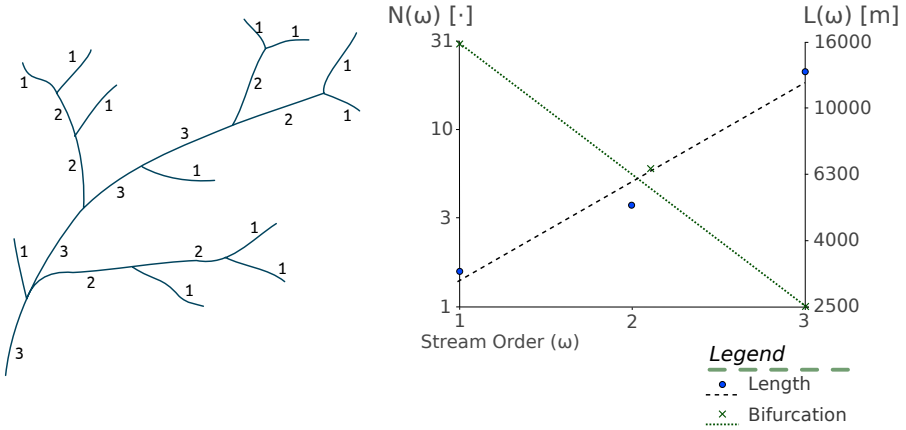

Figure 3.1: Horton-Strahler ordering procedure. On the left: a drainage network is classified according to Horton-Strahler ordering procedure; the numbers next to the links are the orders ω evaluated with that procedure. On the right: an example of the semi-log plot used to evaluate R_B and R_L.

where $\bar{L}(\omega)$ is the arithmetic average of the lengths of streams of order ω and R_L is called *length ratio*. Typical values of R_B and R_L are 4 and 2 respectively, with a range of [3 ; 5] for R_B and [1.5 ; 3.5] for R_L ([53], [34], [19]).

Horton found that R_B and R_L are approximately constant through semi-log plot of $N(\omega)$ and $\bar{L}(\omega)$ against order ω. The two ratios R_B and R_L are estimated as the slope of linear fitting of those plots (right side of figure 3.1).

Horton did not explicitly include basin areas in his laws, but he suggested that areas should satisfy a geometric relation like stream lengths and numbers ([19] and [60]). The law of basin areas was explicitly stated by Schumm [58]:

$$\frac{\bar{A}(\omega)}{\bar{A}(\omega+1)} = R_A \tag{3.18}$$

where $\bar{A}(\omega)$ is the mean total area contributing to streams of order ω and R_A is the *area ratio* and has typical value of 5 [53].

Also, Horton did not state any mathematical law to express the relation between average channel slope and order of the stream. Nonetheless, he showed a semi-log plot of average channel slope against stream order in [19], suggesting an inverse geometric-series law. Yang [71] explicitly stated the relation

$$\frac{\bar{S}(\omega)}{\bar{S}(\omega+1)} == e^F = R_S \tag{3.19}$$

where $S(\omega)$ is the average slope of streams of order ω, F is a constant and R_S is called *stream concavity* [71].

3.4.1.1 *Meaning of Horton's laws*

As Rodríguez-Iturbe and Rinaldo pointed out,

> the regular geometric relationships contained in Horton's law and observed in natural drainage networks have been interpreted as the signature of some particular evolutionary criteria in network organization. They have also been interpreted as evidence that drainage networks are topologically random, meaning that chance is the only criteria operating on the organization of the network. ... it has also been argued that Horton's relations are not specific to any kind of networks as they describe the vast majority of networks, random or not[10].

In this work, the focus is not to understand whether Horton's relations are specific for river networks or not. Therefore, we base the use of these relations on the experience of many researchers and hydrologists before us [65], [54], [40]. Horton's relations are used to demonstrate whether model outputs contain valid networks but other evaluation methods are used in order to strengthen the closeness to river networks.

3.4.2 *Hack's law*

Hack applied a power function to relate length and area of streams in the Shenandoah Valley, Virginia. Gray[11] and many other researchers later refined and corroborated the original analysis by Hack's and nowadays the following equation (3.20) is generally accepted and called Hack's law:

$$L \propto A^{h} \tag{3.20}$$

L is the length of the longest stream from an outlet to the divide, A is the drained area at that point[12] and h is generally accepted to be slightly below 0.6, even if it may vary from region to region. Rigon et al. [50] also suggested that

$$\gamma = \frac{\beta}{h} \tag{3.21}$$

where h is the exponent in Hack's law, β comes from

$$P[A > a] \propto a^{-\beta} \tag{3.22}$$

as [54] found[13], and γ is the exponent in

$$P[L > l] \propto l^{-\gamma} \tag{3.23}$$

10 Rodríguez-Iturbe and Rinaldo, *Fractal River Basins*, page 6.
11 cited in [50].
12 [50] demonstrates the validity of Hack's law for any point inside a basin.
13 A is the contributing area at a randomly chosen point in a drainage network.

where l is the stream length from any point to the divide. Typical values for β and γ are $0.43 \div 0.45$ and $0.70 \div 0.90$, respectively [50]. This rather comprehensive set of relations and the consistency of the measured exponents lead Rigon et al. to suggest that this scaling theory is a complete description of the planar organization of basins and their fractal behaviour.

3.4.3 *Model Outputs Evaluation*

Hack's and Horton's relations, together with the analysis of rivers longitudinal profiles, are going to be the assessment method for the 3D river networks produced by the model developed in this thesis. The descriptive indexes above explained are, in fact, used to understand which landscapes generated by the optimization process are a reasonable representation of natural landscapes. Actually, they are assessed for the basins produced and their values are then compared with the natural ones. This allows the understanding of the Pareto front produced by the optimization and therefore a critical analysis of the hypothesis assumed into the model, e. g. the shape and number of the optimality principles, the $g(\cdot)$ functions and the procedure used to extract river networks from the landscape.

3.5 HIDDEN ASSUMPTIONS ON THE COMPARISON WITH NATURE

In order to compare the results of the model with natural landscapes, two more hypotheses are needed. The first arises from a temporal analysis of the model structure. In fact, natural landscapes are the product of thousands of years of geological processes like tectonic uplift, river dynamics e. g. erosion, transport and deposition, ... The model here developed emulates the effect of a certain rate of rainfall, i. e. it searches for the landscape shape that minimizes energy expenditure principles, under the assumption of the existence of such principles. It does not take into account any previous rain event and, when the interpolator is inserted in the model, the previous shape of the landscape i. e. the history of that landscape. Comparing model outputs to natural river networks is possible under the assumption that optimality principles used here to derive model outputs are always valid and does not define an optimal point toward which river networks move during a transitory. These optimality principles do not describe any temporal dynamics.

Another strong assumption underlying this model is the isotropy of the landscape. There is no simulation of different geological composition of rocks, sand or clay layers. From the point of view of erosion, transport and deposition, this does not mean that these processes can act indifferently on any part of the landscape, because they are not simulated in the model. In fact, there is no process simulated in the

model. The model just produces a "picture" of a landscape subjected to rainfall and river dynamics. This assumption rather means that the optimal principle searched for explaining landscape evolution is independent from the anisotropy of natural landscapes. This is the second hypothesis needed to use statistics taken from the real world to evaluate the results of the model here presented.

3.6 TESTING OPTIMALITY PRINCIPLES: SOME REMARKS

In the previous sections, the most important aspects of the work-flow used in this work were shown and explained. The framework to test multiple optimality principle to explain landscape evolution was depicted and explicitly shown.

The framework gives a rational procedure to isolate the hypothesis, allowing an assessment of them based on results. Specifically, the hypotheses here used concern:

- the optimality principles chosen, i. e. the shape of the $g(\cdot)$ functions in equation (3.7);
- the optimization process i. e. the $f(\cdot)$ functions;
- the procedure to evaluate the value of the principles on a given landscape, i. e. the model (section 3.2).

From a bottom up perspective, different models can be compared, other hypotheses being equal, by comparing the value of Horton's and Hack's relations. Once the model is set, one is allowed to test different optimization processes and algorithms and to assess them by relative comparison. The same can be done with the chosen optimality principles.

The framework relies on two untested hypotheses:

- landscape evolution under river dynamics follows an optimality principle;
- the set of indexes[14] used in the evaluation part is suitable to identify natural landscapes among many possible landscapes.

Testing them is required to completely validate the results of this work, but a broader review of the literature and multiple experiments are needed. However, many researchers assumed their truthfulness and based their researches on them.

At this point of the thesis, all theoretical concepts about the topic of landscape evolution under river dynamics and about the different parts of the framework we introduce have been explained. The second part of the thesis is devoted to the explanation of the framework technical implementation and the comment of the obtained results.

14 see section 3.4.

Part II

PRACTICE

From this point on the work will be detailed in its technicalities and its results will be shown. If you are eager to find what we have found, jump directly to the conclusions in chapter 6. If you nonetheless decide to read the following two chapter, well, we have warned you.

4

MULTI-OBJECTIVE FRAMEWORK: IMPLEMENTATION AND TECHNICALITIES

For the things we have to learn before we can do them,
we learn by doing them.

— Aristotele, *Nicomachean Ethics*, 350 B.C.E.

The previous chapters introduced many questions and the uncertainty present in the field of landscape evolution. In order to proceed on testing our idea, we had to make a number of assumptions, which were described in chapter 3. At the end of it, the choice of the hypotheses and the thesis to test has been included into a framework. This allows us to rationalize the scientific process of testing hypotheses by explicitly express them. We hope also that the framework would be a valid tool to communicate the methodology here applied in a common language, so that the results we reach can be useful to other researchers. Figure 4.1 shows the operational part of the framework, using the common language of flowcharts. This chapter starts from the inner part of the model, moving towards the final analysis of results, showing the technicalities and methodologies adopted. For this reason, the order of the topics as written in the chapter may sometimes be different from how they appear in the flowchart. We will refer to the flowchart at the beginning of each section, in order to avoid that the reader gets lost.

4.1 THE DIGITAL ELEVATION MODEL

This section refers mostly to the model setup part of the flowchart in figure 4.1 .

In our experiments, DEMs of 51×51 cells were used (each cell having an area of $1\,km^2$).

The use of Digital Elevation Models (DEMs) has significantly changed the way of studying Earth's surface processes. The increasing availability of data in this format and the computational power of computers allows researchers to perform their analyses with a wider and deeper perspective. Therefore, the use of DEMs when studying landscape evolution is convenient. Many landscape evolution models relies on this data structure to represent surfaces [51].

An example of DEM is provided in the left side of figure 4.2.

Also the work by Paik [38], we started this one from, is based on DEMs. In his paper, he uses a square domain of 201×201 cells, each grid cell having an area of $1\ km^2$. In this work, however, the experiments conducted on DEMs of such a dimension requires too many computational resources and becomes too expensive when many experiments with different setups have to be conducted. Therefore, we

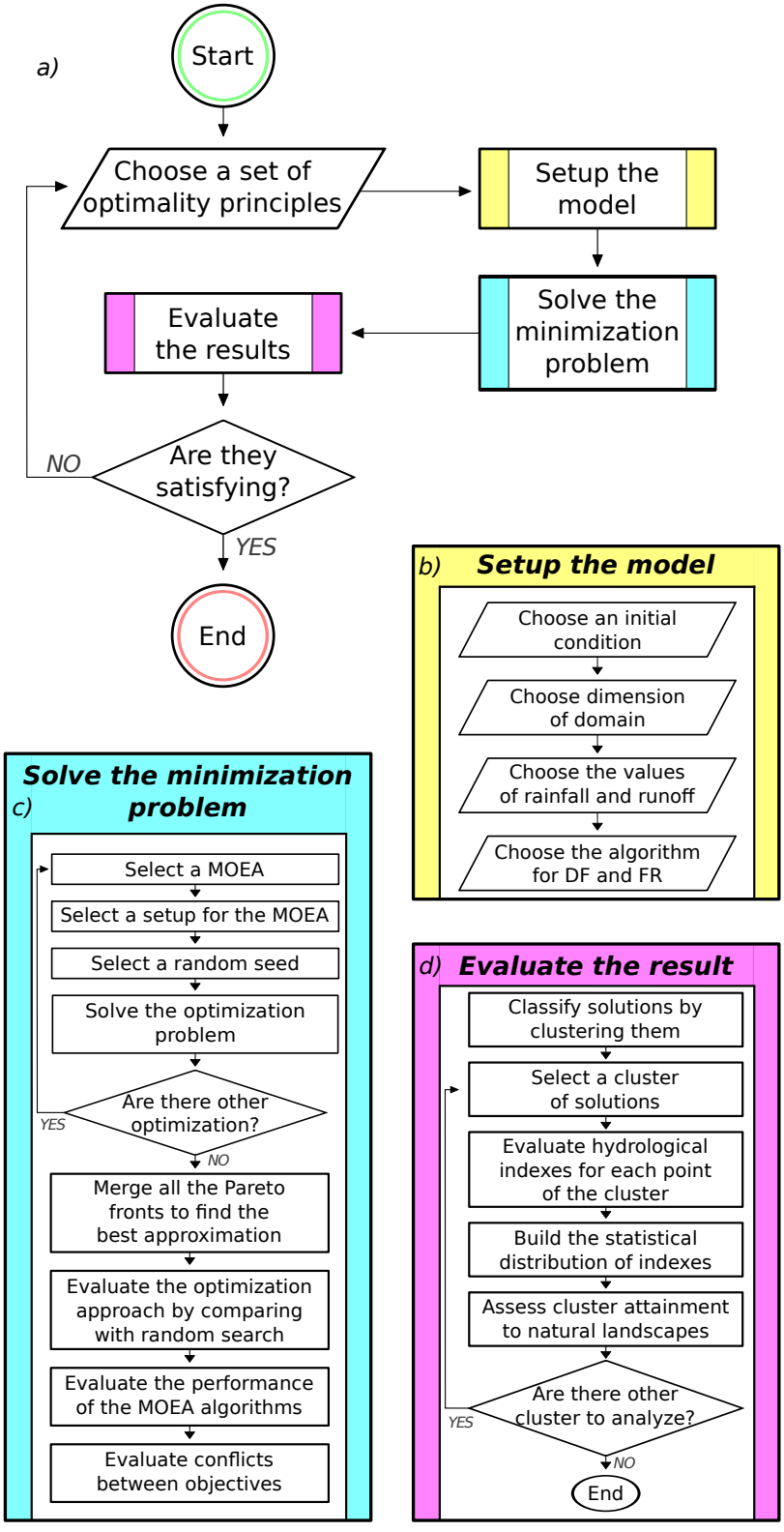

Figure 4.1: Operational flowchart that specifies the framework. The upper part (*a*) represents the operation performed. The parallelograms represent interactive steps where decisions by the user are required. The rectangles indicate generic processing steps: the ones with lateral stripes are complex processes composed by sub-processes that are expanded in parts *b*, *c* and *d*. The rhombuses symbolize conditional operations and usually implement iterative steps.

choose to reduce the dimension by a ratio of 4, performing our simulations on square DEMs of 51×51 cells. Many hydrological and geomorphological researches are based on DEMs of these dimensions: Horton's original work that lead him to formulate the laws of stream composition was based on basins of area between 15.8 Sq. Mi. and 479 Sq. Mi., which roughly corresponds to ones generated by our model. Nonetheless, the effect of the scale is something that should be studied in future research on this topic and the analysis on larger landscapes has to be performed.

The planar shape of the DEM can influence the whole landscape and the hydrological networks grown on it, as found by Rigon et al. [51] in their studies about OCN. They studied triangular domains and hydrological networks grown according to the TEE criterion, finding that a minimum angle of the planar projection of the domain is required by basins to develop without imposed boundary constraints. Similar experiments with different DEM shapes should be performed with the model here presented, but again we leave this topic to future research.

The resolution of DEMs here used is 1 km^2, as in Paik's work. Given the dimension of 51×51 cells, the covered area is 2601 km^2. The resolution can seem too coarse, but it allows to simulate a surface large enough to observe river dynamics on landscape evolution while keeping a reasonable computational cost.

4.1.1 *Boundary conditions*

The DEM boundary elevations are at the sea level, in our experiments.

Boundary conditions for the model and the DEM can deeply affect the simulations results. We used here the same boundary condition as in Paik, i. e. we imposed the contour cells to have an elevation equal to zero. This elevation represents the sea level, therefore, the simulated DEMs are actually islands. It has been suggested that they can represent also other types of landscapes, e. g. the top of a mountain, by translating each cell of a suitable elevation value.[1]

To have an idea, the French island of Réunion, located in the Indian Ocean (East of Madagascar) has a surface equal to 2 512 km^2, about the same as our model DEMs. Digital elevation data of the island, collected from National Aeronautics and Space Administration (NASA), are shown in figure 4.2.

4.1.2 *Initial conditions*

For the first two experiments described in chapter 5 , it is necessary to define an initial condition i. e. an initial shape of the landscape surface. Paik used a pyramid shaped DEM to "maximize the terrestrial

1 We thank Prof.ssa Marina De Maio for the suggestion.

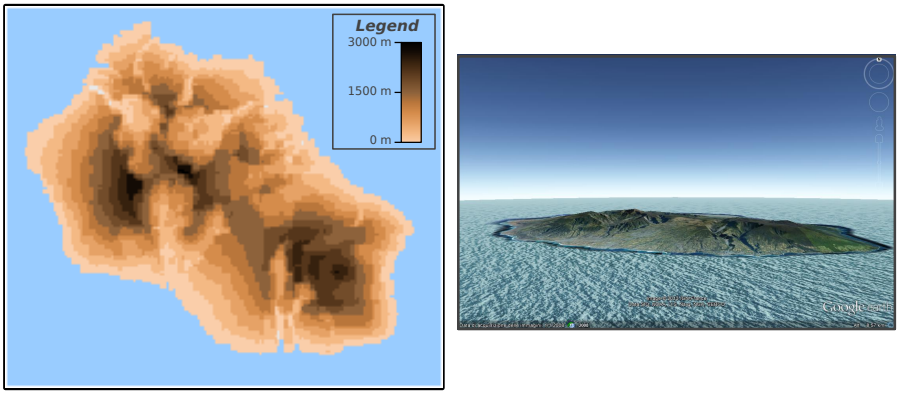

Figure 4.2: On the left, the SRTM v4 digital elevation data from NASA of Réunion island, France, Indian Ocean. Data have been elaborated by the authors. On the right, the same island seen in Google Earth ©, from Terrametrics images, 2013.

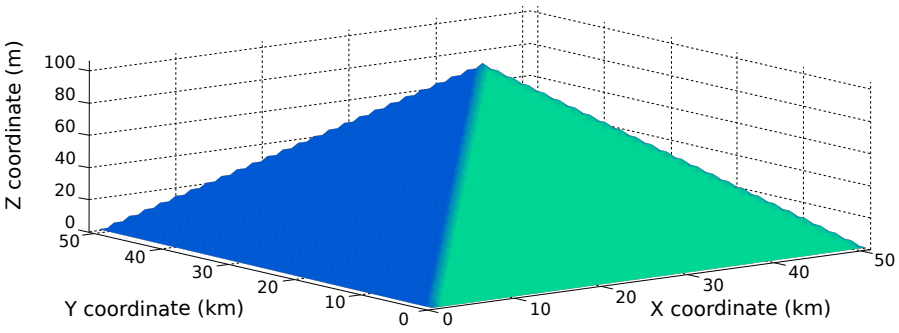

Figure 4.3: DEM initial condition for experiments here performed: the base of the pyramid is a square of 51×51 cells (or square kilometers), covering a surface of 2401 square kilometers, with the same number of cells.

area (effective domain)" [see 38, p. 689]. The pyramid is discr, the slope is $\frac{4}{1000} = 0.004$.

We use the same configuration in the smaller domain of 51×51 cells (or square kilometers). The same slope used by Paik makes the top of the pyramid have an elevation of100 meters above sea level. An example of the resulting initial DEM is given in figure 4.3 . As other parameters, also these settings should be changed to study how they can affect the optimal landscape, but again, these experiments are left to future researches.

4.1.3 *Spatial interpolator*

The amount of cells in the DEM can be noticed in figure 4.3. For each of them, the optimization algorithm has to evaluate function $f(\cdot)$, i. e. the elevation value.

As highlined in subsection 3.2.2 , the great number of values can "puzzle" the optimization algorithm and make it work more as a ran-

dom search procedure, losing part of the connection to optimality principles and guidance from them. In order to avoid this possible failure mode, we reduced the number of elevation data required to the optimizer. Then, a spatial interpolator is used to recreate a surface that actually becomes the landscape. In other words, we ask to the optimizer a sparser set of sample values of function $f(\cdot)$ with a resolution inferior to 1 km^2.

4.1.3.1 *Spatial interpolation*

In numerical analysis, multivariate interpolation or spatial interpolation refers to the interpolation on functions depending on more than one variable. The function to be interpolated is known at given points $(x_i, y_i, z_i, \ldots)$ and the interpolation problem consists of yielding values at arbitrary points $(x, y, z, \ldots)$. Many interpolation methods exist: they differ in terms of precision and complexity of the estimated surface.

INVERSE DISTANCE WEIGHTING Inverse Distance Weighting (IDW) is a type of deterministic method for multivariate interpolation with a known scattered set of points. The values assigned to unknown points are calculated with a weighted average of the values available at known points. The applied weight is an inverse function of the distance between the point to be calculated and each of the known points, from which the name of the methodology. The method is simple to implement and execute and does not require many parameters setup. It is therefore suitable to be used in this framework.

A longer explanation of this method and a snipped code of the algorithm implemented by the authors is given in appendix A.2. By using the interpolation, it was possible to reduce the number of input variables required to the optimizer: from the original 2401 cells belonging to the 51×51 DEM to 16 over the same surface.[2]

4.2 DEM ELEVATIONS SUM CONSTRAINT

In our experiments, the sum of DEM elevations is conserved along the process, keeping its variation within a tolerance.

Before concluding the description of the model setup, i. e. section *(b)* in figure 4.1, with the description of depression filling and flow routing algorithms, one last important feature related to the DEM must be described: the DEM elevations sum constraint. The model by Paik features a constraint called "tectonic condition" based on the hypothesis that the mass gained because of uplift is the same as the total loss of sediment mass from the whole landscape. The basis of this hypothesis is

2 The contour is excluded because it is not modifiable, given the presence of the boundary condition.

> that there can be a balance between erosion and uplift as an increase in tectonic uplift rate can lead to higher relief and then this again will result in a higher erosion rate [see 38, p. 687].

He cites observations from Taiwan, Southern Alps of New Zealand and Swiss Central Alps to support this statement [38].

This condition can be also derived from equation (3.4): the rate b_t represents river dynamics, while $U(x, y)$ represents tectonic uplift. This requirement also means that the sum of elevations is still the same during the optimization process. Therefore, the total amount of potential energy available to the water flow on the surface remains the same and the resulting landscapes can be compared without the need to take into account different energy levels.

This constraint is enforced by checking the mass variation between the initial condition and the optimal landscape. Actually, mass is not the proper term: thanks to the hypothesis of isotropy of the landscape, mass is proportional to the sum of the elevations in the landscape i. e. the sum of the values contained in each DEM cell.[3]

4.2.1 *Feasibility*

This constraint has proved to be very challenging: figure 4.4 shows the probability of randomly choose a landscape that fulfill the constraint. The figure is based on the evaluation of such a probability, given a discrete set of variation in the elevation values, which can be applied to each cell of the DEM, during the whole optimization. The whole dissertation and the algorithm used for the calculus are shown in appendix A.3.

Without any tolerance on mass variation (i. e. the mass of the final DEM is exactly the same of the initial one), the probability of randomly choose a feasible control is less than 0.1 for a 51×51 DEM.

4.2.2 *Tolerance and application*

Figure 4.4 demonstrates how difficult is to randomly select a landscape that fulfill the mass constraint with growing DEM dimension. As in Paik's paper [38], we add a tolerance value to the mass constrain, i. e. we accepted small changes in the total elevations sum. Even a value of tolerance as little as 0.001 is able to increase the probability to more than 80%.

It must be underlined that the Depression Filling (DF) phase can also alter the elevations in the DEM. The mass constrain is checked after this phase. The effect of this change can be assessed empiri-

3 Mass constraint is verified after the depression filling phase, which is explained in subsection 4.3.1 .

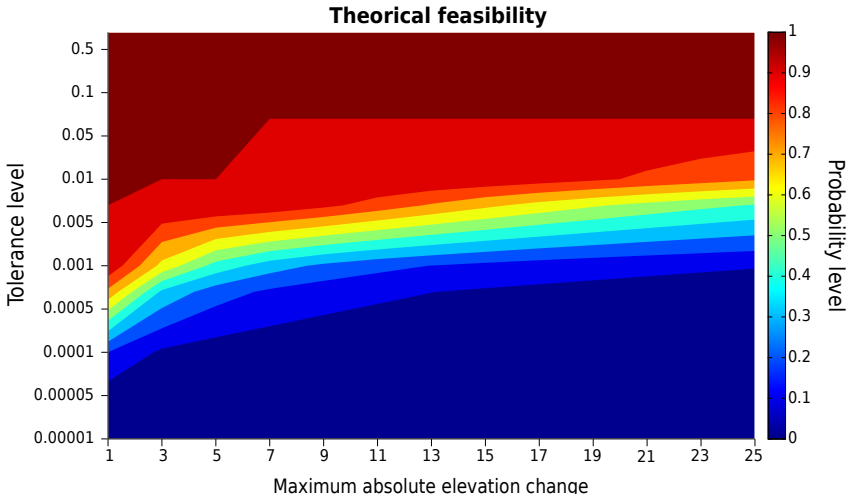

Figure 4.4: Theoretical probability of randomly choose a surface respecting the DEM elevations sum constraint: the blue area represents low probabilities, the red higher ones. On the y-axis there is the tolerance on the accepted mass variation. On the x-axis there is the range of possible variations in meters, e. g. 5 means that each cell can vary from its initial condition of ± 5 meters. DEM dimensions are 51×51.

cally with the following data. On the experiment MOGLE , which will be explained later, according to figure 4.4 with maximum absolute change of 9 meters and tolerance level of 0.001, a random search should have a feasibility probability between 30% and 40%. The random search performed had instead a feasibility value of 3.40% on 30 millions of different DEMs tried.

That said, it is true that MOEAs can manage constraints and tackle them more efficiently than a merely random sampling. For example, the first experiment (see MOGLE and MOGLE_RAINY) which matches exactly the situation analyzed in the figure, should have a percentage of landscapes fulfilling the constraint by 30%. With the effect of DF, we measured 3%. MOEAs instead showed a percentage of approximately 60%. They demonstrates the ability of MOEAs to efficiently understand the problem.

4.2.3 *Spatial interpolator and mass constraint*

In the experiments shown in section 5.4, we use the interpolator presented in subsection 4.1.3. Mass constraint is still verified, in the sense that the mass of optimal landscapes does not differ more than the tolerance with respect to the initial condition. However, the possibility to explore a larger number of landscape surfaces extends the controls range. Therefore, the probability of randomly select a correct landscape is even lowered (with the same tolerance value). We did not evaluate it with a probability calculus, but the experiments with

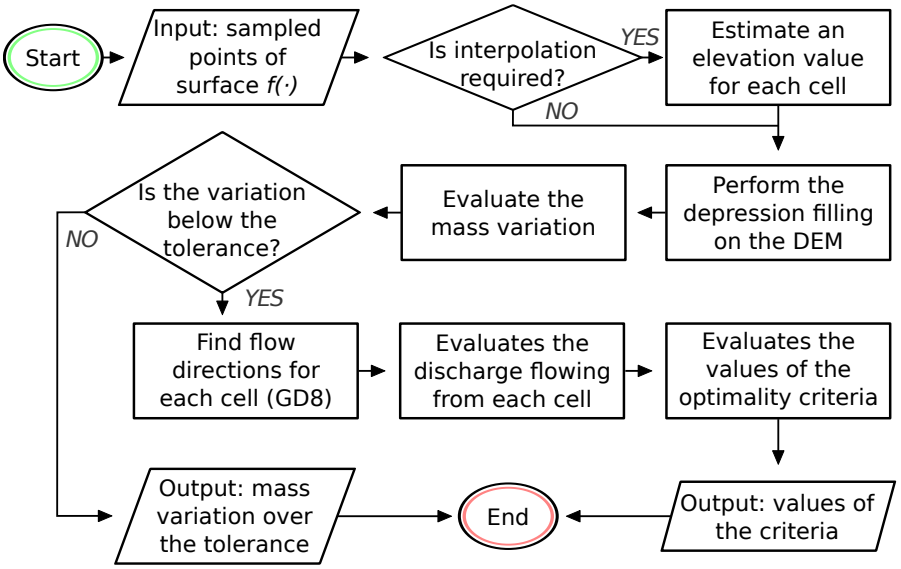

Figure 4.5: Operational flowchart of steps performed by the model developed for this thesis: the parallelograms represents the input and output operations; rectangles are generic processing steps; rhombuses are conditional forks in the work flow; ellipses indicate the start and the end of flowchart.

MOEAs showed a percentage of correct landscapes among the tried ones between 0.4% and 20%. The random sampling of 400 000 different values for each of the 16 input values required by IDW, which created a set of 13 600 000 different DEMs, was not able to find a single landscape respecting the mass constraint.

4.3 THE EXTRACTION OF HYDROLOGICAL NETWORKS

The core part of the work-flow shown in figure 4.1, i. e. what is required to "solve the optimization problem" (sector *(c)* in figure 4.1), is the process to find the solution of equation (3.15) . Hidden inside it, all the operations that connect a given landscape with the values of its optimality criteria are present. Some characteristics of this procedure have already been explained in the previous section 4.1 and section 4.2. The operational part of the DEM analyzing procedure is going to be explained in the following paragraphs. An overview of this procedure is given in figure 4.5.

The implementation of the following algorithms has been made by the authors of this thesis in C plus plus (C++) software, which is detailed in appendix A.1.

4.3.1 *Depression filling*

Planchon and Darboux's DF algorithm was used

As explained in section 3.2, depression filling operation is performed in order to remove pits and allows each cell to be connected with an

outlet. The algorithm which was chosen and implemented for carrying out this passage is described and then compared with the one used by Paik in his GLE model, in the next paragraphs.

4.3.1.1 *DF: the algorithm*

The algorithm used in the model proposed within this thesis is the extended version of the one conceived by Planchon and Darboux in [45]. In few words, it "first adds a thick layer of water over all the DEM and then drains excess water" [see 45, p. 159], so that all pits result filled. Their algorithm is now illustrated:[4]

INITIALIZATION In this initial phase, the following elements are defined:

- $Z_{transient}$: it is a transient elevation matrix. It has the same dimensions as the initial DEM ones and the elevation values of all its cells, apart from the ones on the border, are set to a very high number. In our C++ model, considering that elevation cells assume integer values, they were set equal to the value INT_MAX $= 2\,147\,483\,647$, which is the max value an integer number can assume in C++. As for the border cells, they are set equal to the Z_{DEM}, being Z_{DEM} a matrix containing the depressed DEM elevations;
- ε: it is called minimum positive elevation distance required. It is the positive elevation difference which a cell is required to have with respect to the lowest of its neighbouring cells, in order not to be considered depressed or produce flat areas. In our model, the value chosen for ε is 1 cm.

DEPRESSION FILLING This is the core of the algorithm. The operations executed after the initialization phase are essentially two:

- the value of $Z_{transient}$ in the positions related to the cells not depressed in the initial DEM are lowered and set equal to the values in the DEM:

$$Z_{transient}(x, y) = DEM(x, y) \qquad \forall (x, y) \text{ not depressed} \quad (4.1)$$

- correction of depressions: the value of $Z_{transient}$ in the positions related to the cells depressed in the initial DEM are set equal to the elevation of their lowest neighbour, (x_n, y_n), plus the minimum positive elevation ε, as shown in equation equation (4.2) .

$$Z_{transient}(x, y) = Z_{transient}(x_n, y_n) + \varepsilon \quad (4.2)$$

4 Here the description is summarized; for a more complete one see [45].

In particular, the two mentioned operations are performed by exploring the DEM and $Z_{transient}$ iteratively:

1. first of all, starting from each cell of the border and going upwards iteratively, values of $Z_{transient}$ for not depressed cells are corrected according to equation (4.1) ;
2. secondly, the DEM and $Z_{transient}$ are explored varying the direction of scrolling and $Z_{transient}$ values are changed, both for depressed and not depressed cells, according respectively to equations equation (4.2) and equation (4.1) .

TERMINATION At this point, matrix $Z_{transient}$ is equal to the initial DEM, where it was not depressed, and corrected, where it was depressed. Therefore, the algorithm ends and DEM elevations are substituted with $Z_{transient}$ ones.

4.3.1.2 *A comparison with Paik's DF algorithm*

A comparison between the DF algorithm used in our model and the one used in Paik's GLE model is needed, in order to explain the reason for having used another algorithm.

Paik's DF, as it is described in [38], works as follows:

1. each depressed cell is compared with the lowest one among its neighbouring cels;
2. the elevation difference between the two is evaluated;
3. finally, "the depression cell is lifted by half of the gap and and the neighbouring cell is lowered by the same amount" [see 38, p. 688].

According to Paik's DF algorithm, not only depressed cells are filled, but also the elevations of the neighbouring cell is modified, in order to grant the conservation of the total elevations sum. A comparison between the behaviour of the two DF algorithms is provided in figure 4.6 .

The main reason for having chosen an alternative algorithm with respect to Paik's one is that, as emerged from the testing and debugging activity performed on our model, Paik's DF works fine as long as there are single cell depressions, but it may enter an endless loop when there are extended depressions, i. e. depressions including two ore more cells. In this latter case, in fact, elevation gap is continuously moved to and fro the depressed cell, without solving the depression and reaching a termination condition. It might be argued that, even if the algorithm we used is more stable, it does not respect the elevations sum constraint detailed in subsection 4.2. In response to that, it is possible to say that, even if the DF algorithm by itself does not provide any elevations constraints, it is placed in the model in such

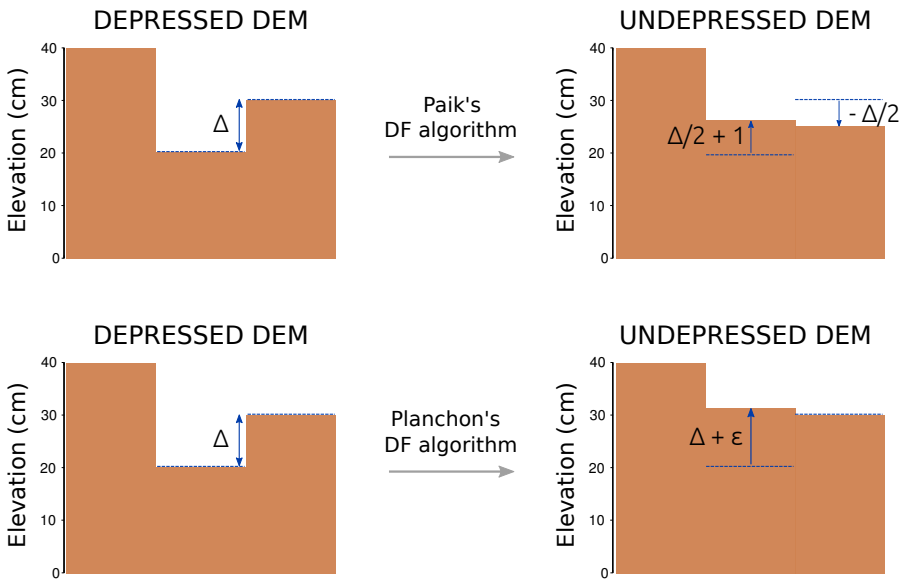

Figure 4.6: Depression filling techniques comparison. In the upper part of the figure, Paik's algorithm is shown[38]. Since $\frac{\Delta}{2} + 1$ is added to the depressed cell and $\frac{\Delta}{2}$ is subctracted from its lowest neighbour, elevations sum is conserved apart from 1 cm. In the lower part of the figure, Planchon and Darboux's algorithm is shown[45]. Since the only operation is adding $\Delta + \varepsilon$ to the depressed cell, being ε the minimum positive elevation distance, elevations sum is not conserved.

a position that the fulfillment of the constraint is ensured. In fact, it is performed after the controls (i. e. the value of function $f(\cdot)$ in every point (x, y, z) of the DEM) are applied, before verifying the elevations sum constraint. Doing so, DEMs corrected with DF are submitted to the constraint and it is guaranteed that only control masks which respect it are accepted and applied to the DEM, being otherwise rejected.

4.3.2 *Flow routing extraction: GD8*

Paik's GD8 algorithm was used for flow routing extraction

The problem of performing a good flow direction extraction is illustrated in [37]. In our model, the improved version of D8 called GD8 and proposed by Paik in [37] is implemented, as already written in chapter 3.

The reason for the choice is double: first of all, as the author affirms as a concluding remark, based on the application of his method,

> the proposed algorithm successfully reduces the uncertainty residing in local searches and produces more natural flow patterns, while it is still simple, computationally efficient, and easy to use [see 37, p. 9].

Secondly, it was chosen in order to implement a model coherent with Paik's GLE model and be able to consistently compare the output net-

works of the two models. The algorithm is described and commented by comparing it with simple D8 algorithm in the following paragraph.

4.3.2.1 *GD8: the algorithm*

The algorithm, implemented according to its features described in [37], is executed with this work-flow:

INITIALIZATION: the primary and secondary directions are defined for each cell of the DEM.

- The PRIMARY DIRECTION is defined according to the concept of Local Steepest Direction (LSD). Given the fact that each DEM cell is surrounded by other eight cells, the slopes between the central cell and each of its eight neighbours are compared and the direction following the maximum slope is assigned as primary direction.
- The SECONDARY DIRECTION is "the steeper direction between clockwise and counterclockwise directions adjacent to the LSD" [37].

DIRECTION CHOICE: this is the core phase of the algorithm, consisting in choosing whether to assign the primary or the secondary direction. The choice is performed by comparing the cell itself with its upstream neighbour, on the basis of three criteria:

1. the primary direction of the cell and its upstream neighbour is the same;
2. the secondary direction of the cell and its upstream neighbour is the same;
3. the gradient between the source of the flow passing onto the cell and the downstream neighbour defined by the secondary direction is higher than the gradient between the same source and the downstream neighbour defined by the primary direction.

If the three of these criteria are satisfied, secondary direction is chosen; in the opposite case, the primary one is assigned.

TERMINATION: when all DEM cells have been assigned a flow direction, the algorithm stops.

4.3.2.2 *Short comparison between D8 and GD8*

The improvement provided by GD8 algorithm in comparison with the D8 one is significant. In fact, for non-dispersive methods i. e. the ones which set only one flow direction to each cell, like D8 and GD8, there is an uncertainty when the direction is chosen starting from the central cell to one of its neighbouring cells. The reason for this uncertainty is that among all the directions that the flow might assume in a real

condition, discretization allows only the eight directions related to the eight neighbouring cells. As it is easy to understand, this uncertainty is equal to $\frac{2\pi}{8} = \frac{\pi}{4}$, being 8 the neighbouring cells for each cell of the DEM. Given this matter of fact, the difference among the two algorithms is the following:

- D8 algorithm does not include any correction option, since it considers only the local gradients, i. e. the gradients between a cell and its neighbours and it only chooses the direction as the LSD. Therefore, if a direction different from the real one is undertaken, then the error is cumulated along the flow and the simulated directions might be very distant from the real ones;
- GD8 algorithm presents two options of direction, i. e. the primary and the secondary directions and it considers not only local slopes, but also slopes given by "cells up to the highest-order neighbors" [37], being a global search. Therefore, it is able to reduce the cumulative error by evaluating global slope conditions and, on the basis of that, choosing the direction that follows the maximum global slope, between the two options it has.

4.3.3 *TEE, EEL, EE, EEE in the model*

The formulation of the criteria must be rewritten, according to DEM cell discretization

As it is shown in figure 4.5, the last operation performed by the model, after having exctracted the river network, is evaluating the values of the chosen criteria. In subsection 2.4.1 it was explained that the four objectives to test with our framework are Total Energy Expenditure (TEE), Energy Expenditure in any Link (EEL), Energy Expenditure (EE) and Equal Energy Expenditure (EEE). The definition previously provided for the four objectives was referred to a river network considered as composed by links and knots. In our model, since the basis is a DEM discretized with a certain number of cells, the objectives formulation needs to be translated according to this discretization, so that the river networks elementary components are not anymore links and knots, but cells. According to this assumption, the new formulation of the four objectives for a DEM having a number of rows of cells equal to N_{rows} and a number of columns equal to $N_{columns}$ is:

MINIMUM TOTAL ENERGY EXPENDITURE:

$$TEE = \min \left(\sum_{i=1}^{N_{rows}} \left(\sum_{j=1}^{N_{columns}} Q_{i,j}^{0.5} \, L_{i,j} \right) \right) \tag{4.3}$$

MINIMUM ENERGY EXPENDITURE IN ANY LINK:

$$EEL = \min \left(Var \left(\mathbf{Q^{0.5}L} \right) \right) \tag{4.4}$$

where $\mathbf{Q^{0.5}L}$ is the matrix containing the product $Q_{i,j}^{0.5}L_{i,j}$ for every (i-th, j-th) cell, with:

- $i \in [1; N_{rows}]$
- $j \in [1; N_{columns}]$

MINIMUM ENERGY EXPENDITURE PER UNIT AREA:

$$EE = \min\left(\sum_{i=1}^{N_{rows}}\left(\sum_{j=1}^{N_{columns}} Q_{i,j}^{0.5}S_{i,j}\right)\right) \tag{4.5}$$

EQUAL ENERGY EXPENDITURE PER UNIT AREA:

$$EEE = \min\left(\mathrm{Var}\left(\mathbf{Q^{0.5}S}\right)\right) \tag{4.6}$$

where $\mathbf{Q^{0.5}S}$ is the matrix containing the product $Q_{i,j}^{0.5}S_{i,j}$ for every (i-th, j-th) cell, with:

- $i \in [1; N_{rows}]$
- $j \in [1; N_{columns}]$

4.3.3.1 *Evaluating the objectives on a cell basis: is it reasonable?*

A question which rises at this point, given the new definition of the objectives based on a DEM cell basis discretization is: is this kind of discretization reasonable with respect to the evaluation of the four objectives?

Three reasons can be advanced in order to support the effectiveness of this discretization choice. The first one is that the formulation of the objectives changes according to the discretization, but their meaning does not: when Rodríguez-Iturbe et al. enunciated the TEE in [55], in the way it is written in subsection 2.4.1, it already was evaluated as an aggregated objective of discretized elements, having as elementary components the links of the network, which may vary their length. The evaluation of the objectives based on DEM cells only affects the aggregation as for the discretization technique, in the sense that now a regular grid is imposed on the analyzed network, but its features are not conditioned (the total length, discharge and slopes are the same). Therefore, the aggregation for objectives evaluation only changes the scale of the disaggregated elements, but not their overall aggregation. As an example, if a stream link has length $L = 10\,m$ and constant discharge $Q = 25\,m^3/s$, its TEE will be equal to $50\sqrt{(m^3/s)}m$; hypothesizing that the link is split into two cells, once a DEM grid is superimposed on it, each cell will have $L = 5\,m$ and $Q = 25\,m^3/s$, therefore its TEE is equivalent $TEE = 5 \times 5 + 5 \times 5 = 50\sqrt{(m^3/s)}m$. Of course, a proper DEM scale should be chosen, in order to perfectly maintain the same networks features and having exactly the same values for the objectives.

Nevertheless, as Rigon et al. prove through a multiscale analysis of river networks, that fractality property of river networks and subnetworks grants that "the networks of different sizes exhibit consistently the same statistic" [see 51, p. 1644]. Of course, changing the DEM scale causes a variation in the absolute values of the objectives, but the river network properties and scaling laws are not affected, therefore the objectives maintain their meaning and are suitable descriptors of the considered networks.

Finally, other important scientific studies evaluating optimality principles on DEM cell basis have been previously carried out: among them we cite [51] and [38].

4.3.3.2 *Drained area threshold for objectives evaluation*

Another topic related to DEM scaling and river networks extraction is the one of drained area support, or drained area threshold. As asserted by Tarboton, Bras, and Rodriguez-Iturbe, there is a particular drainage density value which should be set as minimum threshold for river networks extraction from a DEM, defined as

> a point of transition between the stable smoothing effects of diffusive processes at small scale and the unstable effects of concentrative processes, such as overland or open channel flow [see 66, p. 59].

In particular, it is shown in the same article that this value can be found as the maximum of the function relating slopes values to drained area values of a river network [67], [66].

This concept of drained area threshold was not considered for the objectives evaluation in our model. The reason is that, before introducing the spatial interpolator, the overall system (composed by model and optimizer) was structured requiring a control mask with a value for the variation in elevation for each DEM cell. As a consequence, all the controls affected the objectives values and, therefore, excluding the ones under the threshold from objectives evaluation would have lead to a lack of information in the controls-objectives correlation.

On the contrary, the concept of threshold is then considered during the evaluation of river networks according to naturality indexes, as the reader will notice while reading section 4.6 . In particular, it was set to 4 cells, i. e. $4\,km^2$, both for naturality indexes evaluation and river networks visualization, coherently with Paik's GLE model in [38], [37] and [39].

4.4 OPTIMIZATION ALGORITHMS

εNSGA-II, GDE3 and OMOPSO are the optimization algorithms used in our experiments, apart from random search.

In this section, the elements necessary to understand the phases described in box *(c)* of figure 4.1 are explained. As outlined in section 3.3, to search for the optimal landscape, i. e. the functions $f(\cdot)$

that minimize equation (3.15), an evolutionary algorithm approach is used. The following section shows the algorithms used, their differences and history and the reason for their use.

These algorithms are common and already implemented. We used a library that provides implementation together with managing functions, the *MOEA Framework* [15] created by Hadka, D. et al. As the website states,

> The MOEA Framework is a free and open source Java library for developing and experimenting with multiobjective evolutionary algorithms (MOEAs) and other general-purpose multiobjective optimization algorithms. The MOEA Framework supports genetic algorithms, differential evolution, particle swarm optimization, genetic programming, grammatical evolution, and more. A number of algorithms are provided out-of-the-box, including Nondominated Sorting Genetic Algorithm II (NSGA-II), epsilon Multi Objective Evolutionary Algorithm (εMOEA), Generalized Differential Evolution 3 (GDE3) and Multi Objective Evolutionary Algorithm based on Decomposition (MOEA/D). In addition, the MOEA Framework provides the tools necessary to rapidly design, develop, execute and statistically test optimization algorithms. [from 15, http://www.moeaframework.org/]

The library is actively developed with five releases in the last year, according to the website [15], easy to understand thanks to the object oriented framework and simple to extend with new problems. Documentation for its use is provided on the website and on the blog of the research group that mainly uses it [16].

Now, the algorithms used will be shown and explained. The choice of them is based mostly on the considerations in [49] and the availability of free versions. Additional information about epsilon Nondominated Sorting Genetic Algorithm II (εNSGA-II) and Generalized Differential Evolution 3 (GDE3) can be found in appendix B.

4.4.1 *eNSGAII*

εNSGA-II is a MOEA built on the Nondominated Sorting Genetic Algorithm II (NSGA-II), with the additional capabilities of ε-dominance archiving, adaptive population sizing and automatic termination to minimize the need for extensive parameter calibration [24]. The primary goal of εNSGA-II is to provide a highly reliable and efficient MOEA which minimizes the need for parameterization [24].

The parameters required to set up an optimization run of εNSGA-II are the initial population size, the maximum Number of Function Evaluations (NFE), the injection rate into the archive and the parameters related to simulated binary crossover and mutation operator.

Algorithm	Parameter	Suggested Values
Any	Number of Function Evaluations	10 000 ÷ 200 000
	Population Size	10 ÷ 1000
εNSGA-II	Injection rate	0.1 ÷ 1.0
	SBX rate	0.0 ÷ 1.0
	SBX distribution index	0.0 ÷ 500.0
	PM rate	0.0 ÷ 1.0
	PM distribution index	0.0 ÷ 500.0
GDE3	DE step size	0.0 ÷ 1.0
	Crossover rate	0.0 ÷ 1.0
OMOPSO	Archive size	10 ÷ 1000
	Perturbation index	0.0 ÷ 1.0

Table 4.1: Parameters needed for each MOEA used: if the algorithm requires the parameter, a range is given as in [49].

Suggested possible values for these parameters are shown in table 4.1.

4.4.2 *GDE3*

As the name suggests, Generalized Differential Evolution 3 [25] is the third improvement of the Generalized version of Differential Evolution EA [63]. It is a multiobjective variant of the DE algorithm. The GDE3 was one of the top rated in a competition for MOEAs [73].

Among GDE3 features, there is its mutation operator, which uses the scaled "difference" between two population members' decision variable vectors to generate new candidate solutions. This operator is called rotationally invariant and it does not assume explicit search directions when it creates new solutions. It also means that GDE3 does not require decisions to be separable and independent i. e. , they can have conditional dependencies.[5]

Another interesting feature of GDE3 is its constraint handling method: it reduces the number of needed function evaluations, being more efficient in finding solutions for constrained problem.

The parameters required to set up an optimization run of GDE3 are: initial population size, maximum NFE, crossover rate and step size of DE operator. With only four parameters, GDE3 appears to be very suitable for applications. As for εNSGA-II, suggested possible values for these parameters are shown in table 4.1.

5 SBX operator used by εNSGA-II assumes problems have independent decisions that can be optimized using only vertical or horizontal translations of the decision variables.

4.4.3 *OMOPSO*

Optimal Multi Objective Particle Swarm Optimization (Sierra and Coello Coello [61]) is one of the most successful multiobjective Particle Swarm Optimization algorithms to date. It is notable for being the first multiobjective Particle Swarm Optimization (PSO) algorithm to include ε-dominance and a crowding-based selection mechanism to identify the leaders to be removed when there are too many of them. It is also highly competitive, as the authors found after performing a comparative study with respect to three other PSO-based approaches and two MOEAs (the NSGA-II and Strength Pareto Evolutionary Algorithm 2 (SPEA2)).

The parameters required to set up an optimization run of OMOPSO are: initial population size, maximum NFE, archive size and perturbation index. As for εNSGA-II and GDE3, suggested possible values for these parameters are shown in table 4.1 .

4.4.4 *Random Search*

Among the algorithms included into the MOEA Framework, one is named Random Search. At each search step, it generates a new population with random sampled values of the input, evaluates it and adds the newly Pareto dominant solutions to an archive. Of course, this is neither an EA nor an efficient way to solve a MOP.

However, it is included into the following analysis as a benchmark of the ability of a proper MOEA to perform better than a random sampling of input values. In fact, this kind of search is not based on the connection between input values and optimal principles. Therefore, the comparison between the two procedure is an indirect assessment of the strength of that connection and gives an hint for understanding whether landscape evolution under river dynamics follows an optimality principle[6].

4.5 MULTIPLE APPROXIMATIONS OF THE PARETO FRONT

Again, this section is about the phases described in box *(c)* of figure 4.1. Subsection 3.3.4 introduced the choice of the use of EAs, but also underlined two important drawbacks of those algorithms. The first is that when the solution is unknown, it is impossible to know how far is the solution found by the MOEA from the real Pareto front. The second drawback is that parameterization can greatly impact the performance of an MOEA [49] [17] [18]. There is also a third point that is worth to be mentioned: the algorithms used here rely on random number generation to initialize the first population or to go on with the optimization process [49] [18]. The first one is deeply related with

6 see section 3.6 .

the other two: poor parameterization and unlucky random seed can prevent the MOEA to find good approximation of the Pareto front.

The proposed problem solving methodology tries to take care of these problems by increasing the number of optimization runs for each experiment. In other words, given a model setup and a choice of the optimality principles to test, the optimization process is repeated multiple times to overcome the dependency from the random seed number generator. Given the computational burden, it is repeated from five to ten times.[7]

As highlighted, the choice of the algorithm and the fine tuning of its parameter can deeply affect the quality of Pareto front produced. Lacking previous experiences with optimizations of this kind of problems, more than one algorithm has been selected. GDE3, εNSGA-II and OMOPSO are recognized to be top performing algorithms in water resources management field, which is the closer field of applications to the problem faced here. The parameterization would have required a random sampling of parameter values and multiple optimization with each of them. Computational burden and time availability prevent us to perform this operation: we therefore address this analysis to further research and present the results with hand-tuned parameters , aware of the limitations that comes with this.

4.5.1 *Recent trend in MOEAs*

Using multiple optimization algorithms means that we applied different selection, crossover and mutation operators to find the Pareto front. In particular, the algorithms take advantage of Simulated Binary Crossover and Differential Evolution crossover operators, of Polynomial Mutation and perturbation mutation operators and of different selection strategies, like archive or re-injection.

This is the recent trend in the development of MOEAs. Given the variety of fitness landscapes and the complexity of search population dynamics, Vrugt and Robinson [69] proposed to adapt the evolutionary operators used during multiobjective search, based on their success in guiding search. The multiobjective A Multi ALgorithm Genetically Adaptive Multiobjective (AMALGAM) MOEA [69] exploits multialgorithm search that combines the NSGA-II, PSO, DE, and Adaptive Metropolis (AM). The new Borg MOEA [17] features a multiple recombinations operator to enhance the search in a wide assortment of problem domains.

Another feature used by εNSGA-II, Borg and other MOEAs is the ε-box dominance archive for maintaining convergence and diversity throughout the search. It is also used to compose the best approx-

7 We will call experiment a set of optimization runs with the same model setup and same optimality criteria to be followed.

imation from different MOEA runs. It will be described in the next section.

4.5.2 *Epsilon box Pareto dominance*

The ε-box dominance is a concept that helps MOEAs to maintain any dominant solution they found during the optimization process. The same concept is used to aggregate multiple Pareto fronts which result from different optimization runs.

The problem that ε-box solves is called deterioration. It occurs whenever the solution set discovered by an MOEA at time i contains one or more solutions dominated by a solution discovered at some earlier point in time $j < i$, discarded during the optimization. Laumanns et al. [27] (2002) effectively eliminate deterioration with the ε-dominance archive and guarantee simultaneous convergence and diversity in MOEAs. Hadka and Reed gives this definition of ε-dominance archive:

Definition 1. For a given $\varepsilon > 0$, a vector $\mathbf{u} = (u_1, u_2, \ldots, u_M)$ ε-dominates another vector $\mathbf{v} = (v_1, v_2, \ldots, v_M)$ if and only if $\forall i \in \{1, 2, \ldots, M\}$, $u_i \leqslant v_i + \varepsilon$ and $\exists j \in \{1, 2, \ldots, M\}$, $u_j < v_j + \varepsilon$.

The ε-dominance provides also a minimum resolution that bounds the archive size and allows to specify different ε values for each objective. Conceptually, the ε-box dominance archive discretizes the objective space into subspaces with side-length ε, called ε-boxes. Therefore, the user of the algorithm is able to define the desired resolution of the objective values.

This very important concept is used to compose the multiple Pareto fronts resulting from the different executions of various algorithms. The resulting Pareto front will therefore contain the ε-dominant solution across all the solution points in all the Pareto front produced for a given experiment.

4.6 OUTPUT ANALYSIS TOOLS

The last operation conduced in our framework consists in evaluating the results according to naturality indexes.

From this point till the end of the chapter, the tools implemented for performing the phases included in box *(d)* of figure 4.1 are described. Once the Pareto front is obtained according to the techniques explained in section 4.5, each of its points can be visualized in the objectives space, i. e. the coordinates of each point are objectives values. An example of Pareto Front is provided in figure 5.1. Moreover, each point of the front represents a landscape, characterized by its elevation data and by the river network which develops on it. The objectives values related to each point are the values of TEE, EE, EEL, and EEE for the landscape hidden behind the point itself. Given that and

the workflow described in chapter 3 and figure 4.1, each point must be analyzed according to the naturality indexes defined in section 3.4:

- Horton's ratios R_B, R_L, R_L and R_S;
- Hack's law exponent;
- probability distribution of contributing area exponent;

In order to do that, some Matlab© functions were developed, as described in the following subsections.

4.6.1 *Matlab© functions for evaluating Horton's indexes*

Horton's indexes are evaluated, for each model output network, i. e. for each Pareto front point, using the base DEM, the values of the drained area and the flow directions for each of its cells. The procedure implemented in Matlab© is the following:

1. springs are identified. More precisely, a minimum threshold equal to 4 cells i. e. 4 km^2 is set, in accordance to Paik's work [38] and springs are so identified as cells draining such an area;
2. Strahler order is set to 1 for the identified spring cells;
3. flow directions are followed downstream and a Strahler order value is set for each cell of the DEM, in the same way as shown in the left side of figure 3.1. Of course, cells belonging to the same river branch will assume the same order. When two branches of orders i and j meet, the resulting branch order k is evaluated as in equation (4.7):

$$k = \max\left(i, j, \operatorname{int}\left(1 + \frac{i+j}{2}\right)\right) \tag{4.7}$$

4. Horton's ratios i. e. R_B, R_L, R_L and R_S are evaluated. In general, in order to simplify the analysis, and at the same time have a significant number of sample for analyzing the results, the mentioned ratios are evaluated only for the three networks of the DEM having the biggest drained area.

   Moreover, R_B, R_L, R_L and R_S are evaluated as 10^{ε} where ε is the average slope of the interpolating line of semilogarithmic plots of, respectively, number of streams for each order, average channel length, average channel drained area and average channel slope against order of stream, as shown in the example graphs in figure 4.7. As for the interpolation, in the case of R_B plot, it is imposed that the interpolating line passes through point $(\omega, 0)$, being ω the maximum order of the basin. The reason is that in a network there must be only one branch with maximum Strahler order, therefore $N(\omega) = 1$ and $\log(N(\omega)) = 0$.

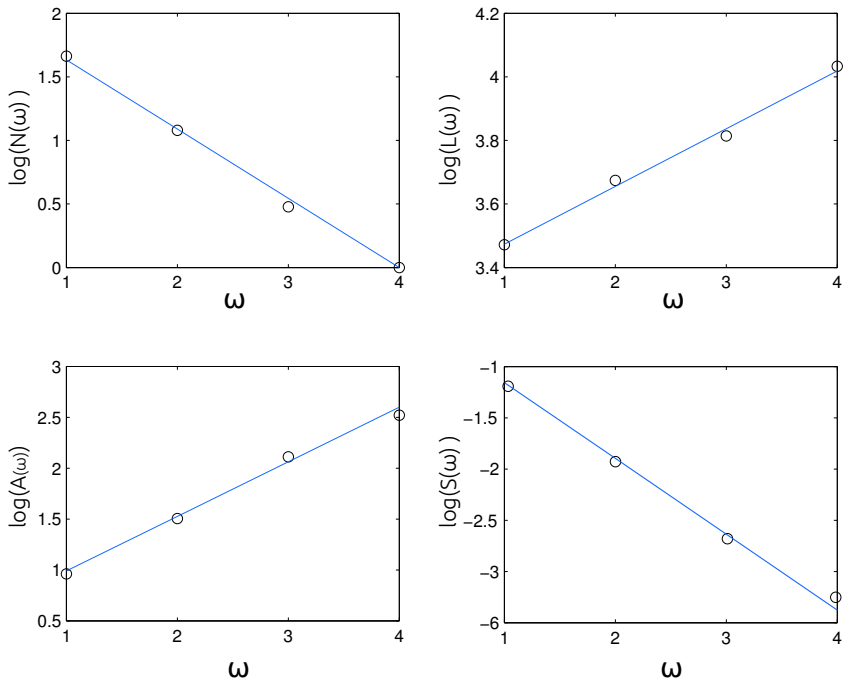

Figure 4.7: Horton indexes semilogarithmic plots. ω is the stream order. In the upper-left plot, N(ω) is the number of stream for each stream order. In the upper-right plot, L(ω) is the aveage channel length for each stream order. In the lower-left plot, A(ω) is the average drained area for each stream order. In the lower-right plot, S(ω) is the average slope for each order. The blue line in each plot represents the linear interpulation, whose slope is exponent ε for evaluating Horton ratios.

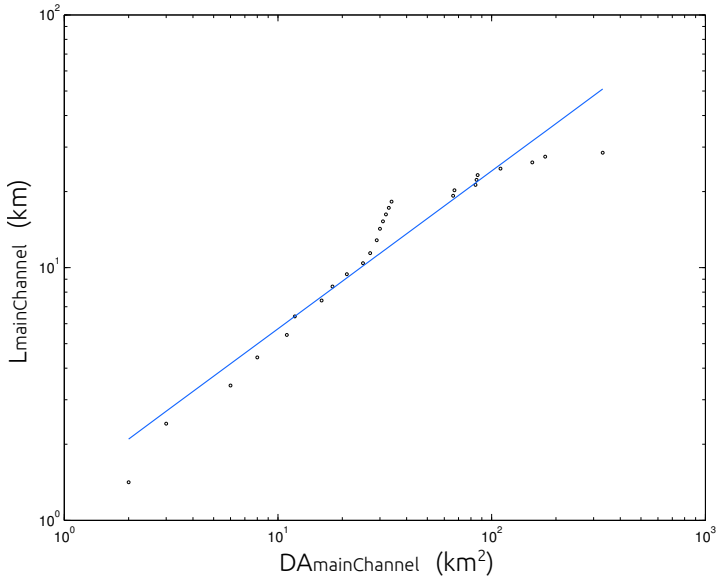

Figure 4.8: Hack's law logarithmic plot. $DA_{mainChannel}$ represents the drained area of the main channel of a network, at different distances $L_{mainChannel}$ from its spring. The blue line represents the linear interpulation, whose slope is Hack's law exponent h.

4.6.2 *Matlab© function for evaluating Hack's law exponent*

Remembering that Hack's law states that $L \propto A^h$ as in equation (3.20), the value of interest for evaluating the naturality of a river network is h. Moreover, since the law is valid for the longest stream from an outlet to the divide, as asserted in [12] it is evaluated including only the main channel of the considered basins (in our case the three biggest basins of each landscape). It is therefore estimated, for the main channel of each basin, using this algorithm:

1. the main channel is scrolled from the most upstream cell to the outlet, and the cumulative length $L_{mainChannel}$ is iteratively evaluated for each of its cells;

2. the cumulative drained area of each cell belonging to the main channel $DA_{mainChannel}$ is retrieved from the drained area matrix obtained as output of the model;

3. Hack's law exponent h is evaluated as the slope of the interpolating line in the logarithmic plot showing the relation between $DA_{mainChannel}$ and $L_{mainChannel}$ as the example presented in figure 4.8 .

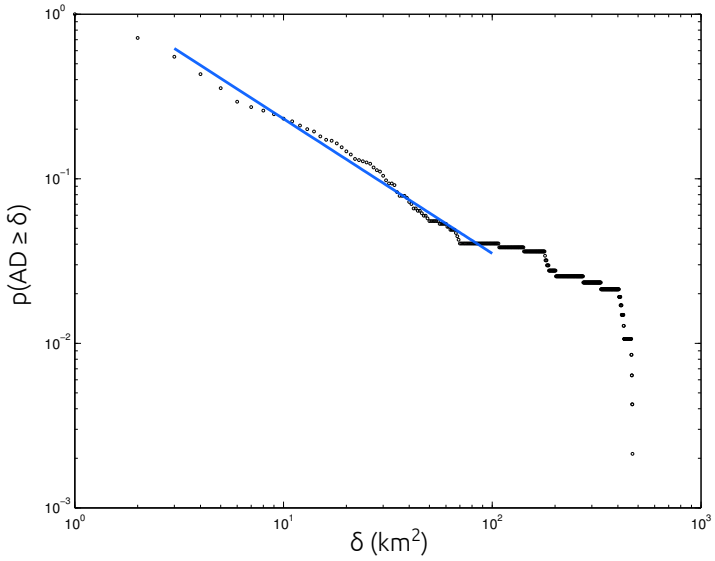

Figure 4.9: Probability distribution of drained area. δ is the drained area value the probability $p(DA \geqslant \delta)$ is iteratively evaluated for the considered basin. The blue line represents the linear interpolation, whose slope is the probability distribution of contributing area exponent.

4.6.3 *Matlab© function for evaluating the probability distribution of contributing area exponent*

The function for evaluating the exponent of the probability distribution of contributing area, i. e. β in equation (3.22), is implemented according to the following algorithm, which is repeated for each considered basin (in our case the three biggest ones for each landscape):

1. a probability distribution of drained area values is computed, considering the values for the cells belonging to the current basin. It is important to remind that the values of drained area for each cell are produced as outputs of the model. Again, only cells draining more than 4 cells (i. e. 4 km^2) are considered;
2. the cumulative probability distribution of drained areas is computed, starting from the probability distribution generated at step 1;
3. β is evaluated as the slope of the interpolating line in the logarithmic plot showing the cumulative distribution of drained area, as the example presented in figure 4.9 .

4.6.4 *Evaluating the number of indexes*

After analyzing each point of the Pareto front using the functions just described, the number of indexes obtained is the following:

NUMBER OF HORTON INDEXES N_{Horton}:

$$N_{Horton} = N_{points} \times N_{basins} \times N_{ratios} \tag{4.8}$$

where:

- $N_{ratios} = 4$ since it considers R_B, R_L, R_L and R_S;
- N_{points} is the number of points in the Pareto front;
- N_{basins} is the number of considered basins, for each point (in our analysis it is set to 3).

NUMBER OF HACK'S LAW EXPONENTS N_{Hack}:

$$N_{Horton} = N_{points} \times N_{basins} \tag{4.9}$$

NUMBER OF EXPONENTS OF THE PROBABILITY DISTRIBUTION OF CONTRIBUTING AREA $N_{probability}$:

$$N_{probability} = N_{points} \times N_{basins} \tag{4.10}$$

TOTAL NUMBER OF INDEXES ($N_{indexes}$):

$$N_{indexes} = N_{Horton} + N_{Hack} + N_{probability} \tag{4.11}$$

Assuming as an example a Pareto front composed by 1 000 points and considering the biggest 3 basins for each DEM, we would obtain a number of indexes to analyze equal to $N_{indexes} = 18\,000$. For this reason, a clustering technique was adopted, in order to simplify and speed the result analysis phase. It is described in the following paragraph.

4.6.5 *Clustering technique*

A clustering technique is needed, in order to face the extremely high number of results and analyze all of them.

As explained in the previous section , since the number of indexes produced analysing all the points of the Pareto front might be very big, a clustering technique is adopted, in order to be able to group points of the front and jointly analyze them.

> Cluster analysis [...] takes a sample of elements and groups them such that the statistical variance among elements grouped together is minimized while between-group variance is maximized [20].

The strategy is to group points of the Pareto front, based in the values of their objectives, select some representative clusters and then evaluate the distribution of naturality indexes for each of them. These two phases, i. e. clustering and building the distribution of naturality indexes are described in the next sections.

4.6.5.1 *Building the clusters: k-means clustering and silhouette*

In order to group the Pareto front points in meaningful clusters, the two following tools were used:

K-MEANS: it is the algorithm which, once a parameter k is set, organizes the points in k clusters;

SILHOUTTE: it is the criterion considered for setting the number of clusters, i. e. k for k-means algorithm.

These two elements are now detailed.

K-MEANS CLUSTERING ALGORITHM It divides a set of data into k exclusive clusters. Since clusters are exclusive, i. e. each point of the data set belongs to one and just one cluster, the clustering method is so called "hard" clustering. Each class is characterized by the number of points it includes and the coordinates of a centroid. A centroid is defined as "the point to which the sum of distances from all objects in that cluster is minimised" [30]. In order to set the position of the k centroids and define clusters in a way that "the distances from all objects in the cluster is minimised", the algorithm is iteratively computed: "The entire procedure is essentially a gradient-based algorithm" [23]. We used the Matlab© implementation of this algorithm.

SILHOUETTE It is a criterion which helps finding the number of clusters which best fits for the given data set. It works as described in [30]:

1. a function $\omega(i)$ is defined for the i-th point as the average distance from the points itself to the other points of the same cluster;
2. a function $b(i)$ is defined for the same i-th point as the minimum average distance from the point itself to the points of another cluster;
3. silhouette is computed, for the i-th point as in equation (4.12)

$$s(i) = \frac{b(i) - \omega(i)}{max[b(i), \omega(i)]} \tag{4.12}$$

It is therefore a measure of how well a point fits with the points belonging to the same cluster, in comparison with how it fits in other cluster. It assumes values in the range $[-1; +1]$: is close to 1 when the point well fits with its belonging cluster, i. e. it is distant from the neighbouring ones, and vice-versa when it is close to -1.

CHOOSING THE NUMBER OF CLUSTERS Since the "average silhouette width for the entire data set" [30] can be evaluated as the average of single points silhouette over the entire data set, the following iterative procedure was implemented, in order to chose a good number of clusters k for k-means algorithm:

1. k-means algorithm is run with $k = 2$ i. e. two clusters;
2. the average silhouette width for the entire data set is computed, for the given k number of clusters;
3. k is incremented and the procedure is iterated from step 1.

In order to avoid a too large number of clusters, a maximum value of cluster k equal to $\sqrt{\frac{n}{2}}$ was imposed according to [20], where n is the number of data in the dataset.[8]

Moreover, since the Pareto front we obtained present a situation of conflict at least between two objectives, we usually required a minimum number of clusters equal to three. In fact, if the Pareto front is projected on two dimensions (the ones of the conflicting objectives), a number of clusters equal to three allows the identification of two extremes areas (where only one objective is minimized, while the other is not, and vice-versa) and one compromise among the previous two. Applying the procedure just described, a clustered Pareto front is obtained; an example is shown in figure 5.12.

4.6.5.2 *Naturality indexes for each cluster*

Once the clustering of the Pareto front is performed, and given the fact that naturality indexes were evaluated for each of the considered biggest basins, for each point of the front, the values of the naturality indexes obtained from the synthetic landscapes (i. e. the outputs of the model) must be compared to typical values characterizing natural basins. For doing so:

1. for each naturality index, for each cluster, the statistical distribution of the current index values obtained for the basins of the points in the cluster is computed;
2. the area of the distribution laying within the natural range of the index is integrated;
3. the distributions of the current indicator are compared among different clusters.

An example of this kind of analysis is represented in figure 4.10 where the naturality index R_A is contemplated and 3 clusters are considered. The bounds represent the typical range assumed by the

8 As an example, a Pareto front of 1 000 points will be organized in maximum 22 clusters.

NATURALITY INDEX	NATURAL RANGE/VALUE
R_B	$3 \div 5$
R_L	$1.5 \div 3.5$
R_A	$3 \div 6$
R_S	$1.5 \div 3.5$
h exponent of Hack's law	0.6
β exponent of drained area probability distribution	$0.43 \div 0.45$

Table 4.2: Typical natural ranges for naturality indexes.

index in natural networks. A remainder of the values is summarized in table 4.2.[9]

9 Ranges and indexes are defined in section 3.4.

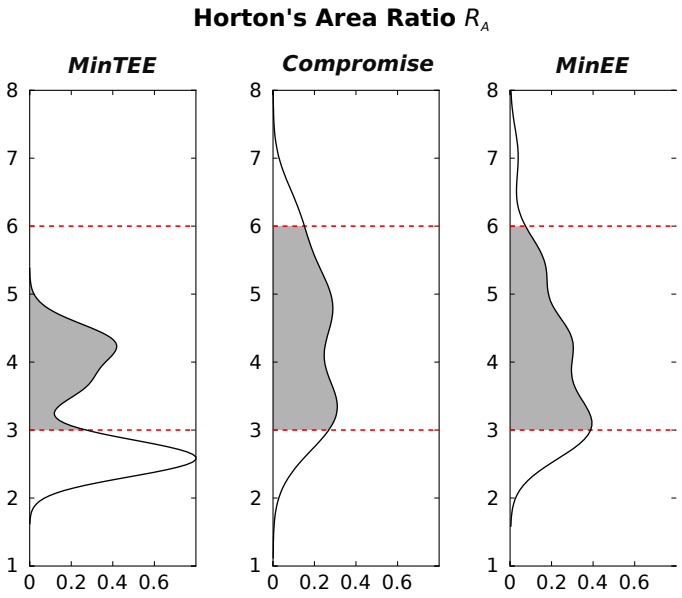

	MIN TEE	COMPROMISE	MINEE
Number of analyzed points	40	118	40
Sample mean and standard deviation	3.258 ± 0.811	4.343 ± 1.184	4.037 ± 1.157
Probability within natural range	0.4831	0.7463	0.7153

Figure 4.10: Statistical distribution of Horton's area ratio within clusters. The chosen clusters are the same of figure 5.12: they are the two extremes of the Pareto front shown in figure 5.10 and a compromise between them. The three graphs show the statistical distribution of the Horton's area ratio for each of the three biggest basin of each Pareto front point within the cluster i. e. of each DEM member of the cluster. On the y there is the ratio value, on x axis the percentage value. The gray area corresponds to the probability within the natural range of variations of the index.

5 SIMULATIONS AND FINDINGS

Science, my boy, is made up of mistakes, but they are mistakes which it is useful to make, because they lead little by little to the truth.

— Verne *Journey to the Center of the Earth*

The reader should now be aware of all the concepts, tools and methods hidden behind the multi-objective framework detailed in the previous chapters. This chapter constitutes the last point before concluding with some final remarks and open issues. In fact the results obtained by running our framework with several experiments are now exposed. The hypotheses onto which this thesis is built on, explained in previous chapters are now going to be tested through the analysis of the results of the experiments.

5.1 OVERVIEW ON THE EXPERIMENTS PERFORMED

Three main experiments were carried out. The logic order adopted for presenting them is the same adopted during the research. Each experiment is performed with the goal of bringing some improvements to the results of the previous ones. The three experiments will be called from this point on MOGLE , MOGLE_RAINY and MOGLE_RAINY_IDW . Here they are briefly described:

MOGLE a multi-objective GLE is performed with our framework, including the four objectives TEE, EE, EEL and EEE. The hydrological parameters adopted by Paik in [38] are used, i. e. rainfall equal to 0.1 mm/h and runoff coefficient equal to 1.0.

MOGLE_RAINY this experiment is equal to the previous one but for the input rainfall parameter that is increased from 0.1 mm/h to 10.0 mm/h. Moreover, the range of possible values which control variables can assume is increased;

MOGLE_RAINY_IDW IDW spatial interpolator is added to the model of experiment MOGLE_RAINY .

More precisely, the common model settings of the three experiments are summarized in table 5.1, their model settings differences are written in table 5.2, while the different optimization settings for them are listed in table 5.3.

In addition to the information in table 5.3, the following two parameters were set, in the same way for each algorithm:

COMMON FEATURE	DESCRIPTION / VALUE
Optimality principles	TEE EE EEL EEE
Initial DEM shape	square pyramid (top elevation 100 masl)
DEM cell dimension	1 km × 1 km
DEM number of cells	51 × 51
Elevations sum conservation tolerance	0.001 (i. e. 1‰)
Depression filling algorithm	Planchon's DF
Flow directions algorithm	GD8

Table 5.1: Common model settings for all the three analyzed experiments: MOGLE , MOGLE_RAINY and MOGLE_RAINY_IDW.

	MOGLE	MOGLE_RAINY	MOGLE_RAINY_IDW
Rainfall (mm/h)	0.1	10.0	10.0
z **range (m)**	$(-10; +10)$	$(-20; +20)$	$(0; 400)$
z **discretization (cm)**	100	2	2
Interpolator	-	-	IDW

Table 5.2: Different model settings for all the three analyzed experiments: MOGLE , MOGLE_RAINY and MOGLE_RAINY_IDW.

- population size of 500 individuals. It represents the number of initial individuals for the GAs;
- ε values for ε-box widths equal to 100.0 for TEE, 100.0 for EEL, 0.1 for EE and 0.001 for EEE.

5.1.1 *Computational effort*

One last important comment which is due before starting the real analysis of the results is about the computational effort which was required to perform the just described experiments, both in term of time spent and number of operations executed. As it is possible to read from table 5.3, a total number of 530 millions of NFE run for the three experiments we are commenting in this chapter, requiring a total execution time of over 1400 hours (about two months!). In addition, other preliminary and testing experiments were performed, for an additional execution time of approximately 326 hours.[1]

1 All experiments were run on Lion-XO, a computational cluster run by the High Performance Computing Group (PennState University) with a total number of 192

EXPERIMENT	GENETIC ALGORITHM	SEEDS	NFE
MOGLE	εNSGA-II	2	10M
	GDE3	3	10M
	Random	5	10M
MOGLE_RAINY	εNSGA-II	2	10M
	GDE3	4	10M
	Random	5	10M
MOGLE_RAINY_IDW	εNSGA-II	11	10M
	GDE3	11	10M
	OMOPSO	10	10M

Table 5.3: Different optimization settings for MOGLE , MOGLE_RAINY and MOGLE_RAINY_IDW experiments. In the column SEEDS, the number of initial random seeds for each algorithm is listed. NFE stands for Number of Function Evaluations.

5.2 FIRST EXPERIMENT RESULTS: MOGLE

This preliminary experiment, as said, was performed using the same hydrological parameters used in [38] and considering the four selected formulations of the optimality principle. A control variable corresponds to each DEM cell and makes it change its elevations. In particular, the range for control variables was set equal to $[-10; +10]$ meters[2], and the discretization step of this interval was set to 1 m (the same discretization step used by Paik in his GLE model.

5.2.1 *Pareto front*

The Pareto front obtained as a result of the optimization of this experiment is the one represented in figure 5.1.

In the figure, it is possible to see that the Pareto front has four dimensions, due to the choice of four criteria to test: three are given by x, y and z axis, while the fourth one is represented through a color bar. All the points composing the front are therefore optimal, with respect to the the four objectives of the minimization problem. The fact that they appear spread into the 4 dimensional space might suggest that, among them, some kind of conflict exists. If no conflict existed, probably a single optimum point would be found, in spite of the Pareto front. The topic of conflict will be treated soon, but firstly some technical features of the front are described.

processors *AMD Opteron 250 2.4 GHz* and *AMD Opteron 852 2.6 GHz* and a total RAM of 768 GB.

2 The interval was chosen in order to have a good theoretical feasibility, which, according to figure 4.4, should be between 30% and 40%, with such a control range.

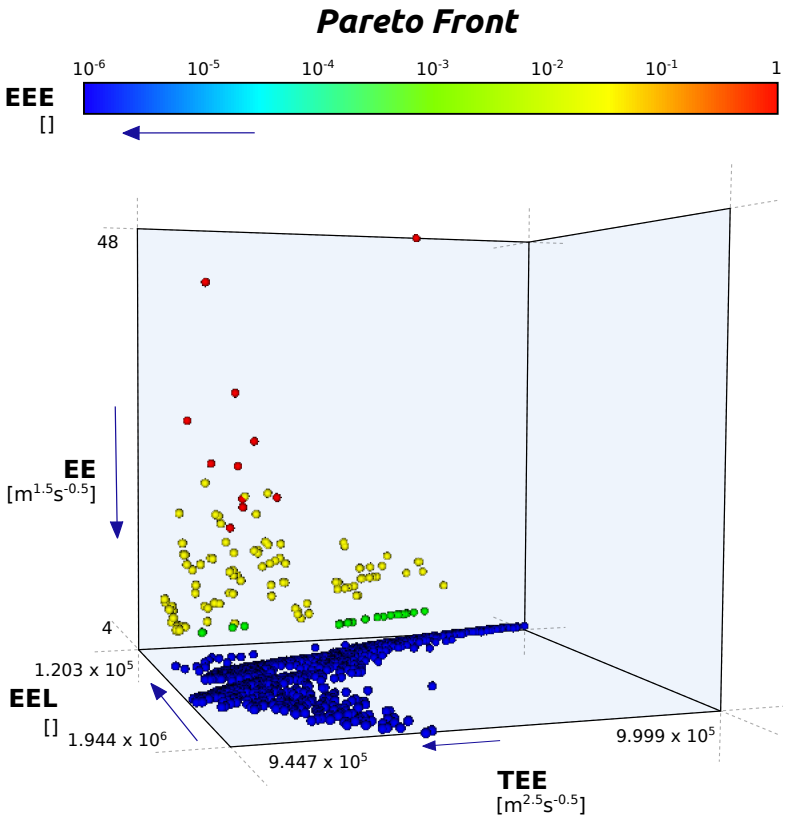

Figure 5.1: Pareto front obtained from MOGLE experiment. The front was represented using AeroVis©.

5.2.1.1 *Algorithms performance*

Table 5.4 provides some information on the just shown front. In particular, the number of points of the front each algorithm contributed to is shown, together with the feasibility. As for feasibility, it represents the number of control sets respecting the mass constraint over the total number of generated sets, for each algorithm in the first three rows and for the total number of function evaluations in the last row.

ALGORITHM	NUMBER OF FRONT POINTS	FEASIBILITY (%)
εNSGA-II	1103	58.70
GDE3	102	64.44
Total	1205	61.57

Table 5.4: MOGLE: Pareto front features.

The largest contribution is therefore coming from εNSGA-II algorithm, covering the 91.5% of the front, and the feasibility of the two algorithms are comparable. Since the average feasibility is higher than 60%, it is possible to say that the two algorithms are quite good at recognizing the mass constraint and find feasible control sets.

5.2.1.2 *Comparison with Random search*

It is possible to assess the effectiveness of the use of EAs also by comparing their results to the ones obtained with a random search algorithm. As written in table 5.3, this experiment was executed also running random search algorithm on five seeds. The result, which has to be compared with EAs performance, is the following:

- the capability of the random search algorithm to find control sets which respect mass constraint is around 3.38%, which is very low if compared to the one just mentioned of EAs, higher than 60%. This means that EA permorm better in understanding the mass constrain;
- the feasible points found with random search algorithm can be compared with the ones produced by EAs, in the objective space. As it is represented in figure 5.2, two fronts are compared: the blue front is the one presented at the beginning of this section, while the red one is computed considering the feasible points of random search. It clearly appears that the red front is dominated by the blue one: that means that EAs perform better than random search as for the minimization problem. Moreover, again due to the higher feasibility of EA, the number of points

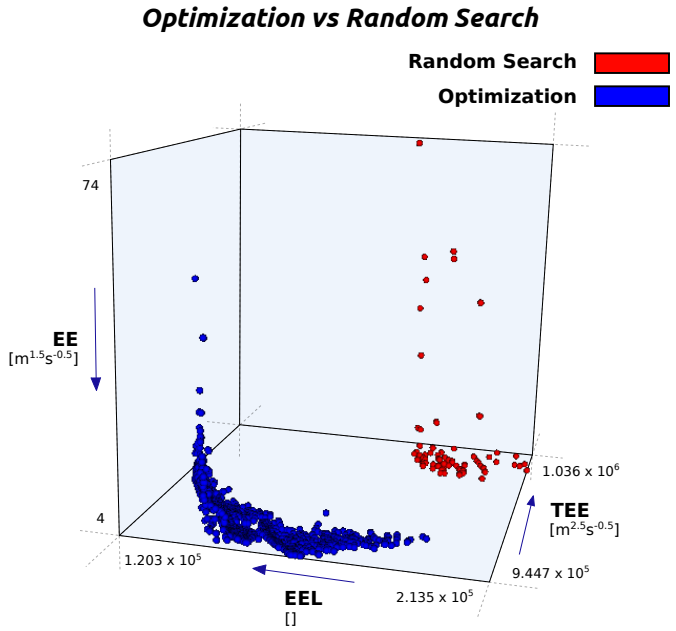

Figure 5.2: MOGLE : Pareto front obtained with EAs compared with the one obtained with Random search. The front was represented using AeroVis©.

in the blue front is larger than the one of the red ones, which are only 80.

The use of EA seems then justified.

5.2.2 *Analysis of the conflict*

It appears from the front, even if it is not very clear, that a possible conflicting situation might intercur between TEE and EE objectives. It is highlighted in figure 5.3. This conflict can be expected and explained, if Rodríguez-Iturbe et al. considerations are balanced:

> If the rate of energy expenditure per unit area of channel is maintained the same [...], then the minimum total rate of energy expenditure, corresponds to the network with the largest Ω.[...] If one maintains the total rate of energy expenditure, as a constant in all cases [...] implies a rate of energy expenditure per unit area of channel largest for the network with the minimum Ω and smallest for the network with the minimum Ω [see 55, p. 1098].

In fact, since in our model TEE is the total rate of energy expenditure and EE is the rate of energy expenditure per unit area of channel, it seems that the theory hypothesizes a conflict between them.[3]

3 Ω is the order of basin network which for a fixed number of sources is also a measure of the degree of branching.

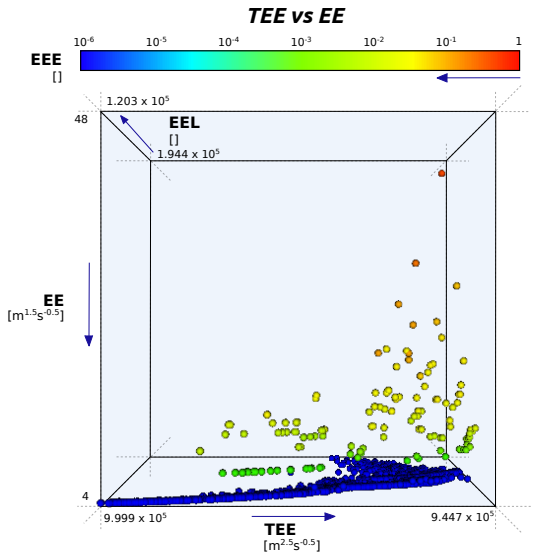

Figure 5.3: Pareto front view on the plane (TEE; EE) for MOGLE experiment. The front was represented using AeroVis ©.

Furthermore, also the relation between TEE and EEL is not clear: it is not possible to clearly establish whether they are conflicting or not. Their behaviour is highlighted in figure 5.4.

One evident thing, on the other hand, is that EE and EEE are no conflicting. For this fact, it is possible, for the next analysis, i. e. clustering, to consider just three objectives, in order to reduce the dimensionality of the objectives space, keeping into account that minimizing EE means also minimizing EEE.

5.2.3 *Clustering and naturality indexes analysis*

In this experiment, five clusters were obtained with k-means clustering and are represented with different colors in figure 5.5.

Despite the fact that conflict appears to be a bit confused, in order to simplify the analysis, only three clusters were selected for carrying out the assessment through naturality indexes. They were chosen in order to have two extreme values and one compromise among TEE and EE objectives. They are the following:

MINTEE: this cluster minimizes TEE objective, counting against EE objective;

COMPROMISE: this cluster represents the compromise between TEE and EE objectives;

MINEE: this cluster minimizes EE objective, counting against TEE objective;

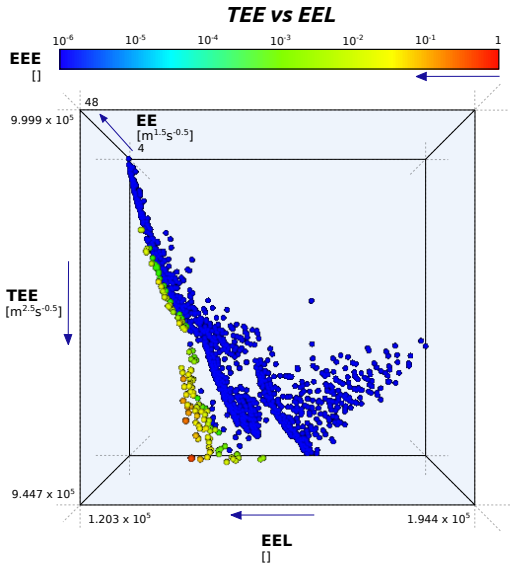

Figure 5.4: Pareto front view on the plane (TEE; EEL) for MOGLE experiment. The front was represented using AeroVis ©.

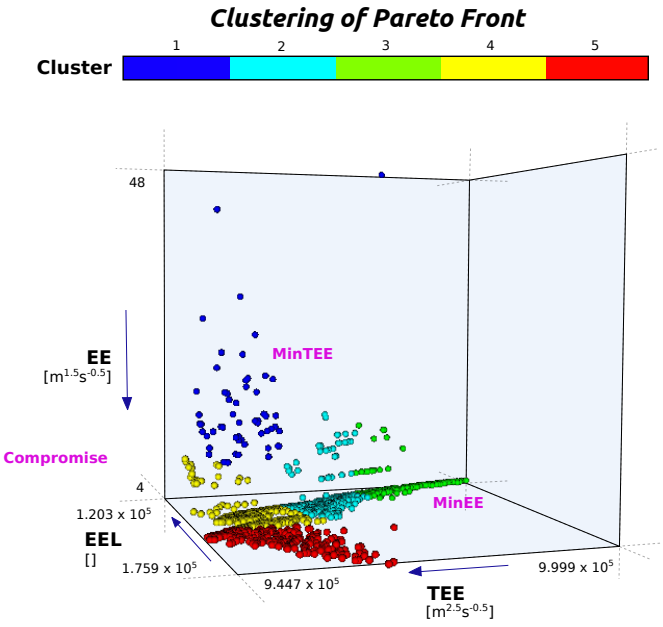

Figure 5.5: Pareto front clusters for MOGLE experiment. The upper colorbar shows the colors of the different 5 clusters. Cluster *Min*$_{TEE}$ is the blue one, *Compromise* is the yellow one and *Min*$_{EE}$ the green one. They are selected for naturality indexes analysis. The front was represented using AeroVis ©.

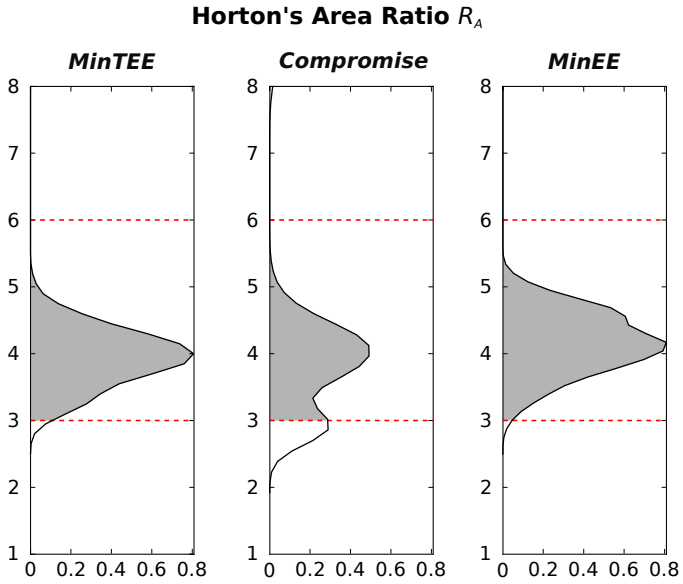

Figure 5.6: Statistical distribution of values of Horton's R_a for the clusters of experiment MOGLE . The chosen clusters are the same of figure 5.5. On the y there is the ratio value, on x axis the percentage value.

Coherently with the framework described in the previous chapter, naturality indexes were computed for the three largest basins of each point of the three clusters. Probability distributions were built on their values, and the most important results about them are commented in the following paragraph. All less relevant results are included in appendix C.

5.2.3.1 *3D networks features*

As just mentioned, probability distributions of naturality indexes were created for the analyzed clusters, as the example shown in figure 5.6 for Horton's R_a index.

As it is possible to see from figure 5.6, the gray area represents the area of probability within the natural range. Statistics about this area, for all Horton's ratios are summarized in table 5.5.

From the data in the table, no particular trends among the different clusters can be found, but a clear result appears: it seems that on the indexes assessing the 2D naturality of river networks, i. e. R_b, R_a and R_l, selected clusters do not perform so bad, being their probability higher than 50% for R_a and R_l, with also values higher than 90% of probability, and maintaining values around 30% for R_b. On the contrary, it is evident that slope is really badly reproduced, since none of the values are inside the natural range.

The obtained result for this preliminary experiment is therefore partial, in the sense that it fails at reproducing the natural features

	MIN TEE	COMPROMISE	MIN EE
Number of cluster points	58	382	185
Area within natural range of R_b [%]	32.73	26.56	29.59
Area within natural range of R_l [%]	61.79	60.41	52.62
Area within natural range of R_a [%]	82.84	61.31	95.23
Area within natural range of R_s [%]	0	0	0

Table 5.5: Naturality indexes statistics for MOGLE. The three cluster for which data are shown, are the same of figure 5.5.

of river networks with respect to the dimension of elevation and its consequent slopes.

A reason for that can be that the model, as it was set for this experiment had strong limitations:

- the range variable controls can assume values in maybe is too narrow and does not allows control variables to assume values which could better satisfy the chosen optimal criteria and reproduce better synthetic landscapes;
- the number of control variables maybe is too high: there is a control variable for each DEM cell. Because of that, the relation between controls and objectives could be weak;
- the first two points might also affect the capability of the model to reproduce the conflict among objectives and distinguish among the networks related to their trade-offs;
- the choice of the hydrological parameter of rainfall, equal to 0.1 mm/h, may limit the system. In fact, in the nature, rivers shape the landscape when they are in a condition of bank-full discharge. It can be supposed that a strong rainy event increase the system action in transferring mass and shaping itself. Therefore, it might be possible that 0.1 mm/h is too low.

5.2.3.2 *General conclusion on MOGLE*

In light of the results obtained for this first experiment, it appears that a large part of the optimized networks, obtained from the Pareto front points, are characterized by acceptable values for those indexes which evaluate the 2D features of a river network, but show bad distributions with respect to Horton's slope ratio. Therefore, as in Paik's

GLE model, there are problems in properly representing the third dimension of river networks. As a consequence, the following question rises: What are the limitations causing the inability of simulating good longitudinal profiles for river channels?

The experiments which are analyzed in the following two sections were made in order to answer this question.

5.3 INCREASING RAINFALL: MOGLE_RAINY

Experiment MOGLE_RAINY is commented in this section. As written in the experiments description at the beginning of this chapter, this second experiment differs from the previous one as for the value given to the rainfall input parameter. It was increased from 0.1 to 10 mm/h, in order to consider a rainfall value typical of an average natural rainy event. [4]

Another important feature of this experiment is the discretization of control variables ranges. In fact, as underlined in the comments of the previous experiment, the chosen range limited the actions of control variables, therefore, a new setting was adopted:

- in MOGLE , the elevation of each cell could vary in the range $[-10; +10]$ meters, discretized with the resolution of 1 meter;
- in this MOGLE_RAINY , the elevation of each cell is allowed to change in the range $[-20; +20]$ meters, discretized with the resolution of 2 centimeters.

This change could increase the complexity of the search for feasible control variables sets, but allows the control variables to have a bigger degree of freedom in their acceptable range, since they can assume a greater number of values within it, which can recombine in many different control sets.

All other features and model settings are equal to the ones of the first experiment: they were summarized in table 5.1 , at the beginning of this chapter.

5.3.1 *Pareto front*

The Pareto front obtained as a result of the optimization of this experiment is the one represented in figure 5.7.

5.3.1.1 *Algorithms performance*

As for the first experiment, some important features of the Pareto front shown in the previous section are summarized in table 5.6. We

4 Such a value can be considered as representative of extreme rainy events, as confirmed, for example, by the data gathered in [13].

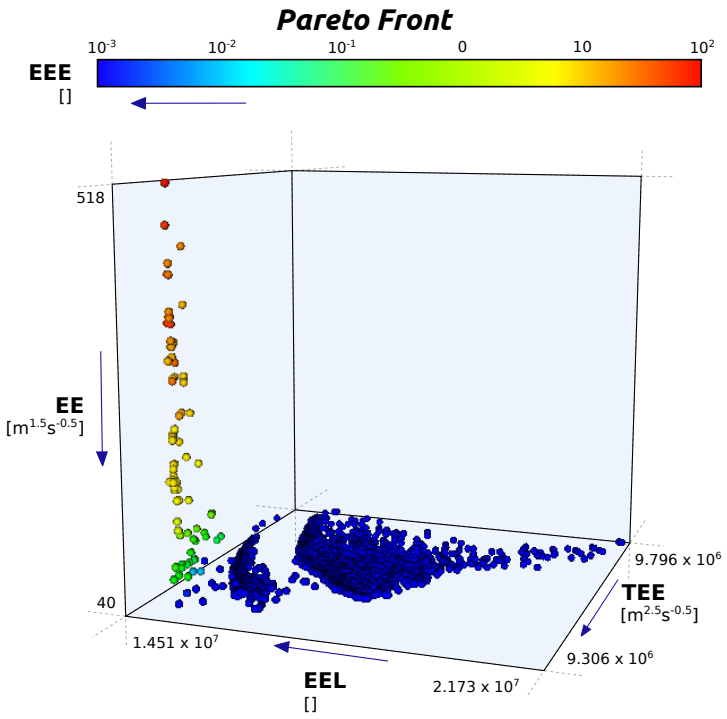

Figure 5.7: Pareto front obtained from MOGLE_RAINY experiment. The front was represented using AeroVis©.

remind that, as for feasibility, it represents the number of control sets respecting the mass constraint over the total number of generated sets, for each algorithm in the first three rows and for the total number of function evaluations in the last row.

ALGORITHM	NUMBER OF FRONT POINTS	FEASIBILITY (%)
εNSGA-II	2145	62.05
GDE3	115	44.61
Total	2260	53.33

Table 5.6: MOGLE_RAINY: Pareto front features.

The largest contribution is therefore coming from εNSGA-II algorithm, covering over the 94% of the front. εNSGA-II is also the algorithm having the largest feasibility suggesting that is the one which best recognise the mass constraint.

5.3.1.2 *Comparison with Random search*

Also for this experiment, the performance of EAs is compared to the one of Random search algorithm. In this case, the performance of EA is extremely superior, if compared to Random search. In fact, random

search feasibility of finding control sets respecting the mass constraint is 7.2×10^{-5} (on 50 millions of NFE, only 36 feasible control sets were found and all of them are dominated by the front given by EAs). This fact confirms that EAs can better recognise the mass constraint and now, since the range for control variables is larger and the resolution is finer, random search is very limited in finding proper combinations of controls, while EAs lowered a bit their feasibility with respect to the one they had in MOGLE, especially GDE3, but they work much better that random search.

5.3.2 *Analysis of the conflict*

The conflict can be analyzed again looking at the front. In particular:

- it is very clear that EE and EEE are not in conflict at all;
- the conflict between TEE and EE,supposed thanks to [55], is now more clear than in the first experiment and the front is concave with respect to their projection;
- the relation between TEE and EEL is still unclear, but, despite the points are still widespread, it seems there is not much conflict between them.

Given these considerations, it is possible to say that the new configuration of the model better allows to show the conflict among objectives, with respect to the first experiment. Clustering and naturality index analysis might help the interpretation of this conflicting situation.

5.3.3 *Clustering and naturality indexes analysis*

In this experiment, five clusters were obtained with k-means clustering and are represented with different colors in figure 5.8.

As in the previous experiment, only three clusters were selected for carrying out the assessment through naturality indexes. They were again chosen in order to have two extreme values and one compromise among TEE and EE objectives. They are the following:

MINTEE: this cluster minimizes TEE objective, counting against EE objective;

COMPROMISE: this cluster represents the compromise between TEE and EE objectives;

MINEE: this cluster minimizes EE objective, counting against TEE objective;

Furthermore, coherently with the previous experiment, distributions of naturality indexes were built, and the most important results

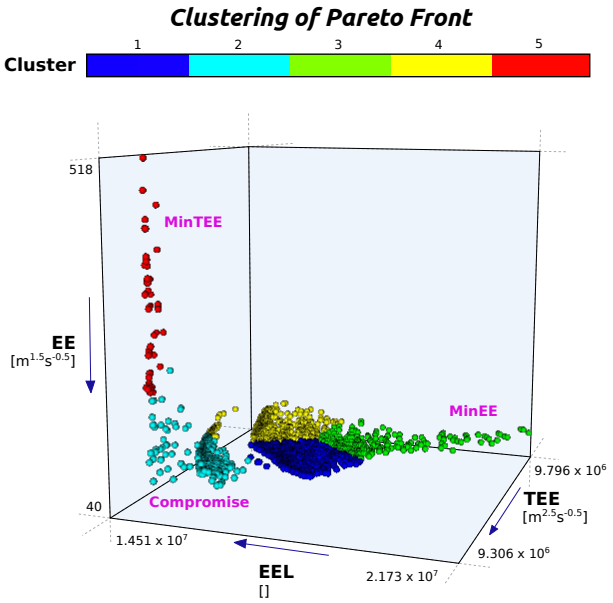

Figure 5.8: Pareto front clusters for MOGLE_RAINY experiment. The upper colorbar shows the colors of the different 5 clusters. Cluster *Min*$_{TEE}$ is the red one, *Compromise* is the light blue one and *Min*$_{EE}$ the green one. They are selected for naturality indexes analysis. The front was represented using AeroVis ©.

about them are commented in the following paragraph. We remind that all less relevant results are included in appendix C.

5.3.3.1 *3D networks features*

Again, considering the values of naturality indexes and their probabilities of being in a natural range, the results is quantitatively different from the previous experiment, but not qualitatively. Important values for Horton's ratio and Hack's law, for each cluster, are summarized in table 5.7.

Given the values in the table, it is possible to assert that, with the settings adopted for this experiment, again no particular trends and trade-offs among the clusters are shown, but the 2D features of river networks are really well represented, in the sense that their values of naturality indexes are for the majority inside natural ranges with high probability. The areas of Horton's ratios distributions (R_b, but mainly R_a and R_l) inside natural ranges are very high and many o them higher than 90%. Moreover, another index which describe the planar orgnization of river networks, i. e. Hack's law exponent is very close to 0.6, its "natural" value. Its distributions are show in figure 5.9.

On the other hand, the model is again limited when the slope, and therefore the third dimension should be reproduced. Comments on

	MIN TEE	COMPROMISE	MIN EE
Number of cluster points	55	598	243
Area within natural range of R_b [%]	77.69	54.87	91.58
Area within natural range of R_l [%]	94.40	81.83	92.00
Area within natural range of R_a [%]	96.36	96.24	95.03
Area within natural range of R_s [%]	1.79	0.3	0
Hack's law exponent	0.67	0.68	0.66

Table 5.7: Naturality indexes statistics for MOGLE_RAINY.

that are present in the last paragraph of this section, introducing the third experiment.

5.3.3.2 *General conclusion on MOGLE_RAINY*

It appears that the changes introduced in the model with respect to MOGLE , were useful in order to improve the performance on reproducing 2D networks, but still 3D features are missing. The hypothesis for that are, now:

- the range of control variables, even if it was enlarged and a finer resolution was adopted, remains a limitation for them and does not let the landscape evolve completely freely;
- apart from the range of control variables, their number is the main issue. When the number of controls is too high, it looses the link with the objectives;
- if each DEM cell is related to a single control value, different, even neighbouring, cells of the DEM evolve too independently from the closest ones. Therefore, the surface of the landscape is not enough smoothed and this fact, together with the action of depression filling algorithm, contributes in creating sudden steps, peaks and unnatural slopes.

Mainly for the last reason, a spatial interpolator is integrated with the next, last experiment.

5.4 SPATIAL INTERPOLATION: MOGLE_RAINY_IDW

Experiment MOGLE_RAINY_IDW is commented in this section. As written in the experiments description at the beginning of this chapter,

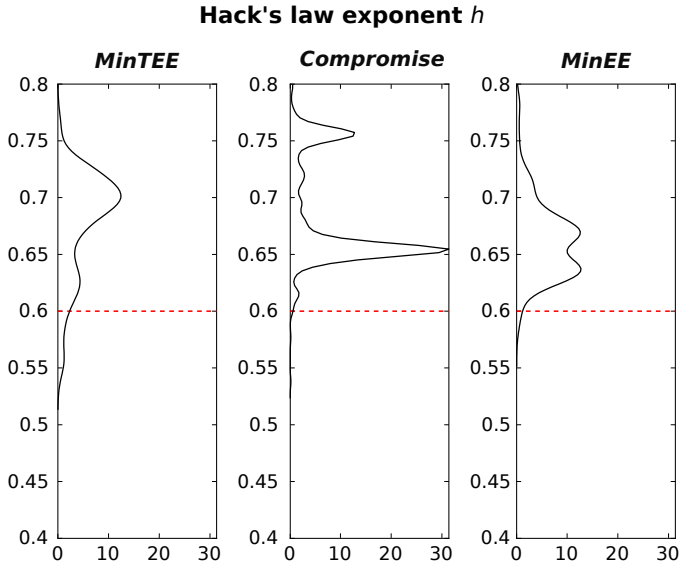

Figure 5.9: Statistical distribution of values of Hack's law exponent for the clusters of experiment MOGLE_RAINY . The chosen clusters are the same of figure 5.8. On the y there is the ratio value, on x axis the percentage value.

this third experiment includes the IDW spatial interpolator algorithm, explained in subsection 4.1.3 .[5]

5.4.1 *Spatial interpolator settings*

The following parameters were set for IDW:

- FREQUENCY: 10 cells. It means that on a 51×51 cells DEM, since the border is excluded, the number of $f(\cdot)$ values to optimize is reduced to 16. All the other elevations are obtained through interpolation;
- WINDOW: 15 cells. It means that the elevation of each cell is interpolated only on the optimized $f(\cdot)$ elevation values present in the square mask composed by its neighbouring 225 cells.

5.4.2 *Pareto front*

The Pareto front obtained as a result of the optimization of this experiment is the one represented in figure 5.10 .

5 It is useful to remind that the spatial interpolator was implemented in order to let the optimizer create the concave bed profile and to reduce the number of points the optimizer has to evaluate function $f(\cdot)$ for, so that the connection between objectives and controls is reinforced.

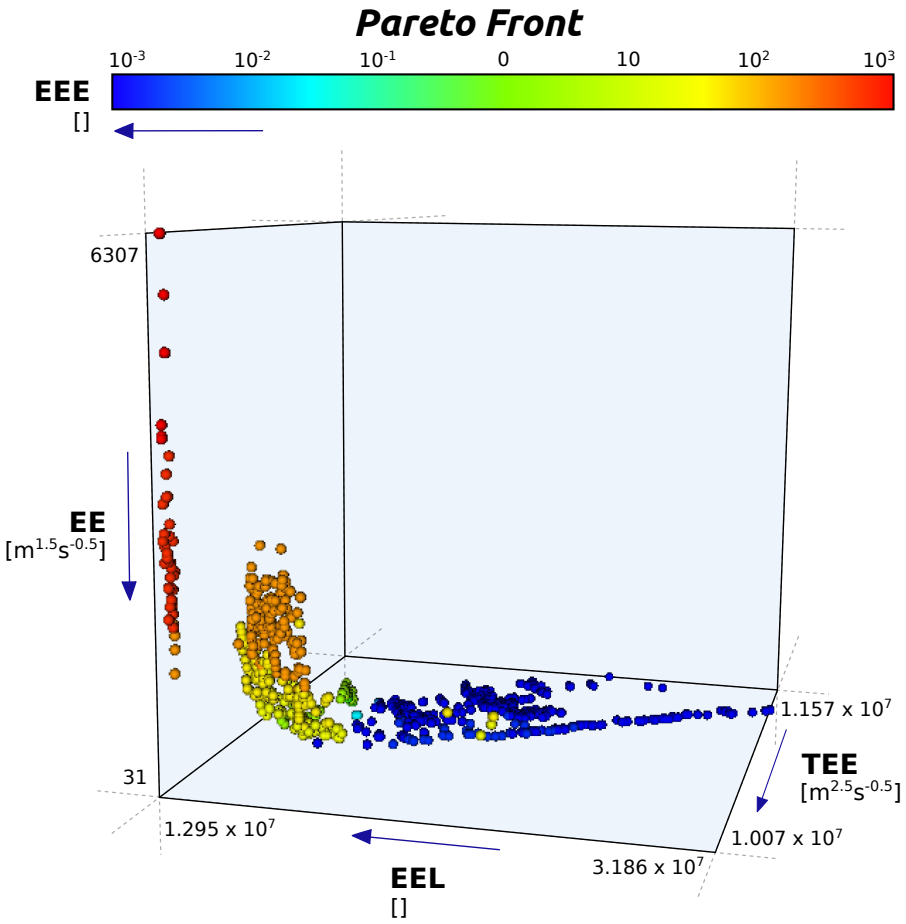

Figure 5.10: Pareto front obtained from MOGLE_RAINY_IDW experiment. The front was represented using AeroVis©.

5.4.2.1 *Algorithms performance*

Some important features of the Pareto front shown in the previous section are summarized in table 5.8. In particular, the number of points of the front each algorithm contributed to is shown, together with the feasibility. As for feasibility, it represents the number of control sets respecting the mass constraint over the total number of generated sets, for each algorithm in the first three rows and for the total number of function evaluations in the last row.

ALGORITHM	NUMBER OF FRONT POINTS	FEASIBILITY (%)
εNSGA-II	396	4.72
GDE3	654	18.83
OMOPSO	55	0.31
Total	1105	8.19

Table 5.8: MOGLE_RAINY_IDW: Pareto front features.

The largest contribution is therefore from GDE3 algorithm, covering over the 59% of the front. GDE3 is also the algorithm having the largest feasibility suggesting that is the one which best recognise the mass constraint.

As in the previous two experiments, also the results of this experiment support and justify the use of GAs. In fact, the following comparison with random control generation was performed:

- a sample of 400 000 different random values for each control was generated;
- 13.6 millions of different control sets were created as combinations of the previously generated controls by the use of Saltelli's method implemented in the MOEA framework. The magnitude order of control sets is therefore comparable to the NFE for the GAs, which was set equal to 10 millions, as shown in table 5.3.
- Among all the control sets generated, none of them was able to respect the mass constraint.

This fact, again, confirms that evolutionary algorithms are effective in understanding the mass constraint and produce proper control sets.

5.4.2.2 *A comparison with MOGLE_RAINY*

It is possible to compare the Pareto fronts obtained for MOGLE_RAINY and MOGLE_RAINY_IDW. They are both represented in figure 5.11.

In particular, it is possible to say that as for the objectives values, the pareto Front obtained in MOGLE_RAINY is dominant. Nevertheless the following thing is important: the front obtained with the

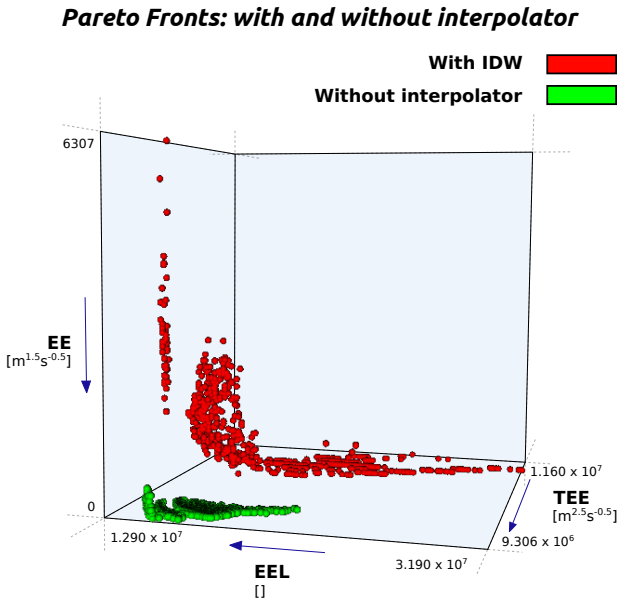

Figure 5.11: Comparison between the Pareto fronts of MOGLE_RAINY without the interpolator and MOGLE_RAINY_IDW with IDW interpolatro. The front was represented using AeroVis©.

interpolator is much more extended. This fact confirms the comments written at the end of the previous section, i. e. that a range for control variables is a limitation in reproducing very different control sets and representing the conflict among the objectives. Now, since the interpolator is directly applied to the DEM surface, and the surface itself is directly optimized, a bigger degree of freedom is given to the optimizer, allowing it to explore very different areas in the objectives space.

5.4.2.3 *Analyzing the conflict*

Looking at the Pareto front, it appears that the conflict among objectives, already treated in the previous two sections, is now more present and clear. This evidence supports the hypothesis of conflicting objectives, since it now clearly emerges. Moreover, the main conflicts are the ones expected:

- TEE and EE are conflicting;
- TEE is not conflicting with its variance EEL, but the front points on the quarter (TEE, EEL) are spread;
- EE is not conflicting with its variance EEE;
- as a consequence of the previous observations, TEE is conflicting also with EEE, and EEE with EEL.

According to the methodology adopted for analyzing the previous two experiments, considering the conflict between TEE and EE as the

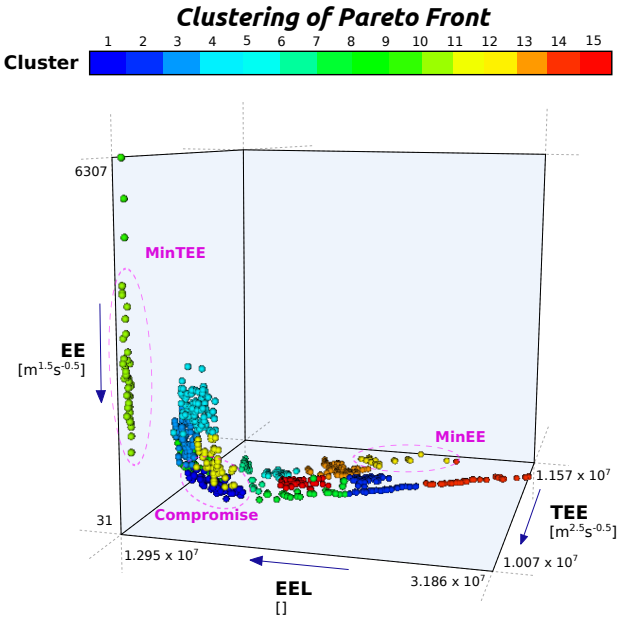

Figure 5.12: Pareto front clusters for MOGLE_RAINY_IDW experiment. The upper colorbar shows the colors of the different 15 clusters. Clusters *MinTEE*, *Compromise* and *MinEE* are surrounded by a coloured circle, since they are the selected clusters for naturality indexes analysis. The front was represented using AeroVis ©.

most evident, it is possible to exclude EEE from the representation of the front being it concordant with EE. We proceed with the clustering and the naturality indexes analysis, as commented in the following subsections.

5.4.3 *Clustering and naturality indexes analysis*

In this experiment, fifteen clusters were obtained with k-means clustering and are represented with different colors in figure 5.12.

As in the previous experiments, only three clusters were selected for carrying out the analysis through naturality indexes and again, the three clusters were chosen in order to have two extreme clusters and one compromise. They are the following:

MinTEE: this cluster minimizes TEE objective, counting against EE objective. This class was chosen in spite of class 9, the one composed just by three green points above class MinTEE, in order to have a larger amount of points and therefore basins for the naturality indexes analysis;

Compromise: this cluster represents the compromise between TEE and EE objectives;

MINEE: this cluster minimizes EE objective, counting against TEE objective;

Coherently with the previous experiments, naturality indexes were computed for the three largest basins of each point of the three clusters. Probability distributions were built on their values, and the most important results about them are commented in the following two paragraphs. All less relevant results are included in appendix C.

5.4.3.1 *2D networks features*

Some first comments about the landscape and river networks generated with this third experiment may be done considering the indicators which refer to the 2D features of river networks, i.e. all apart from R_s (which includes the third dimension in the evaluation of the slope).

In general, no significant improvements are observed when considering the distributions of Horton's ratios R_b, R_l and R_a. Also, no significant trends can be identified for those indexes while moving from one extreme cluster to another passing through the compromise. Anyway, the following elements appear:

- usually the area of R_b, R_l and R_a which is inside the natural range is larger for clusters *Compromise* and *MinEE*. Anyway, the index distributions for those clusters have a bigger standard deviation, if compared to the ones for *MinTEE* cluster, therefore the distribution is not concentrated and some basins are far from the natural range. As a consequence, it is not possible to affirm which cluster performs better with respect to those three Horton's ratios;

- on the contrary, considering Hack's exponent, as shown in figure 5.14, the average value is closer to the natural value 0.6 for *MinEE* cluster, which also shows a smaller standard deviation, if compared to the others. It seems so that *MinEE* performs better than *Compromise* and *MinTEE*, which is the one whith the worst behaviour;

- in general, river networks appear worst and less realistic than the ones obtained for the previous experiment. An example of them is provided in figure 5.13 . This fact is for sure due to the combined effect of IDW and depression filling algorithms, which create almost flat areas in some points of the DEM and, in this way, act against more articulated and branched river networks.

As a consequence of the commented observation, we conclude that river networks simulated within MOGLE_RAINY_IDWdo not show particular pattern and trends while moving along the Pareto front points when considered as 2D networks without the elevation dimension.

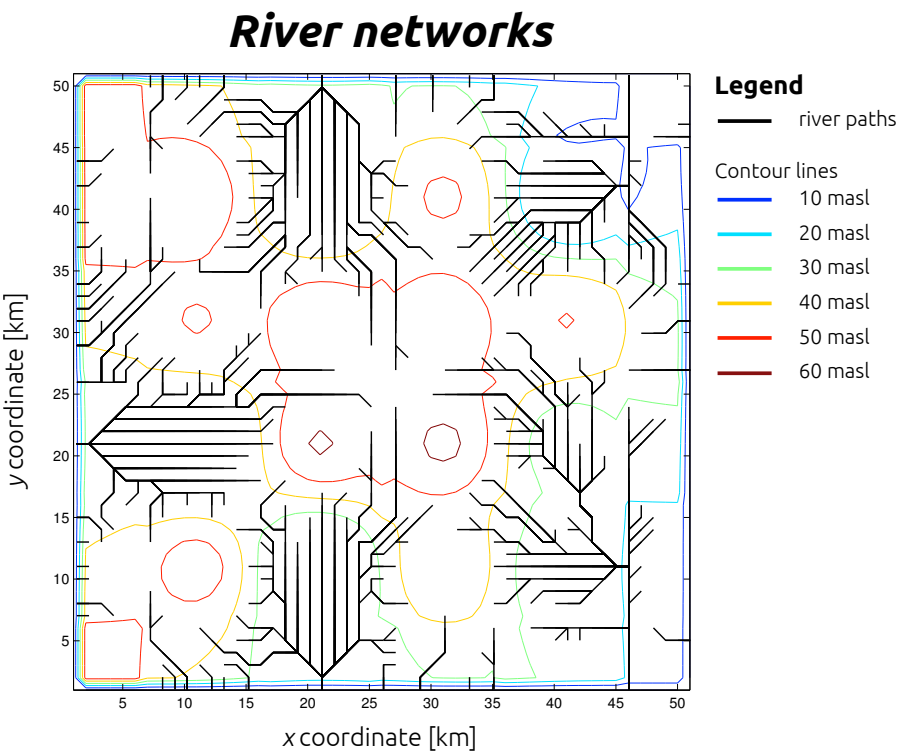

Figure 5.13: Example of river networks for MOGLE_RAINY_IDW . Black lines represent river networks exctracted from the DEM of the centroid point of *MinTEE* cluster.

5.4.3.2 *Slope and river longitudinal profiles*

The interesting results of this experiment come when analyzing the 3D features of river networks. That means looking at the distributions of R_s index for the three clusters; they are represented in figure 5.15. Even if the part of the distribution inside the natural range does not change very much among the clusters, and it is always below 60%, big differences exist among the clusters:

- R_s distribution for *MinTEE* cluster (left side plot in figure 5.15) has over 50% of its area included in the natural range. Anyway, the fact that its average value is approximately 13 and its standard deviation is the largest, suggests that the distribution is very widespread and values with high probability are very far from the natural range $[1.5;\ 3.5]$ and they lie on the portion of distribution which is outside the plotted one;

- R_s distribution for *Compromise* (central plot in figure 5.15) shows that less than 50% of its area is included in the natural range (about 44%). Anyway, this distribution is better than the one for *MinTEE* cluster, because the average value of 2.27 is closer to the mean value of the natural range and its standard deviation is much smaller, if compared to the one for *MinTEE* cluster. This

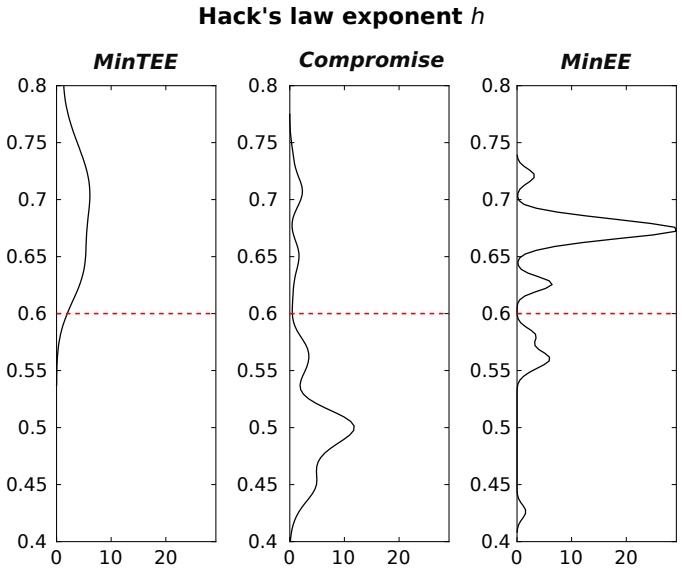

	MIN TEE	COMPROMISE	MIN EE
Number of cluster points	40	118	40
Sample mean and standard deviation	0.7040 ± 0.06832	0.5287 ± 0.07906	0.6465 ± 0.05714

Figure 5.14: Statistical distribution of values of Hack's law exponent for the clusters of experiment MOGLE_RAINY_IDW. The chosen clusters are the same of figure 5.12. On the y there is the ratio value, on x axis the percentage value. The table below integrates the graphics with simple statistics.

means that almost all the values which are not inside the natural range are close to it;

- R_s distribution for *MinEE* (right side plot in figure 5.15) is the one which better approximates the natural range. In fact, it has the largest area inside it, its average value is close to the center of the natural range and its variance is the smallest among the distributions of the three clusters.

As a consequence, it is possible to state that the cluster which minimizes the objective containing the 3D term of slope, i. e. EE, is also the one which best performs according to Horton's slope ratio, while the performance gets worse when moving along the Pareto front toward the opposite extreme cluster, i. e. the ones that minimizes TEE.

In order to verify if the performances on R_s index really reflect on networks patterns, rivers longitudinal profiles were analyzed. Specifically, one significant Pareto front point for each cluster was taken as sample, i. e. the one closest to the cluster centroid. The main channel of the largest network developing on the DEM represented by those front points was identified and its longitudinal profile is represented in figure 5.16.

As it is possible to appreciate from the figure, the only profile showing some promising results with respect to concavity, is the one belonging to *MinEE* cluster, which is also the one with the best results with respect to R_s. On the other hand, the one belonging to *MinTEE* can be considered the most convex. Since natural profiles are characterized by concavity, in our experiment *MinEE* cluster is the one which better approximates natural patterns with respect to that feature. Moreover, even if only one significant profile for each cluster was represented here, the analysis of other points confirmed the just affirmed comments.

Even if the result is good, further improvements can be done. In fact, as it is possible to see again from figure 5.16 , almost flat areas and sudden steps are present. They are probably due to depression filling algorithm and the settings chosen for IDW interpolator algorithm, or to the algorithm itself.

5.4.3.3 *General conclusion on MOGLE_RAINY_IDW*

The summarizing comment on this last experiment is positive. Despite a not good performance of the model with respect to the 2D features of river networks independently from the objectives values, very good results were obtained with respect to the third dimension represented by rivers longitudinal profiles. It seems that the integration of a spatial interpolator in the model reduces its limitations and helps the optimizer to interpret the objectives, especially regarding the ones including the slope term i. e. EE and EEE. With respect to 3D

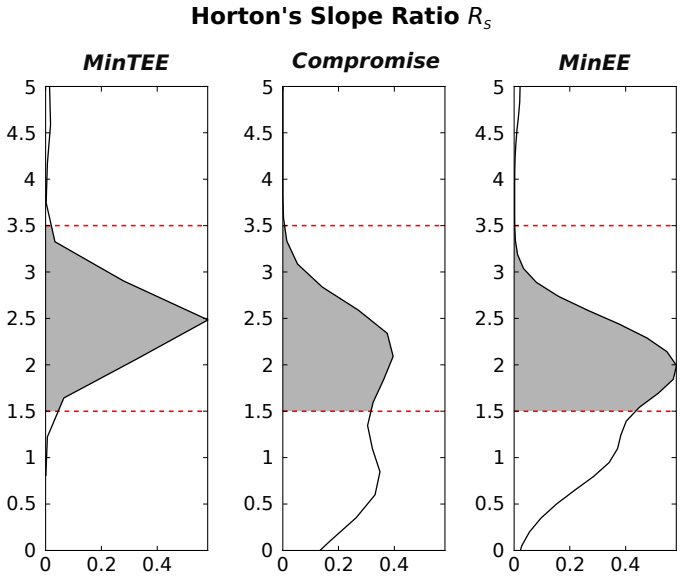

	MIN TEE	COMPROMISE	MIN EE
Number of cluster points	40	118	40
Sample mean and standard deviation	13.64 ± 13.25	2.270 ± 3.523	2.117 ± 2.241
Probability within natural range	0.5184	0.4387	0.5699

Note on the left plot: the sharp distribution showed in the first plot is due to the distribution interpolator algorithm used. In fact, its Matlab© implementation builds the statistical distribution of the dataset, then samples it with a fixed amount of point. Since the range of values covered by the Horton's slope ratio in this case is very wide, the sampling step is wide too. In this particular case is about 0.5: this explain the shape of the plot.

Figure 5.15: Statistical distribution of Horton's slope ratio for the clusters of experiment MOGLE_RAINY_IDW. The chosen clusters are the same of figure 5.12.

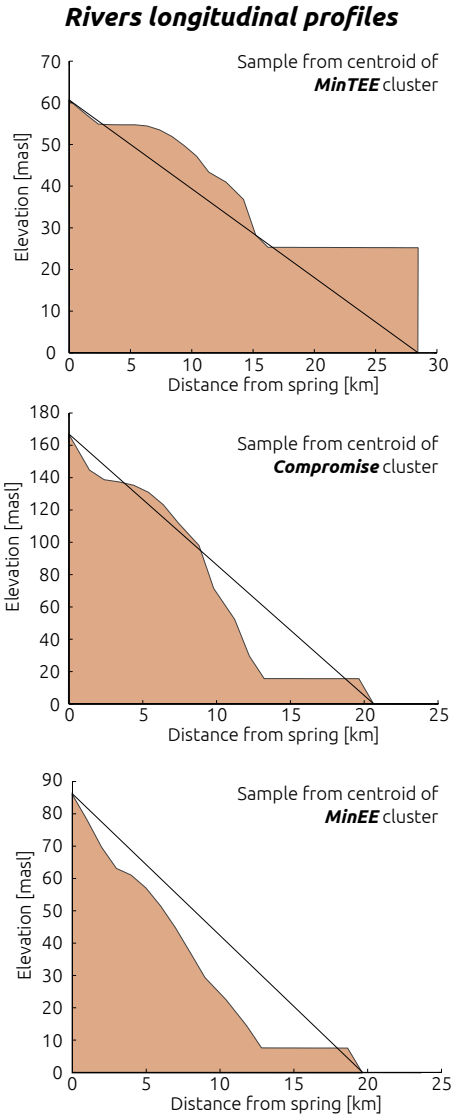

Figure 5.16: Rivers longitudinal profiles for MOGLE_RAINY_IDW experiment. Starting from the top, the three plots represent the longitudinal profile of the main channel for the largest network in, respectively, *Min*TEE, *Compromise* and *Min*EE clusters centroids. The straight line in each sub-plot connects the spring to the outlet. Pay attention to the different scales on x- and y-axes.

river networks, this is the first promising attempt in simulating concave longitudinal profiles of river, if compared to the previous studies mentioned in subsection 2.3.3 studies.

6

FINAL REMARKS: OUR CONTRIBUTION AND SOME OPEN QUESTIONS

May the principle be used to represent the landscape evolution process in time and space using Digital Elevation Models?

Would a multi-objective framework be suitable to take advantage of the existing knowledge and to assess the trade-offs among different simplified version of the "optimality" criterion in order to find the proper expression for 3D modeling?

The previous two questions were written in the introduction as the goal of this thesis. Now, after having commented the results, are we able to answer?

It is important to remind that, for reaching the goals, we detailed a multi-criteria optimization framework which describes river and landscape evolution over a 3D spatial domain.

After the simulations run, the results obtained and the analysis performed, we are ready to assess the value of the framework proposed. The effort in the analysis and reduction of the aspects around modeling landscape evolution under multiple principle allows to assess the different criteria. We found that some of them are conflicting, validating the hypothesis of opposite phenomena captured by the LAP as in [55]. Studying this conflict means understanding which drivers of landscape evolution are captured by each formulation. Several trade-offs between criteria formulations should be relate to hydrogeological features such as different degrees of equilibrium between soil erodibility and channel incision or to geological constraint such as bedrock properties. This should give more awareness of the meaning of the LAP.

In addition to the identification of the conflict, creating the framework i. e. a complete methodology, tools for studying the phenomenon and assessment strategies for evaluating the outputs forced us to deepen and expand the questions on landscape evolution modeling. We had to provide mathematical formulations for the simplified versions of the LAP), in a suitable form for DEMs.

Therefore, by considering each part of the framework separately:

- as for its core, i. e. the model, some important improvements and tests were put in practice. In particular, with respect to the main modeling reference of this work, i. e. Paik's GLE model [38], a spatial interpolator was integrated in the model, showing promising results with respect to the simulations of slopes and

the study of river profiles. Moreover, the rainfall parameter of the model was tested;

- as for the optimization phase, it was executed rigorously, adopting top performing state of the art algorithms. Additionally, the performances of these algorithm and the advantage of using them in spite of simple random search, were quantified and assessed;
- the outputs analysis was based on many hydrological indexes, consistently with other important works. Moreover, the dimensional burden of the results was tackled by implementing clustering and statistical, allowing them to be globally considered.

Finally, it is possible to say, as an answer, that the framework we developed is suitable to study the criteria and evaluating their tradeoffs, and is a complete tool for developing further studies.

6.1 OUR CONTRIBUTION TO THE FIELD OF STUDY

This thesis contributes to the field studying landscape and river evolution as follows:

- as for modeling purposes, it is the first attempt that provides a model to reproduce the 3D features of landscapes and river networks based on multiple criteria optimization;
- as for sistem understanding purposes, it deepened the knowledge about the different formulations of least action principle and the way they affect the features of river networks developing on landscapes.

The deliverables of this work are, therefore, good basis for future researches towards the right formulation of the LAP driving landscape and river evolution. For this reason, many improvements and open questions are suggested, in the next, last section.

6.2 PROPOSED IMPROVEMENTS AND OPEN QUESTIONS

Given the largest amount of topics touched by this thesis, some relevant issues are proposed to future development.

The first idea is to better setup and configurate the IDW interpolator. The results of MOGLE_RAINY_IDW are promising but they also show significant limitations. This is something we are already working on with the perspective of validiting the framework with the comparison with a real case study. In case additional problems should arise, would the implementation of a different interpolator be better?

At the same time the optimization part of the framework can be improved by performing sensitivity analysis and trials on different algorithms parameterizations. The goal is to find the best parameterization and the best performing algorithms to reduce the amount of time and resources needed for the optimization. Alternatively, algorithms which do it automatically, like Borg or Amalgam can be used. Also a parallelization of model and algorithm could take advantage of High Performance Computing (HPC) and lighten the computational costs.

A part from this improvements, the open issues become more complicated. The first fundamental one is related to time. In order to really explore the concept of evolution, the time dimension should be integrated in the model. In this case, hydrological parameters, like rainfall, would assume values directly comparable to the ones measured in natural events. Moreover, the DEM configuration would be relatable to time itself and the rate of change in its elevation would be linked to natural erosion and deposition rates.

Questions related to this issue that need to be answered can be:

- what is the resilience of the system over time? is it stable somehow? what kind of equilibrium does it reach?
- what is the right scale, both in term of time and space, for reproducing the action caused by phenomena explained by the optimality principle?
- further exploiting the concepts of control theory, is a control policies a proper structure for aggregating the criteria over time?

The second issue, is related to conflict. Given the fact that conflicting behaviour was shown by the different formulations of the LAP, how is it possible to enforce the theoretical interpretation of such a conflict? Moreover, is the conflict really related to different features in the landscapes? Or does it express a form of multifinality in landscape evolution? How the time dimension affect the conflict shown? And more simply, what are the variations in values of the objectives to be considered as significant with respect to natural systems? All these questions are promising topics for research. They can also be a theorical base to study the principle of equifinality in landscape evolution, e. g. to analyze different DEM shapes that lead to the same optimized landscape after the operations described in the framework.

Among the biggest issues, one last topic is worth to be mentioned: our model is based on DEMs, given the advantages explained in the text. The landscape is discretized on a cell basis, it is made evolve and then river networks are extracted. An alternative approach would be to base the analysis on a finer discretizations which would better describe river networks, like TINs. These structures can also allow to directly optimize river networks without losing the z dimension, in

spite of landscapes. Would such an approach better describe the 3D features of river networks?

Other improvements and open questions are given below in sparse order.

On the modeling side:

- Planchon's DF algorithm should be improved, in order to better recognize real depressions from false depressions, caused by abnormal isolated small peaks and, consequently, better respect the mass constraint. Are there algorithms which can do it?
- the sensitivity of the model to different hydrological parameters, DEM dimension and shape should be evaluated;
- the choice of the threshold for river network extraction must be better defined, according to state of the art methods.

On the results analysis tools:

- a stronger study on the correlation between naturality indexes and DEM features should be performed, in order to understand if they properly describe the 3D features. Moreover, the definition of their natural ranges should be enforced. Are there any more suitable and correct indexes?
- the comparison between synthetic landscapes and natural ones should be enforced and supported by data. Therefore, which set up of the model allows it to output landscapes really comparable to natural ones? What is the best method for proving that?

Challenges appear to be many because our framework is a completely new perspective on a complex issue.

Plus grand est l'obstacle, plus grande est la gloire de le surmonter [1]
Molière wrote some time ago.

1 The greater the obstacle, the more glory in overcoming it.

BIBLIOGRAPHY

[1] J.R.L. Allen. *Principles of Physical Sedimentology*. Allen & Unwin London, 1985 (cit. on p. 11).

[2] Aristotele. *Nicomachean Ethics*. 350 B.C.E. (Cit. on p. 47).

[3] R. Bringhurst. *The Elements of Typographic Style*. Version 3.2. Point Roberts, WA, USA: Hartley & Marks Publishers, 2008 (cit. on p. 138).

[4] C. A. Coello Coello. "Evolutionary multi-objective optimization: a historical view of the field." In: *Computational Intelligence Magazine, IEEE* 1.1 (2006), 28–36 (cit. on pp. 36–38, 125).

[5] J. Cohon and D. Marks. "A review and evaluation of multiobjective programing techniques." In: *Water Resources Research* 11.2 (1975), pp. 208–20 (cit. on p. 35).

[6] K. Deb et al. "A fast and elitist multiobjective genetic algorithm: NSGA-II." In: *Evolutionary Computation, IEEE Transactions on* 6.2 (2002), 182–197 (cit. on p. 126).

[7] K. Deb et al. "Scalable test problems for evolutionary multiobjective optimization." In: *Evolutionary Multiobjective Optimization* (2005), pp. 105–145 (cit. on p. 126).

[8] P. DuBoys. "Le Rhône et les rivières à lit affouillable." In: *Ann. Ponts Chaussees* 18 (1879), pp. 141–148 (cit. on p. 13).

[9] H.A. Einstein. *The Bed-load Function for Sediment Transportation in Open Channel Flows*. Technical bulletin (United States. Dept. of Agriculture). U.S. Department of Agriculture, 1950 (cit. on pp. 11, 12).

[10] D. E. Goldberg. "Genetic algorithms in search, optimization, and machine learning." In: (1989) (cit. on p. 125).

[11] W.H. Graf and S. Altinakar. *Fluvial Hydraulics: flow and transport processes in channels of simple geometry*. Wiley, 1998 (cit. on p. 11).

[12] D. M. Gray. "Interrelationships of watershed characteristics." In: *Journal of Geophysical Research* 66.4 (1961). ISSN: ISSN: 0148-0227 ; E-ISSN: 2156-2202 (cit. on pp. 42, 69).

[13] U. Haberlandt. "Geostatistical interpolation of hourly precipitation from rain gauges and radar for a large-scale extreme rainfall event." In: *Journal of Hydrology* 332.1 (2007), pp. 144–157 (cit. on p. 87).

[14] J. T. Hack. "Studies of longitudinal stream profiles in Virginia and Maryland." In: *US Geol. Survey Prof. Paper* (1957) (cit. on p. 42).

[15] Hadka, D. et al. *MOEA Framework*. 2009. URL: http://www.moeaframework.org/ (cit. on pp. 62, 117, 137).

[16] Hadka, D. et al. *Pat Reed Group Research Tips Blog*. 2012. URL: http://waterprogramming.wordpress.com/ (cit. on p. 62).

[17] D. Hadka and P. Reed. "Borg: An Auto-Adaptive Many-Objective Evolutionary Computing Framework." In: *Evolutionary Computation* (2012) (cit. on pp. 35, 38, 64–66).

[18] D. Hadka and P. Reed. "Diagnostic assessment of search controls and failure modes in many-objective evolutionary optimization." In: *Evolutionary Computation* 20.3 (2012), pp. 423–452 (cit. on pp. 38, 64).

[19] R. E. Horton. "Erosional development of streams and their drainage basins; hydrophysical approach to quantitative morphology." In: *Geological Society of America Bulletin* 56.3 (1945), 275–370 (cit. on pp. 40, 41, 49).

[20] D. J. Ketchen and C. L. Shook. "The application of cluster analysis in strategic management research: an analysis and critique." In: *Strategic management journal* 17.6 (1996), pp. 441–458 (cit. on pp. 71, 73).

[21] Eugene Kindler and Ivan Krivy. "Object-oriented simulation of systems with sophisticated control." In: *International Journal of General Systems* 40.3 (2011), pp. 313–343 (cit. on p. 117).

[22] D. E. Knuth. "Computer Programming as an Art." In: *Communications of the ACM* 17.12 (1974), pp. 667–673 (cit. on p. 117).

[23] J. Kogan. *Introduction to clustering large and high-dimensional data*. Cambridge University Press, 2006 (cit. on p. 72).

[24] J.B. Kollat and P.M. Reed. "Comparing state-of-the-art evolutionary multi-objective algorithms for long-term groundwater monitoring design." In: *Advances in Water Resources* 29.6 (2006), pp. 792–807. ISSN: 0309-1708. DOI: 10.1016/j.advwatres.2005.07.010 (cit. on pp. 62, 125, 126).

[25] S. Kukkonen and K. Deb. "A fast and effective method for pruning of non-dominated solutions in many-objective problems." In: *Lecture Notes in Computer Science* 4193 (2006), 553–562 (cit. on pp. 63, 127).

[26] W.B. Langbein and T. K. Iseri. *Manual of Hydrology: Part 1. General Surface-Water Techniques*. 604 South Picket Street, Alexandria, VA, USA: United States government printing office, 1960 (cit. on p. 30).

[27] M. Laumanns et al. "Combining convergence and diversity in evolutionary multiobjective optimization." In: *Evolutionary computation* 10.3 (2002), 263–282 (cit. on p. 66).

[28] L. B. Leopold and W.B. Langbein. *The concept of Entropy in Landscape Evolution*. US Government Printing Office Washington, DC, 1962 (cit. on pp. xix, 15, 20, 22, 23).

[29] H. Liu and Y. Lu. "Geostatistical Study on the Formation of Longitudinal Channel Shapes." In: *Remote Sensing, Environment and Transportation Engineering (RSETE), 2012 2nd International Conference on*. IEEE. 2012, pp. 1–4 (cit. on p. 9).

[30] R. Lleti et al. "Selecting variables for k-means cluster analysis by using a genetic algorithm that optimises the silhouettes." In: *Analytica Chimica Acta* 515.1 (2004), pp. 87–100 (cit. on pp. 72, 73).

[31] T. Mann and J. E. Woods. *The magic mountain*. 1924 (cit. on p. 29).

[32] E. Meyer-Peter and R. Müller. "Formulas for bed-load transport." In: *Proceedings of the 2nd Meeting of the International Association for Hydraulic Structures Research*. International Association of Hydraulic Research Delft. 1948, pp. 39–64 (cit. on p. 12).

[33] K. Miettinen. *Nonlinear Multiobjective Optimization*. International Series in Operations Research & Management Science, 12. Kluwer Academic Pub, 1999. ISBN: 9780792382782 (cit. on p. 37).

[34] U. Moisello. *Idrologia tecnica*. La Goliardica Pavese, 1999. ISBN: 9788878303638 (cit. on p. 41).

[35] G. C. Nanson and H. Q. Huang. "Least action principle, equilibrium states, iterative adjustment and the stability of alluvial channels." In: *Earth Surface Processes and Landforms* 33.6 (2008), pp. 923–942 (cit. on pp. 18, 27).

[36] J. F. O'Callaghan and D. M. Mark. "The extraction of drainage networks from digital elevation data." In: *Computer vision, graphics, and image processing* 3.3 (1984), pp. 323–344 (cit. on pp. 32, 33).

[37] K. Paik. "Global search algorithm for nondispersive flow path extraction." In: *Journal of Geophysical Research* 113.F4 (2008), F04001 (cit. on pp. 32, 57–59, 61).

[38] K. Paik. "Optimization Approach for 4-D Natural Landscape Evolution." In: *Evolutionary Computation, IEEE Transactions on* 15.5 (2011), pp. 684–691 (cit. on pp. xx, 4, 8, 24–26, 39, 47, 49–52, 55–57, 61, 67, 77, 79, 86, 105, 117, 120).

[39] K. Paik. "Search for the optimality signature of river network development." In: *Physical Review E* 86.4 (2012), p. 046110 (cit. on pp. 20, 26, 33, 61).

[40] K. Paik and P. Kumar. "Optimality approaches to describe characteristic fluvial patterns on landscapes." In: *Philosophical Transactions of the Royal Society B: Biological Sciences* 365.1545 (2010), pp. 1387–1395 (cit. on pp. 20, 42).

[41] F. J. Pazzaglia. "Landscape Evolution Models." In: *Developments in Quaternary Sciences* 1 (2003), pp. 247–274 (cit. on pp. xix, 3, 7, 17, 19).

[42] S. D. Peckham. "Mathematical modeling of landforms: Optimality and steady-state solutions." In: *Concepts and Modelling in Geomorphology: International Perspectives, Eds. Evans, IS, Dikau, R., Tokunaga, E., Ohmori, H. and Hirano, M* (2003), pp. 167–182 (cit. on p. 19).

[43] J. T. Perron et al. "The root of branching river networks." In: *Nature* 492.7427 (2012), pp. 100–103 (cit. on p. 23).

[44] M. Pidwirny. "The Drainage Basin Concept." In: *Fundamentals of Physical Geography*, (2006) (cit. on p. 32).

[45] O. Planchon and F. Darboux. "A fast, simple and versatile algorithm to fill the depressions of digital elevation models." In: *Catena* 46.2 (2002), 159–176 (cit. on pp. 32, 54, 55, 57).

[46] J. Playfair. *Illustrations of the Huttonian theory of the earth*. Cadell and Davies, 1802 (cit. on p. 3).

[47] K.R. Popper. *Objective Knowledge: An Evolutionary Approach*. Clarendon Press, 1979 (cit. on p. 7).

[48] M. Rãdoane, N. Rãdoane, and D. Dumitriu. "Geomorphological evolution of longitudinal river profiles in the Carpathians." In: *Geomorphology* 50.4 (2003), 293–306 (cit. on p. 10).

[49] P. M. Reed et al. "Evolutionary Multiobjective Optimization in Water Resources: The Past, Present, and Future." In: *Advances in Water Resources* (2012) (cit. on pp. 38, 62–64).

[50] R. Rigon et al. "On Hack's law." In: *Water Resources Research* 32.11 (1996), 3367–3374 (cit. on pp. 42, 43).

[51] R. Rigon et al. "Optimal channel networks: A framework for the study of river basin morphology." In: *Water Resources Research* 29.6 (1993), pp. 1635–1646. ISSN: 0043-1397. DOI: 10.1029/92WR02985 (cit. on pp. 23, 24, 26, 47, 49, 61).

[52] A. Rinaldo et al. "Minimum energy and fractal structures of drainage networks." In: *Water Resources Research* 28.9 (1992), pp. 2183–2195 (cit. on p. 24).

[53] I. Rodríguez-Iturbe and A. Rinaldo. *Fractal River Basins: Chance and Self-Organization*. en. Cambridge University Press, 2001. ISBN: 9780521004053 (cit. on pp. 40–42).

[54] I. Rodriguez-Iturbe et al. "Power law distributions of discharge mass and energy in river basins." In: *Water Resources Research* 28.4 (1992), 1089–1093 (cit. on p. 42).

[55] I. Rodríguez-Iturbe et al. "Energy Dissipation, Runoff Production, and the Three-Dimensional Structure of River Basins." In: *Water Resources Research* 28.4 (1992), pp. 1095–1103 (cit. on pp. xx, xxi, 8, 14, 15, 20–23, 26, 27, 60, 82, 89, 105).

[56] R. Rosenberg. *Simulation of genetic populations with biochemical properties*. 1967 (cit. on p. 125).

[57] J. D. Schaffer. "Multiple objective optimization with vector evaluated genetic algorithms." In: *Proceedings of the 1st international Conference on Genetic Algorithms*. L. Erlbaum Associates Inc. 1985, pp. 93–100 (cit. on p. 125).

[58] S. A. Schumm. "Evolution of drainage systems and slopes in badlands at Perth Amboy, New Jersey." In: *Geological Society of America Bulletin* 67.5 (1956), 597–646 (cit. on p. 41).

[59] D. Shepard. "A two-dimensional interpolation function for irregularly-spaced data." In: *Proceedings of the 1968 23rd ACM national conference*. ACM. 1968, pp. 517–524 (cit. on p. 119).

[60] R. L. Shreve. "Stream lengths and basin areas in topologically random channel networks." In: *The Journal of Geology* (1969), pp. 397–414 (cit. on p. 41).

[61] M. Sierra and C. Coello Coello. "Improving PSO-Based multi-objective optimization using crowding, mutation and ε-dominance." In: *Evolutionary Multi-Criterion Optimization*. Springer. 2005, pp. 505–519 (cit. on p. 64).

[62] N. Srinivas and K. Deb. "Multiobjective optimization using non-dominated sorting in genetic algorithms." In: *Evolutionary computation* 2.3 (1994), 221–248 (cit. on p. 125).

[63] R. Storn, K. V. Price, and J. Lampinen. *Differential Evolution-A Practical Approach to Global Optimization*. Springer, Berlin, 2005 (cit. on pp. 63, 126).

[64] A. N. Strahler. "Hypsometric (area-altitude) analysis of erosional topography." In: *Geological Society of America Bulletin* 63.11 (1952), 1117–1142 (cit. on p. 40).

[65] A. N. Strahler. "Quantitative analysis of watershed geomorphology." In: *Transactions of the American Geophysical Union* 38.6 (1957), 913–920 (cit. on pp. 40, 42).

[66] D. G. Tarboton, R. L. Bras, and I. Rodriguez-Iturbe. "A physical basis for drainage density." In: *Geomorphology* 5.1 (1992), 59–76 (cit. on p. 61).

[67] D. G. Tarboton, R. L. Bras, and I. Rodriguez-Iturbe. "On the extraction of channel networks from digital elevation data." In: *Hydrological processes* 5.1 (1991), 81–100 (cit. on p. 61).

[68] J. Verne. *Journey to the Center of the Earth*. Classics illustrated. Huge Print Press, 1957. ISBN: 9780758311993 (cit. on p. 77).

[69] J. A. Vrugt and B. A. Robinson. "Improved evolutionary optimization from genetically adaptive multimethod search." In: *Proceedings of the National Academy of Sciences* 104.3 (2007), pp. 708–711 (cit. on p. 65).

[70] W. H. Wischmeier, D. D. Smith, et al. "Predicting Rainfall Erosion Losses-A guide to conservation planning." In: *Predicting rainfall erosion losses-A guide to conservation planning* (1978) (cit. on p. 12).

[71] C. T. Yang. "Potential Energy and Stream Morphology." In: *Water Resources Research* 7.2 (1971), pp. 311–322. DOI: 10.1029/WR007i002p00311 (cit. on pp. 13, 15, 20, 41).

[72] C. T. Yang. "Theory of Minimum Rate of Energy Dissipation and its Application." In: *Proceedings of the Pakistan Engineering Congress Annual Convention, Lahor, Pakistan*. 1985, pp. 105–129 (cit. on p. 21).

[73] Q. Zhang and P. N. Suganthan. "Final report on CEC'09 moea competition." In: *Congress on Evolutionary Computation (CEC 2009)*. 2009 (cit. on pp. 63, 127).

Part III

APPENDIX

A

LANDSCAPE EVOLUTION FRAMEWORK: MORE DETAILS ON THE MODEL

We have seen that computer programming is an art,
because it applies accumulated knowledge to the world,
because it requires skill and ingenuity, and especially
because it produces objects of beauty.

— Knuth, "Computer Programming as an Art," 1974

A.1 TECHNICAL OVERVIEW ON THE MODEL SOFTWARE

As said in section 4.3, we created a new software to perform the extraction of river networks from an arbitrary landscape represented by a DEM. The software performs the operations described in the already cited section 4.3 and is provided with an interface that allows the comunication with the optimizer, i. e. the MOEA framework [15].

The baseline for this job is the original code used by Paik in [38], which the author kindly gave us. It is written in Fortran 95, is composed by 7 subroutine and the main body, which defines the main operation the software is able to perform. The configuration of the model is hardly coded and a change in parameters value requires a new compilation.

There are several reasons to rewrite the software. In section 4.3 we mentioned the need of taking control on each part of the model and being able to change it to test new configurations. The other reasons concern the coupling with the optimization software and the need for easing the reusability and maintainability of the software. For these point we choose to re-implement the functionality of Paik's software within an object oriented framework that allows code reusing by definition.

In fact, object oriented is a programming paradigm that represents concepts as "objects" that have data fields (attributes that describe the object) and associated procedures known as methods. Objects, which are usually instances of classes, are used to interact with one another to design applications and computer programs [21].

We chose to implement this architecture in the C++ programming language because of its striking performances and for the availability of state of the art libraries to perform common operations. An example of this is the use of the YAML Ain't Markup Language (YAML) to format the parameter setup: a solid library for C++ is available to perform operations within that data format.

A.1.1 *Software architecture*

We chose to design the new software as a static library of functionalities which can be used for various operations. In fact we needed the same functionalities to be linked within the MOEA framework and to be used again when analyzing the landscapes it produced as outputs.

The core operations performed by the software are already described in the main part of the thesis. The main functionality which is not included is the data handling class i. e. the class OurMatrix. Its header with the data containers and its operators is shown in Listing A.1.

The library included into the software is the *yaml-cpp* library, a YAML parser and emitter in C++ matching the YAML 1.2 spec. Source code and use instructions are available from `http://code.google.com/p/yaml-cpp/` under MIT license. It requires the headers of Boost C++ libraries, which are "free peer-reviewed portable C++ source libraries" and very common when using C++.

A.1.2 *How to write good software: testing and evaluating*

To test the software we wrote, we rely on the Google C++ Testing framework. The site says that it is the

> Google's framework for writing C++ tests on a variety of platforms (Linux, Mac OS X, Windows, Cygwin, Windows CE, and Symbian). Based on the xUnit architecture. Supports automatic test discovery, a rich set of assertions, user-defined assertions, death tests, fatal and non-fatal failures, value- and type-parameterized tests, various options for running the tests, and XML test report generation.

It is available under the "New BSD License"[1] at `http://code.google.com/p/googletest/`. Within the testing framework, we performed eighteen tests on the core functionalities of the software. 658 assertions have been evaluated to ensure code correctness both while writing is and when deployment has been done.

The model relies on a certain amount of data which must be produced and held during the execution of the software. An optimization run usually lasts for tens of hours and therefore the memory management becomes an important issue. Assessment of its correctness and coherence has been performed using Valgrind.

> Valgrind is an instrumentation framework for building dynamic analysis tools. There are Valgrind tools that can automatically detect many memory management and threading bugs, and profile your programs in detail. It runs on

1 `http://opensource.org/licenses/BSD-3-Clause`

> the following platforms: X86/Linux, [...]. Valgrind is Open Source / Free Software, and is freely available under the GNU General Public License, version 2.

Performance is also a critical issue: during the optimization, the operations performed by the model are executed millions of times. Therefore we analyzed performance with a profiler, *gprof*. Profiling allows you to learn where the program spent its time and which functions called which other functions while it was executing. This information can show which pieces of your program are slower than expected and might be candidates for rewriting to make the program execute faster.

The profiling analysis showed that the model spend most of the execution time in extraction of flow direction. Some time is spent also during the depression filling: the amount spent is influnced greatly by the smoothness of the landscape and by the dimension of the depressions. After some improvements, the average perfomance in experiment MOGLE has been about 40 ms per function evaluation i. e. per depression filling, flow routing and objectives evaluation.

A.2 SPATIAL INTERPOLATION: IDW

Inverse Distance Weighting (IDW) is a type of deterministic method for multivariate interpolation with a known scattered set of points. The assigned values to unknown points are calculated with a weighted average of the values available at the known points. The applied weight is an inverse function of the distance between the point to be calculated and each of the known points.

The expected result of the integration of IDW in our framework model is a discrete assignment of the searched function $f(\cdot)$, sampled by the optimizer in the DEM domain:

$$f(x,y) : (x,y) \to \mathbb{R}, \quad (x,y) \in \mathbf{D} \subset \mathbb{R}^2 \tag{A.1}$$

where $\mathbf{D}$ is the study area i. e. the DEM. The set of N known data points can be described as a list of tuples:

$$[(x_1,y_1,z_1),(x_2,y_2,z_2),\ldots,(x_N,y_N,z_N)]\,. \tag{A.2}$$

We applied the Shepard method [59]. The estimated value of function $f(\cdot)$ at a given (not sampled) point is

$$f(x,y) = \sum_{i=0}^{N} \frac{w_i(x,y)z_i}{\sum_{j=0}^{N} w_j(x,y)} \tag{A.3}$$

where

$$w_i(x,y) = \frac{1}{d(x,y,x_i,y_i)^p} \tag{A.4}$$

being p a weighting exponent, $d(\cdot)$ the euclidean distance and (x_i, y_i) is a sampled point. Using this method, the function is smoothed continuously, is once differentiable, and passes through the sampled points ($f(x_i, y_i) = z_i$).

We used the IDW interpolation method with $p = 2$ and a fixed grid of sampling points: one point each ten cell in the DEM. We also implemented a maximum window outside which sampled points are not considered i. e. they have weight 0 by default, in order to speed up the interpolation process. The window dimensions were set to 31×31 cells, centered in the point to be evaluated.

A.3 CONSTRAINT FEASIBILITY

Paik's GLE model features a constraint called "tectonic condition" based on the hypothesis that the mass gained by the uplift is the same as the total loss of sediment mass from the whole landscape. This requirement also means that the sum of elevations is still the same during the optimization process.

This constraint has proved to be very challenging: figure 4.4 in chapter 4 shows the probability of randomly choose a landscape that fulfill the constraint. The figure is based on the evaluation of that probability, given a discrete set of variation in the elevation values that can be applied to each cell of the DEM during the whole optimization.

To evaluate the probability and build the figure, we used this procedure: the variation in elevation at each cell can be treated as a random variable x, whose possible values are the discrete integer in the range of variation, e. g. $X \in \Omega = \{-1, 0, 1\}$. The probability distribution of this variable is a uniform one: therefore, in a one-cell DEM the condition to satisfy the mass constraint is $X = 0$ and its probability is $P[X = 0] = \frac{1}{K}$, K being the number of values that X can take i. e. the cardinality of its range of variation.[2]

When the DEM is composed by more than one cell, the mass constraint condition becomes:

$$z_N = \sum_{i}^{N} x_i = 0 \tag{A.5}$$

where x_i is the variation at cell i and N is the total number of cell in the DEM. Being $X \in \Omega$ a random variable and each X_i being the same i. e. each cell have the same possible variations, Z_N is also a random variable and specifically is the sum of N random variables.

2 In this section, the capital letter indicates the random variable, while the lower case letter indicates the realization of the random variable, when its value is set (and it is no more a random variable). Moreover, the probability that the variable X assumes a certain value, say 0, is expressed as $P[X = 0]$ or $p_X(0)$, $p_X(\cdot)$ being the probability distribution function or pdf. The Greek letter indicates its set of definition.

Its distribution of probability can be calculated iteratively, a method suitable to be implemented in a computer. In fact,

$$P[Z_N = z] = p_{Z_N}(z) = \sum_{\forall x \in \Omega} p_{Z_{(N-1)}}(z-x)p_X(x) \tag{A.6}$$

and of course, $P[Z_1 = z] = p_{Z_1}(z) = p_X(z)$. For example, checking the probability of fullfilling the mass constraint on a 3×1 DEM means to evaluate the following equation (A.8) with $\Omega = \{-1, 0, 1\}$,

$$\begin{aligned} P[Z_3 = 0] = p_{Z_3}(0) &= \sum_{\forall x \in \Omega} p_{Z_2}(0-x)p_X(x) = \\ &= (p_{Z_2}(1)p_X(-1)) + (p_{Z_2}(0)p_X(0)) + (p_{Z_2}(-1)p_X(1)) \end{aligned} \tag{A.7}$$

and each $p_{Z_2}(z)$ terms is

$$\begin{aligned} P[Z_2 = z] = p_{Z_2}(z) &= \sum_{\forall x \in \Omega} p_{Z_1}(z-x)p_X(x) = \\ &= (p_{Z_1}(z-1)p_X(-1)) + (p_{Z_1}(z)p_X(0)) + \\ &+ (p_{Z_1}(z+1)p_X(1)) \,. \end{aligned} \tag{A.8}$$

It's also clear from this example the limit of this method: to evaluate the probability of the sum of three random variables, it is necessary to evaluate other eight probabilities.

Including into the dissertation the effect of the tolerance value is simple: the probability of the event A "a DEM fulfill the constraint" becomes

$$P(A) = \sum_{j=-R}^{R} P[Z_N = j] = \sum_{j=-R}^{R} p_{Z_N}(j) \tag{A.9}$$

being R the range of elevation sums that fulfill the constraint.

The implementation of this simple method is able to evaluate the probability of randomly select of correct landscape for DEM dimension of 51x51 and Ω spanning discreetly from -25 to $+25$ meters. A code snippet of the function which evaluates the probability for a given order is shown in Listing A.2.

The results of the evaluation are shown in figure 4.4.

Listing A.1: Header of the template class OurMatrix.

```
template<class T>
class OurMatrix {
public:
    OurMatrix();
    OurMatrix(int nr, int nc);
    OurMatrix(DEMDimensionType, const T[]);
    OurMatrix(DEMDimensionType, const std::vector<T>);
    OurMatrix(int nr, int nc, const std::vector<T>);
    explicit OurMatrix(int nr, int nc, T defaultValue);
    OurMatrix(const OurMatrix<T>& a);
    ~OurMatrix();
    OurMatrix<T>& operator=(const OurMatrix<T> & a);
    OurMatrix<double> toDouble() const;
    bool operator==(const OurMatrix<T>& a) const;
    bool operator!=(const OurMatrix<T>& a) const;

    const T& getElement(int i, int j) const;
    void setElement(const T& value, int i, int j);
    bool sumMatrix(const OurMatrix<T>& a);
    bool sumMatrix(const T& a);
    bool productMatrixElByEl(const OurMatrix<T>& a);
    bool productMatrixElByEl(const T& a);
    bool squareRootElByEl(); // only if T is a float or double
    bool powerElByEl(int power);
    T sumAll();
    double meanOfEls();
    double varianceOfEls();
    DEMDimensionType getDimension() const;
#ifdef DEBUG
    void printMatrix() const
#endif
private:
    T* data;
    long int nr;
    long int nc;
    long int numberOfZero;
    bool checkDimension(const OurMatrix<T>& a);
};

namespace OurMatrixInternal {
// square root element by element - partial specialization
    outside class scope
template<class T> inline bool squareRootElByEl_part(OurMatrix<T>&
     a);
template<> inline bool squareRootElByEl_part<double>(OurMatrix<
    double>& a);
template<class T> inline OurMatrix<double> toDouble(const
    OurMatrix<T>& a);
template<> inline OurMatrix<double> toDouble<double>(const
    OurMatrix<double>& a);
}
```

Listing A.2: Code snippet with the recursive function to evaluate the pdf of the sum Z_N of N random variables equal to X.

```
std::vector<int> values_of_x(number_of_values_of_x,
    min_value_of_x);
for (unsigned int i = 1; i < number_of_values_of_x; i++) {
    values_of_x[i] = values_of_x[i - 1] + 1;
}
prob_x = 1.0 / number_of_values_of_x;
std::vector<std::vector<double> > p_z;
for (unsigned int idx = 0; idx < p_z.size(); idx++) {
    p_z[idx] = std::vector<double>(
        (max_value_of_x * (idx + 1) - min_value_of_x
            * (idx + 1)) + 1, INIT_VALUE);
}

double prob(int Z, int value_of_z) {
    if (value_of_z < min_value_of_x * Z ||
        value_of_z > max_value_of_x * Z) {
            return 0.0;
    }
    if (value_of_z < min_value_of_z ||
        value_of_z > max_value_of_z) {
            return 0.0;
    }
    int idx_value_of_z = -(min_value_of_z - value_of_z);
    int idx_N = Z - 1;
    if (p_z[idx_N][idx_value_of_z] == -2.0) {
        if (Z > 1) {
            double pp = 0.0;
            for (unsigned int i = 0; i < number_of_values_of_x; i
                ++) {
                pp += prob(Z - 1, value_of_z - values_of_x[i], p)
                    ;
            }
            p_z[idx_N][idx_value_of_z] = prob_x * pp;
        } else {
            if (Z == 1) {
                for (unsigned int j = 0; j <
                    number_of_values_of_x; j++) {
                    if (value_of_z == values_of_x[j]) {
                        p_z[idx_N][idx_value_of_z] = prob_x;
                        break;
                    }
                }
            }
            if (p_z[idx_N][idx_value_of_z] == INIT_VALUE) {
                p_z[idx_N][idx_value_of_z] = 0.0;
            }
        }
    }
    return p_z[idx_N][idx_value_of_z];
}
```

B

LANDSCAPE EVOLUTION FRAMEWORK: A BIT OF HISTORY ON MOEAS

B.1 ε-NSGAII

εNSGA-II is an MOEA built on the NSGA-II, with the additional capabilities of ε-dominance archiving, adaptive population sizing and automatic termination to minimize the need for extensive parameter calibration [24]. The ancestors of εNSGA-II go back to Nondominated Sorting Genetic Algorithm (NSGA), one of the first MOEA to be published into a journal[4]. Recalling this history, the ideas that led to the development of MOEA will be shown.

B.1.1 *NSGA*

NSGA was created by Srinivas and Deb [62] and was one of the first MOEA developed. Actually, the first hint regarding the possibility of using EAs to solve a MOPs appears in a PhD thesis from 1967 [56]. Schaffer [57] is the first to develop an MOEA during the mid-1980s: the Vector Evaluated Genetic Algorithm (VEGA). It consists of a simple genetic algorithm with a modified selection mechanism. At each generation, a number of sub-populations are generated by performing proportional selection according to each objective function in turn. These sub-populations are then shuffled together to obtain a new population, on which the EA apply the crossover and mutation operators in the usual way.[1]

The basic idea for the NSGA comes from Goldberg [10]. He suggested the use of nondominated ranking and selection: the idea is to find the set of solutions in the population that are Pareto nondominated by the rest of the population. These solutions are then assigned the highest rank and eliminated from further contention. Another set of Pareto nondominated solutions is determined from the remaining population and are assigned the next highest rank. This process continues until all the population is suitably ranked.

NSGA is based on several layers of classification of the individuals as suggested by Goldberg and a dummy fitness value, proportional to the population size, is assigned to each of them, in order to provide an equal reproductive potential. To maintain the diversity of the population, these classified individuals are shared with their dummy fitness values. Since individuals in the first front have the maximum

1 Further reading and explanation of the usual way are provided in [57] and in the general overview from Coello Coello [4].

fitness value, they always get more copies than the rest of the population.

The algorithm of the NSGA is not very efficient, because Pareto ranking has to be repeated over an over again. Evidently, it is possible to achieve the same goal in a more efficient way.

B.1.2 *NSGAII*

NSGA-II is a second generation MOEA developed by Deb et al. [6]. Compared to NSGA it uses a more efficient non-domination sorting scheme, eliminates the sharing parameter and adds an implicitly elitist selection method that greatly aids in capturing Pareto surfaces. The enforced algorithm of tournament selection helps in finding solutions along the full extent of the Pareto surface. Deb et al. [7] have shown that the NSGA-II performed as well as or better than other second-generation MOEAs.

B.1.3 *ε-NSGAII*

εNSGA-II created by Kollat and Reed adds ε-dominance archiving, adaptive population sizing and automatic termination to the solid basis of the NSGA-II. The concept of ε-dominance is explained below in subsection 4.5.2 . The population size is automatically adapted based on the number of non-dominated solutions found. These solutions are stored in an archive and used to direct the search by re-injection. In the injection scheme, 25% of the subsequent population will be composed of the ε-non-dominated solutions taken from the archive. This assists the search by directing it using previously evolved solutions and by adding new solutions to encourage the exploration of additional regions of the search space. The search is terminated across all populations used if the number and quality of solutions has not increased above Δ% across two successive runs. The primary goal of εNSGA-II is to provide a highly reliable and efficient MOEA which minimizes the need for parameterization [24].

The parameters required to set up an optimization run of the εNSGA-II are the initial population size, the maximum NFE, the injection rate into the archive and the parameters related to simulated binary crossover and mutation operator. Suggested possible values for these parameters are shown in chapter 4 .

B.2 GDE3

As the name suggest, the Generalized Differential Evolution 3 is the third improvement of the Generalized version of Differential Evolution EA [63].

B.2.1 *DE*

The design principles in the DE algorithm were simplicity, efficiency, and the use of floating-point encoding instead of binary numbers. Like a typical EA, DE has some random initial population, which is then improved using selection, mutation, and crossover operations. The stopping criterion is usually a predefined upper limit for the number of generations or function evaluations.

The basic idea of DE is that the mutation is self-adaptive to the objective function surface and to the current population. At the beginning of generations the magnitude of the mutation is large because vectors in the population are far away in the search space. When evolution proceeds and the population converges, the magnitude of the mutation gets smaller.

B.2.2 *GDE3*

GDE3 [25] is a multiobjective variant of the DE algorithm. GDE3 was one of the top rated in a competition for MOEAs [73].

Among the characteristics features of GDE3 there is its mutation operator which uses the scaled "difference" between two population members' decision variable vectors to generated new candidate solutions. This operator is termed rotationally invariant and it does not assume explicit search directions when it creates new solutions. It also means that GDE3 does not require decisions to be separable and independent i. e. , they can have conditional dependencies.[2]

Another interesting feature of GDE3 is its constraint handling method: it reduces the number of needed function evaluations, being more efficient in finding solutions for constrained problem.

The parameters required to set up an optimization run of the GDE3 are: initial population size, maximum NFE, crossover rate and step size of DE operator. With only four parameters, GDE3 appears to be very suitable for applications. As for εNSGA-II, suggested possible values for these parameters are shown in table 4.1 in chapter 4 .

2 The SBX operator used by εNSGA-II assumes problems have independent decisions that can be optimized using only vertical or horizontal translations of the decision variables.

C

LANDSCAPE EVOLUTION FRAMEWORK: ALL THE RESULTS

C.1 FIRST EXPERIMENT: MOGLE

The Horton's bifurcation ratio statistical distribution for the basin within the clusters analyzed in subsection 5.4.3 is showed in figure C.1.

Horton's length ratio statistical distribution for the basin within the clusters analyzed in subsection 5.4.3 is showed in figure C.2.

Horton's slope ratio statistical distribution for the basin within the clusters analyzed in subsection 5.4.3 is showed in figure C.3.

Contributign area exponenent statistical distribution for the basin within the clusters analyzed in subsection 5.4.3 is showed in figure C.4.

C.2 SECOND EXPERIMENT: MOGLE_RAINY

The Horton's bifurcation ratio statistical distribution for the basin within the clusters analyzed in subsection 5.4.3 is showed in figure C.5.

Horton's length ratio statistical distribution for the basin within the clusters analyzed in subsection 5.4.3 is showed in figure C.6.

Horton's slope ratio statistical distribution for the basin within the clusters analyzed in subsection 5.4.3 is showed in figure C.7.

Contributign area exponenent statistical distribution for the basin within the clusters analyzed in subsection 5.4.3 is showed in figure C.8.

C.3 THIRD EXPERIMENT: MOGLE_RAINY_IDW

The Horton's bifurcation ratio statistical distribution for the basin within the clusters analyzed in subsection 5.4.3 is showed in figure C.9.

Horton's length ratio statistical distribution for the basin within the clusters analyzed in subsection 5.4.3 is showed in figure C.10.

The statistical distribution of the exponents of the probability distribution of drained area for the basin within the clusters analyzed in subsection 5.4.3 is showed in figure C.11.

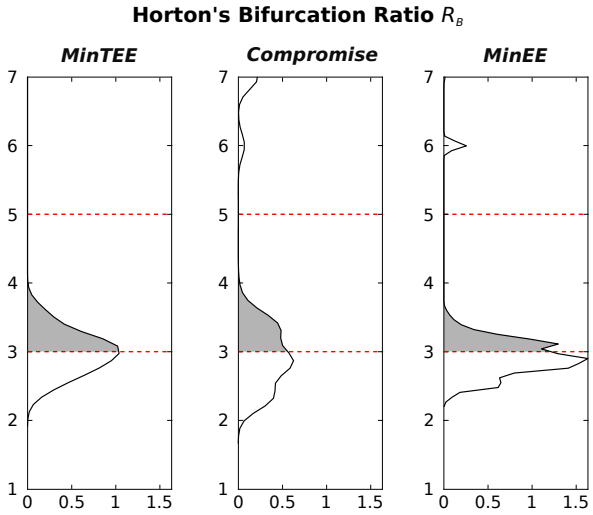

	MIN TEE	COMPROMISE	MIN EE
Cluster points	58	382	185
Mean and std dev	3.954 ± 2.438	4.106 ± 2.132	3.048 ± 0.7599
Cdf within range	0.3273	0.2657	0.2959

Figure C.1: Statistical distribution of Horton's bifurcation ratio for the clusters of experiment MOGLE. For more detailed informations about the image, refer to figure 5.6.

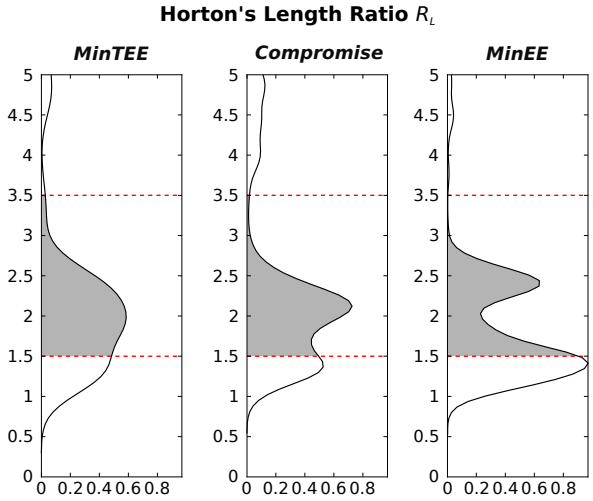

	MIN TEE	COMPROMISE	MIN EE
Cluster points	58	382	185
Mean and std dev	2.319 ± 1.284	2.401 ± 1.210	1.888 ± 0.7986
Cdf within range	0.6179	0.6042	0.5262

Figure C.2: Statistical distribution of Horton's length ratio for the clusters of experiment MOGLE. For more detailed informations about the image, refer to figure 5.6.

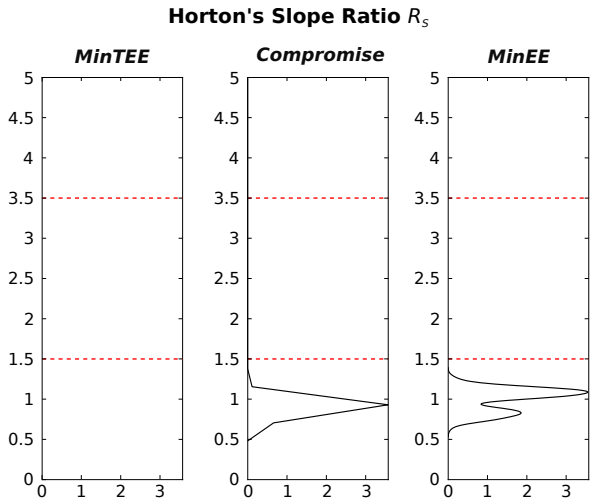

	MIN TEE	COMPROMISE	MIN EE
Cluster points	58	382	185
Mean and std dev	5.560 ± 22.52	1.006 ± 1.279	0.9899 ± 0.1487
Cdf within range	0.0	0.0	0.0

Figure C.3: Statistical distribution of Horton's slope ratio for the clusters of experiment MOGLE. For more detailed informations about the image, refer to figure 5.6.

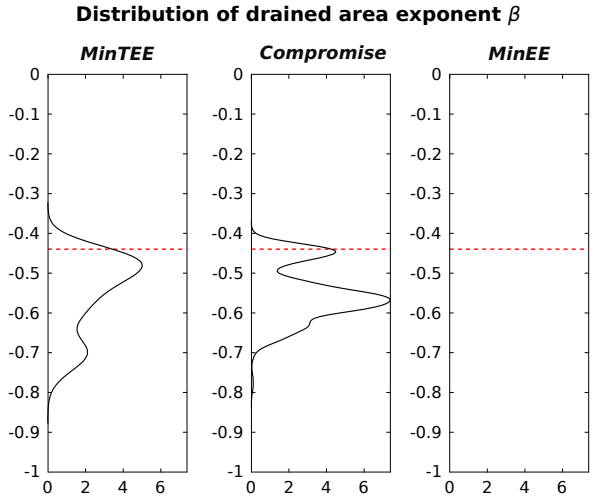

	MIN TEE	COMPROMISE	MIN EE
Cluster points	58	382	185
Mean and std dev	-0.5533 ± 0.1012	-0.5508 ± 0.07141	$- \pm -$

Figure C.4: Statistical distribution of contributign area exponenent for the clusters of experiment MOGLE. For more detailed informations about the image, refer to figure 5.6.

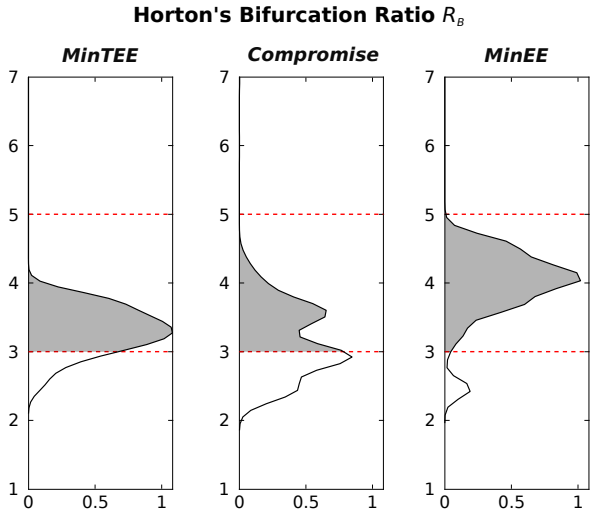

	MIN TEE	COMPROMISE	MIN EE
Cluster points	58	382	185
Mean and std dev	3.954 ± 2.438	4.106 ± 2.132	3.048 ± 0.7599
Cdf within range	0.3273	0.2657	0.2959

Figure C.5: Statistical distribution of Horton's bifurcation ratio for the clusters of experiment MOGLE_RAINY. For more detailed informations about the image, refer to figure 5.9.

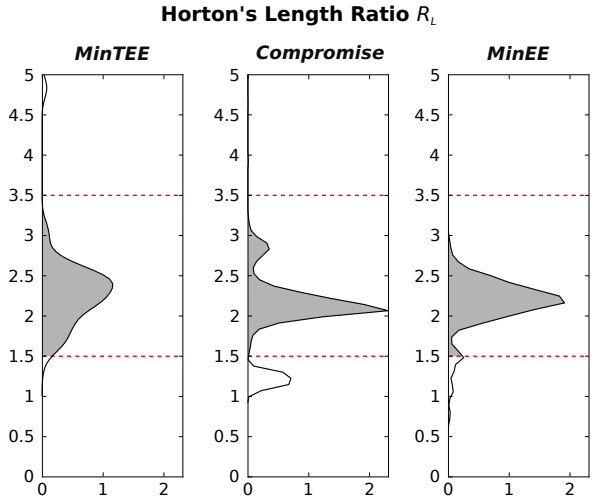

	MIN TEE	COMPROMISE	MIN EE
Cluster points	58	382	185
Mean and std dev	2.319 ± 1.284	2.401 ± 1.210	1.888 ± 0.7986
Cdf within range	0.6179	0.6042	0.5262

Figure C.6: Statistical distribution of Horton's length ratio for the clusters of experiment MOGLE_RAINY. For more detailed informations about the image, refer to figure 5.9.

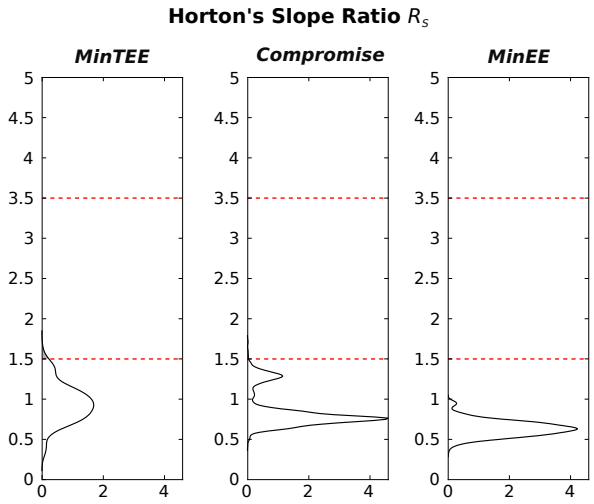

	MIN TEE	COMPROMISE	MIN EE
Cluster points	58	382	185
Mean and std dev	5.560 ± 22.52	1.006 ± 1.279	0.9899 ± 0.1487
Cdf within range	0.0	0.0	0.0

Figure C.7: Statistical distribution of Horton's slope ratio for the clusters of experiment MOGLE_RAINY. For more detailed informations about the image, refer to figure 5.9.

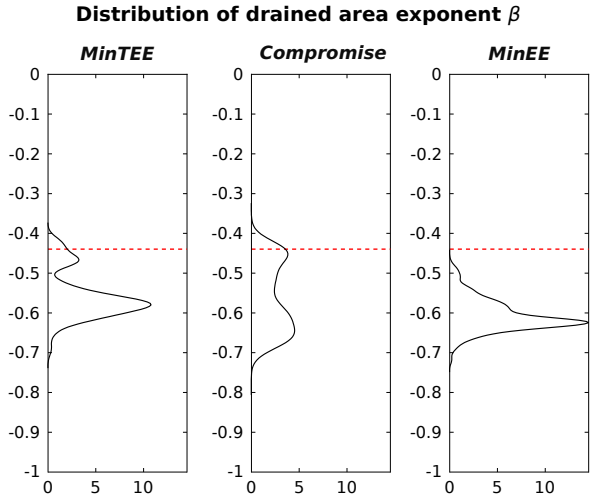

	MIN TEE	COMPROMISE	MIN EE
Cluster points	58	382	185
Mean and std dev	-0.5533 ± 0.1012	-0.5508 ± 0.07141	$- \pm -$

Figure C.8: Statistical distribution of contributign area exponenent for the clusters of experiment MOGLE_RAINY. For more detailed informations about the image, refer to figure 5.9.

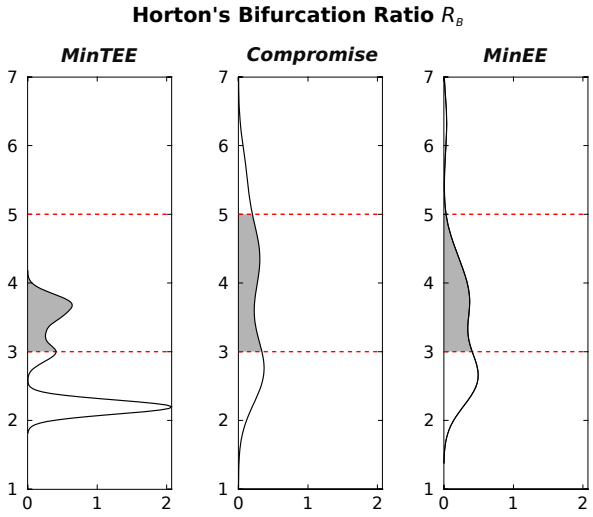

	MIN TEE	COMPROMISE	MIN EE
Cluster points	40	118	40
Mean and std dev	2.755 ± 0.6584	3.750 ± 1.112	3.357 ± 0.9667
Cdf within range	0.3839	0.5297	0.5178

Figure C.9: Statistical distribution of Horton's bifurcation ratio for the clusters of experiment MOGLE_RAINY_IDW. For more detailed informations about the image, refer to figure 5.14.

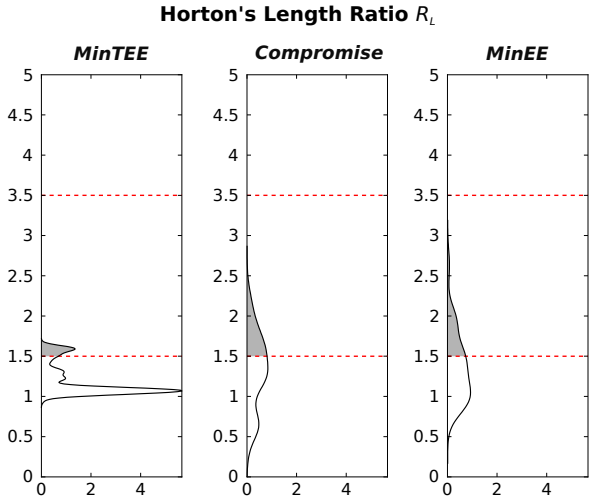

	MIN TEE	COMPROMISE	MIN EE
Cluster points	40	118	40
Mean and std dev	1.203 ± 0.2007	1.324 ± 0.4964	1.367 ± 0.4618
Cdf within range	0.1541	0.3673	0.3387

Figure C.10: Statistical distribution of Horton's length ratio for the clusters of experiment MOGLE_RAINY_IDW. For more detailed informations about the image, refer to figure 5.14.

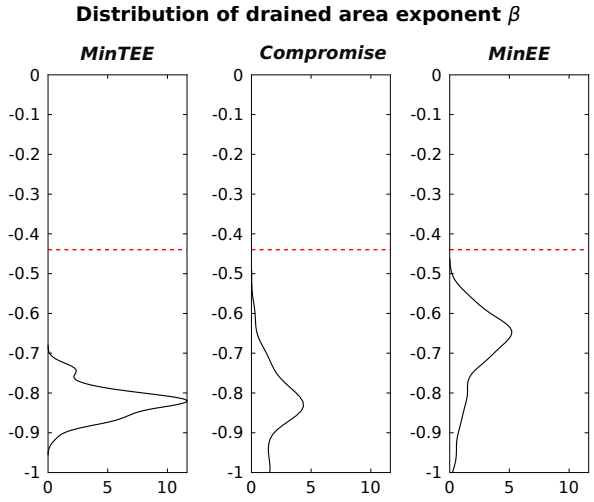

	MIN TEE	COMPROMISE	MIN EE
Cluster points	40	118	40
Mean and std dev	-0.8221 ± 0.04182	-0.9061 ± 0.1979	-0.6961 ± 0.1050

Figure C.11: Statistical distribution of the exponents of the probability distribution of contributing area for the clusters of experiment MOGLE_RAINY_IDW. For more detailed informations about the image, refer to figure 5.14.

D

THE UNSUNG HEROES

We believe that engineering is made by tools, whatever they are. Therefore we present here the tools we have used, which are mainly software tools.

D.1 RESULTS PRODUCTION

The first step to product results was to code the model software. We used the GNU compiler collection for C++. As editor, we choose *Eclipse* because it is open source and because of its plugin structure that allows great extendibility. Is available at `http://www.eclipse.org/`.

To maintain updated the code sources written by us, we needed a code repository. We chose the service from *Google Code* (`code.google.com`) managed by the *Subversion* system. Therefore we used also the *Subversive* plugin to integrate these functionalities within *Eclipse*.

After writing the code, we had to perform the experiments. We used the cluster system Pennsylvania University kindly gave us access to. Control on experiments was based on automatization scripts written in the language of the *bash* textual shell. The scripts automatized the job submission to the cluster computers, the formatting of results file and the launching of the MOEA framework [15] command line utilities to analyze these data under a the perspective of MOEAs.

The images of the Pareto fronts were produced thanks to *Aerovis* which is a visualization software specialized for Pareto fronts. *AeroVis* is currently being site licensed by the Aerospace Corp. through Penn State's Intellectual Property office.

The statistical analysis of Horton's indexes was performed in the *Matlab*© which is an high level language and an interactive environment for numeric calculus. It provides many ready-to-use scientific techniques, like clustering by k-means.

Finally we used *Dropbox* (`www.dropbox.com`) for clouding and hosting services.

D.2 THESIS WRITING

We began the writing of this thesis at the start of March 2013. By that time, we had already imagined most of contents of the thesis and we started the execution of the experiment here shown. We also organized the scientific literature we have read which served as the

basis for the first chapters. The last content which was defined was the conclusion because they are based on experiments results.

D.2.1 *Technical side*

We were asked to use the LaTeXsystem, and we would have chosen it anyway. As the website http://latex-project.org/ states,

> LaTeXis a document preparation system for high-quality typesetting. It is most often used for medium-to-large technical or scientific documents but it can be used for almost any form of publishing. LaTeXis not a word processor! Instead, LaTeXencourages authors not to worry too much about the appearance of their documents but to concentrate on getting the right content. [It] is based on the idea that it is better to leave document design to document designers, and to let authors get on with writing documents. LaTeXis based on Donald E. Knuth's TeXtypesetting language or certain extensions. LaTeXwas first developed in 1985 by Leslie Lamport, and is now being maintained and developed by the LaTeX3 Project.

We can confirm every single word. Indeed, we let the design of the appearance to "document designers". Particularly we chose the style "Classic Thesis" available at http://code.google.com/p/classicthesis/. It's "an homage to the elements of typographic style" and is inspired by the work of Bringhurst *The Elements of Typographic Style* [3].

A little workflow research on the Internet resources was done to find a simple yet powerful bibliography management system. We ended up choosing *zotero* because of its easy connection with most of articles database and with bibtex. As the website states at http://www.zotero.org/,

> Zotero [zoh-TAIR-oh] is a free, easy-to-use tool to help you collect, organize, cite, and share your research sources. It lives right where you do your work — in the web browser itself.

It has also the capability to retrieve the article itself and to link the file with its database, which effectively become our library.

The word "BibTeX" stands for a tool and a file format which are used to describe and process lists of references, mostly in conjunction with LaTeXdocuments. It is supported by *zotero* as well as Google Scholar, Web Of Science and many other research related resources.

Last but not least, we rely on the plugin structure of *Eclipse* to use it as a LaTeXeditor, thanks to the TeXlipse plugin available at http://texlipse.sourceforge.net/. With the *pdf4Eclipse* plugin we were also able to see the changes in the document appearance each time

we saved the TEXfiles, thanks to the automatic compilation that can be triggered in *Eclipse*. We could also rely on the *Google Code* repository to take care of merging the work of both of us and prevent any losses.